Forschungszentrum Karlsruhe
in der Helmholtz-Gemeinschaft

Karlsruhe Institute of Technology

Simulation of Photoproduction on Nuclei and Astroparticle Physics Connection

Ralph Engel

Karlsruhe Institute of Technology

Astroparticle physics connection

Example: Ultra-high energy cosmic rays

- **Sources:**
  interaction of hadrons with dense γ-ray fields
- **Propagation:**
  interaction with cosmic microwave background
- **Detection:**
  interaction with nuclei in the Earth´s atmosphere, extensive air showers

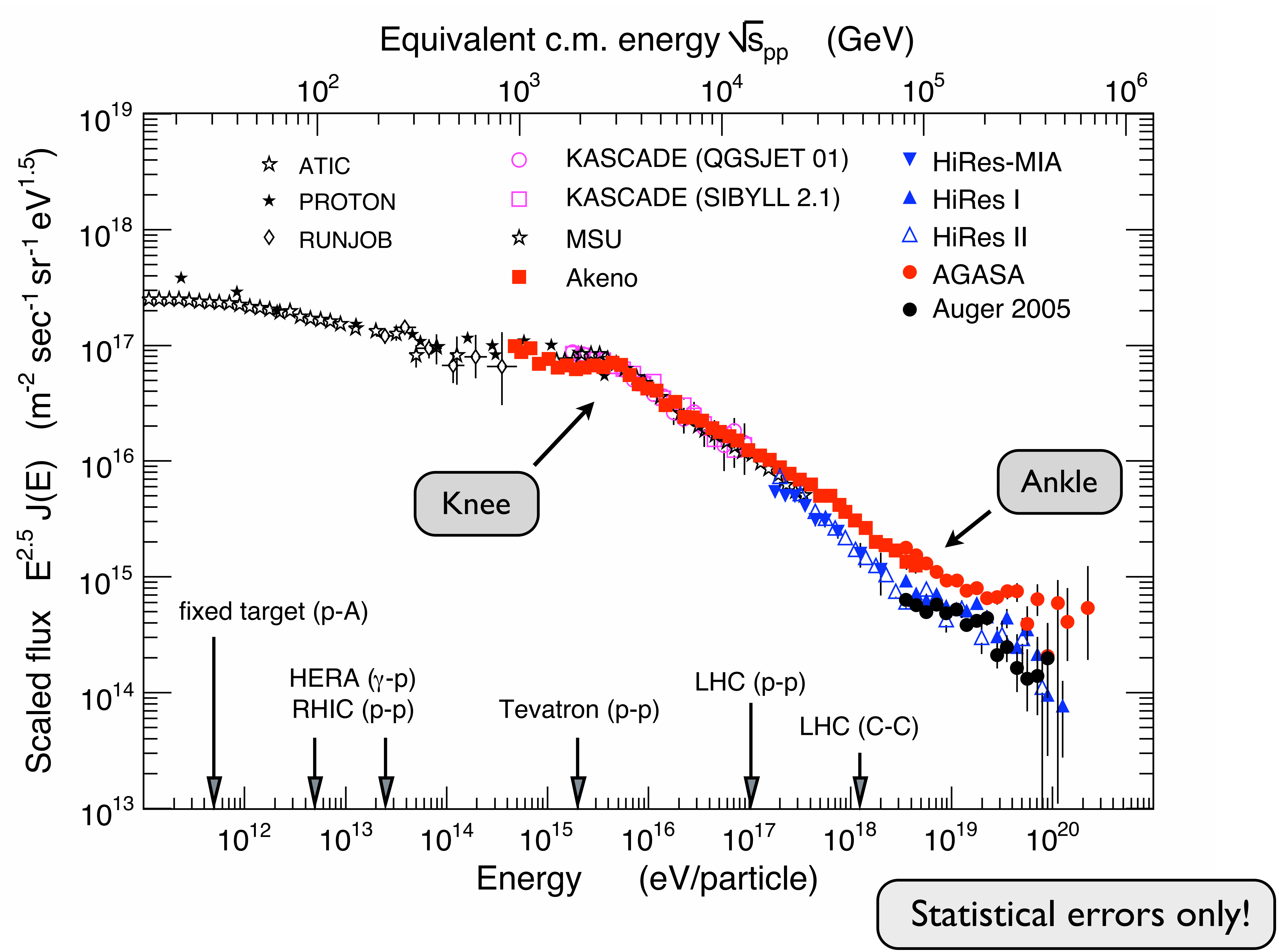

Equivalent c.m. energy $\sqrt{s_{pp}}$ (GeV)
10^2
10^3
10^4
10^5
10^6
10^{19}
10^{18}
10^{17}
10^{16}
10^{15}
10^{14}
10^{13}
Scaled flux $E^{2.5}$ J(E) (m^{-2} sec^{-1} sr^{-1} $eV^{1.5}$)
ATIC
PROTON
RUNJOB
KASCADE (QGSJET 01)
KASCADE (SIBYLL 2.1)
MSU
Akeno
HiRes-MIA
HiRes I
HiRes II
AGASA
Auger 2005
Knee
Ankle
fixed target (p-A)
HERA (γ-p)
RHIC (p-p)
Tevatron (p-p)
LHC (p-p)
LHC (C-C)
10^{12}
10^{13}
10^{14}
10^{15}
10^{16}
10^{17}
10^{18}
10^{19}
10^{20}
Energy (eV/particle)
Statistical errors only!

The first really big air shower

VOLUME 10, NUMBER 4 PHYSICAL REVIEW LETTERS 15 FEBRUARY 1963

EVIDENCE FOR A PRIMARY COSMIC-RAY PARTICLE WITH ENERGY 10^{20} eV†

John Linsley
Laboratory for Nuclear Science, Massachusetts Institute of Technology, Cambridge, Massachusetts
(Received 10 January 1963)

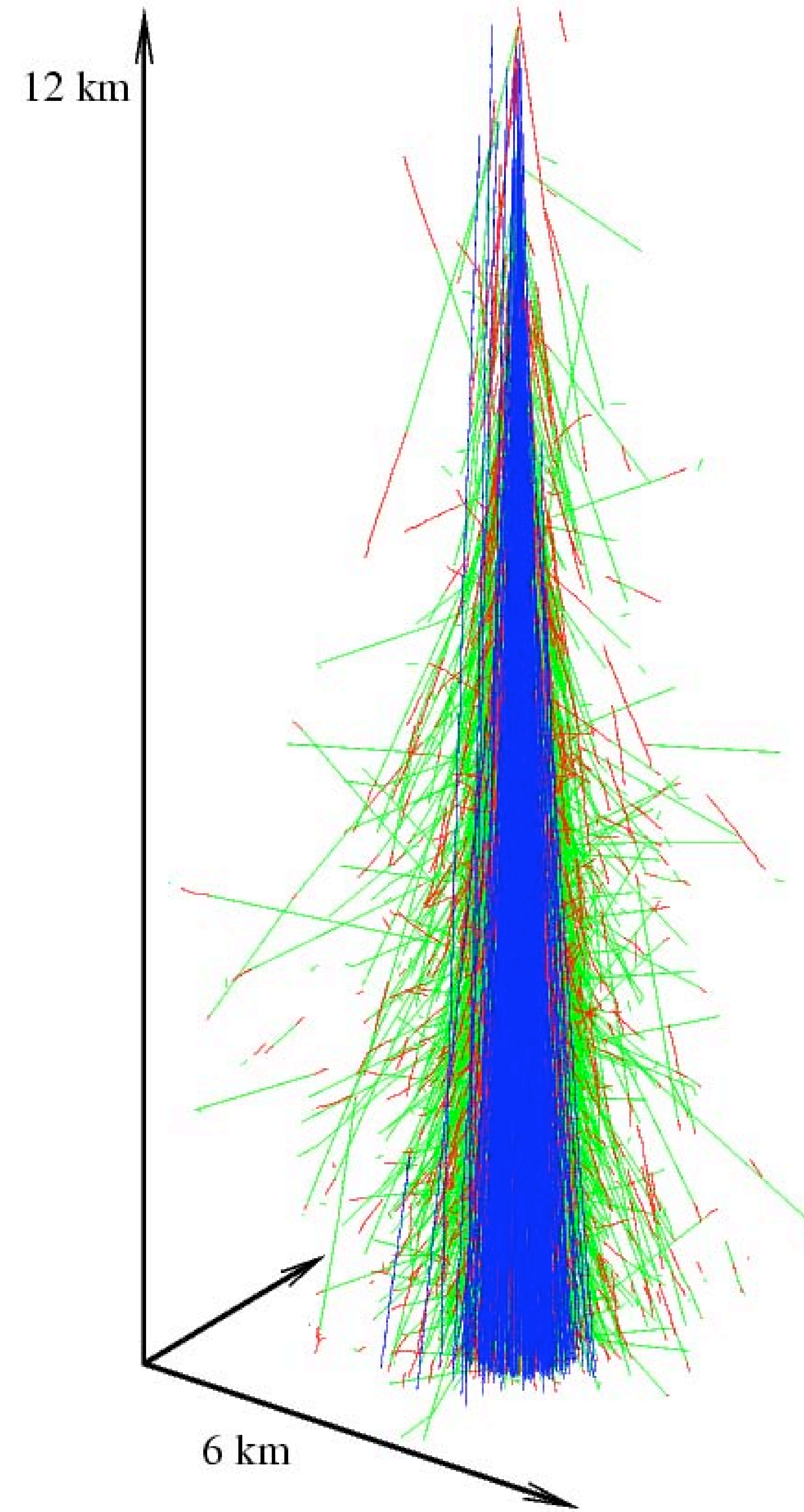

The first really big air shower

VOLUME 10, NUMBER 4 PHYSICAL REVIEW LETTERS 15 FEBRUARY 1963

EVIDENCE FOR A PRIMARY COSMIC-RAY PARTICLE WITH ENERGY 10^{20} eV†

John Linsley
Laboratory for Nuclear Science, Massachusetts Institute of Technology, Cambridge, Massachusetts
(Received 10 January 1963)

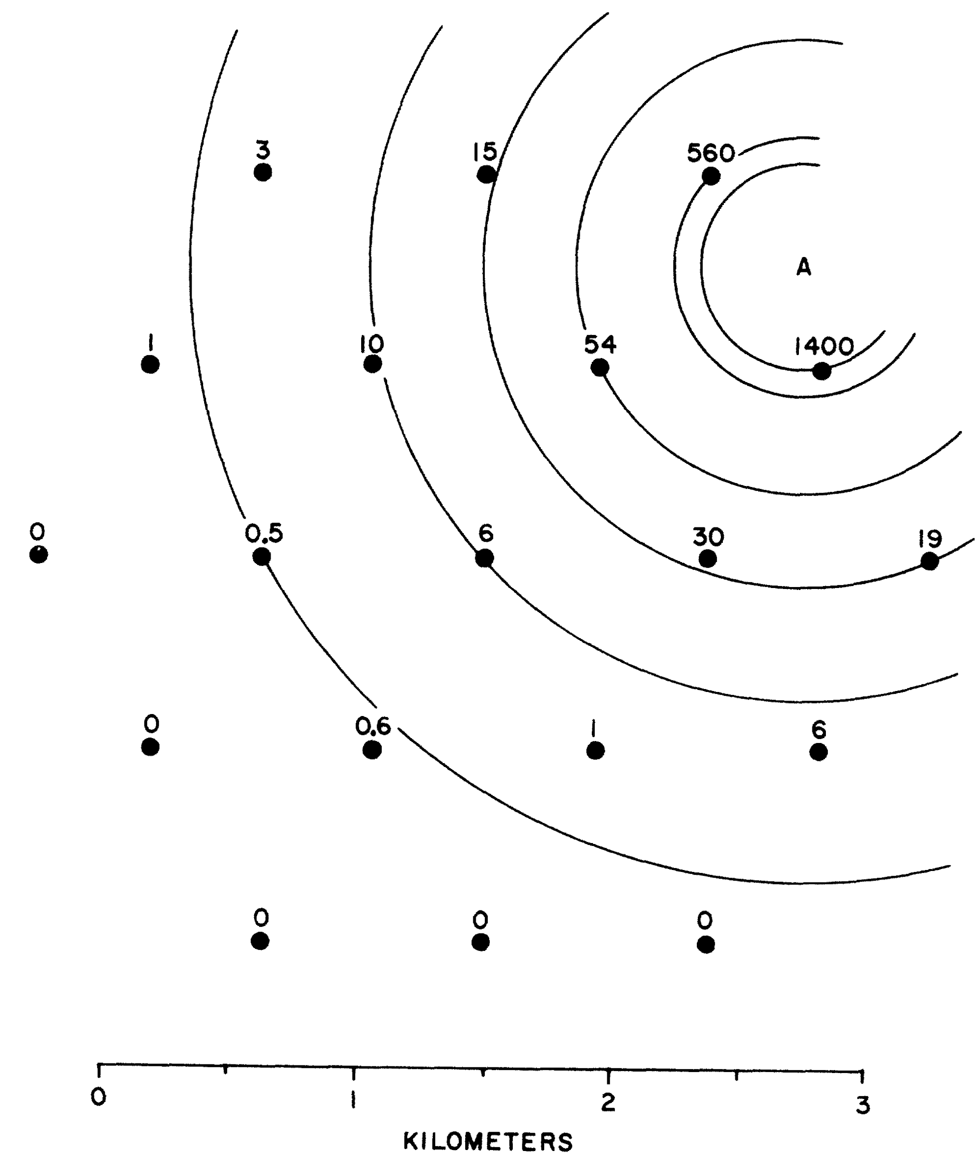

FIG. 1. Plan of the Volcano Ranch array in February 1962. The circles represent 3.3-m^2 scintillation detectors. The numbers near the circles are the shower densities (particles/m^2) registered in this event, No. 2-4834. Point "A" is the estimated location of the shower core. The circular contours about that point aid in verifying the core location by inspection.

Magnetic fields in our Galaxy

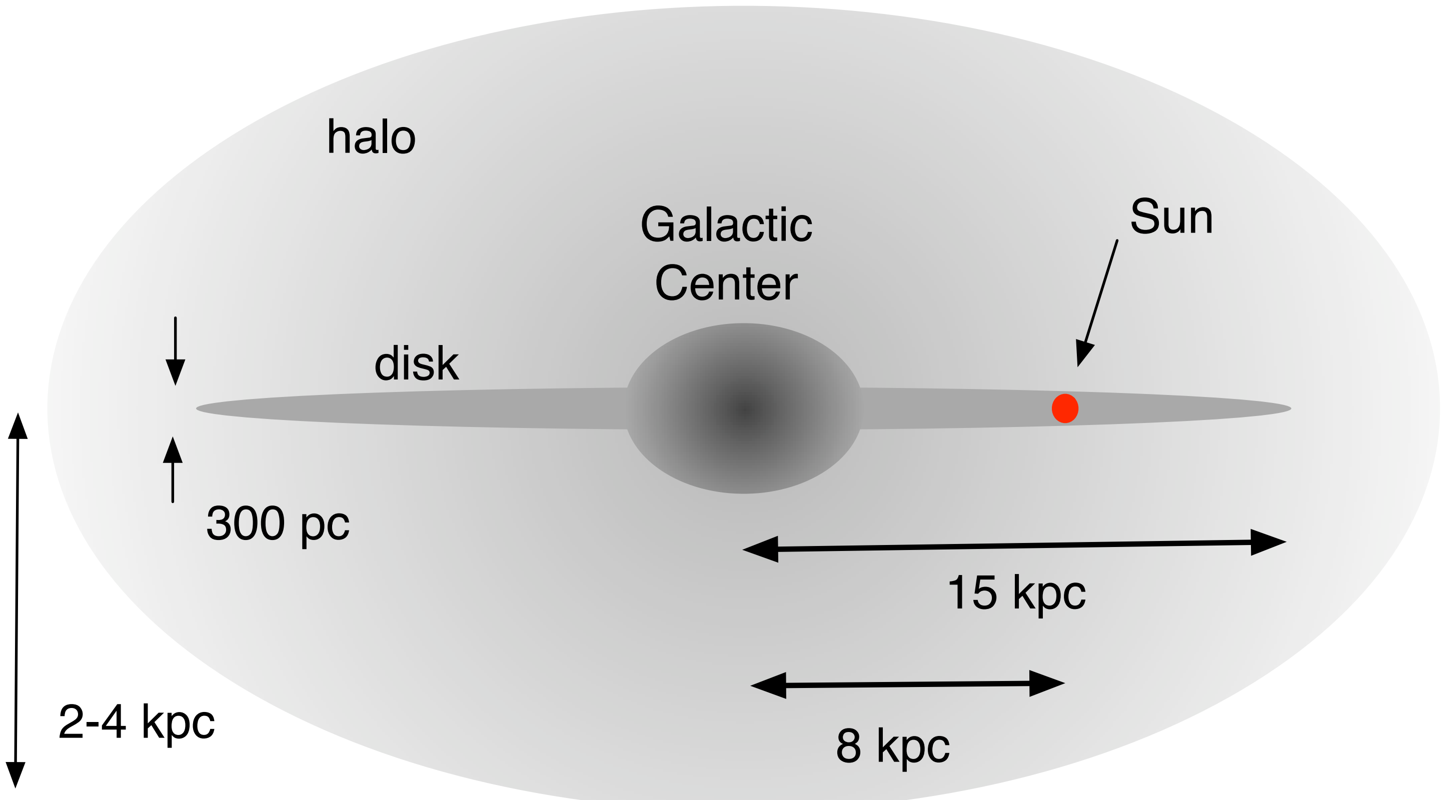

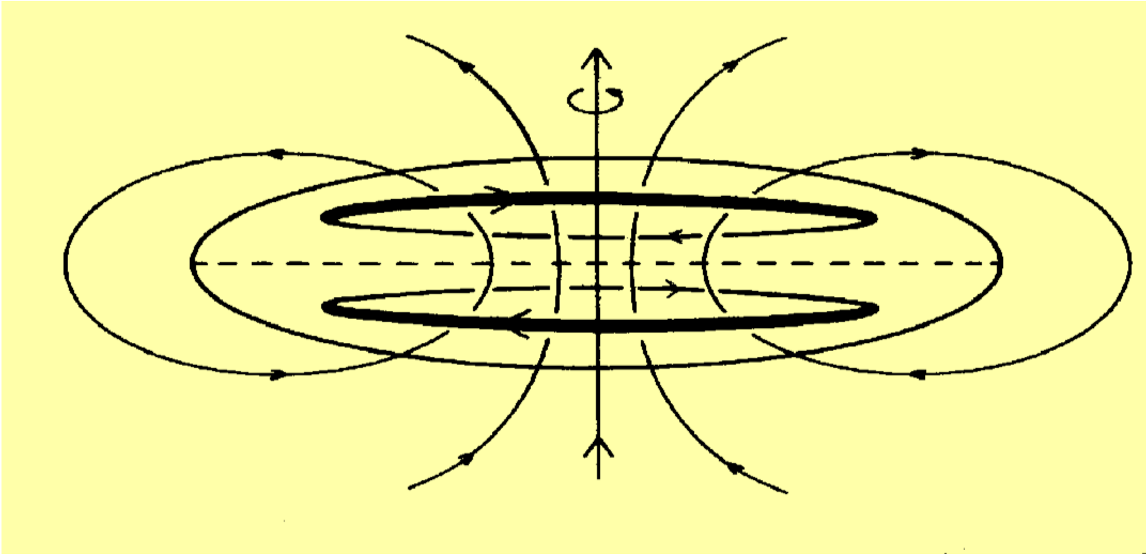

Halo field: A0 dynamo

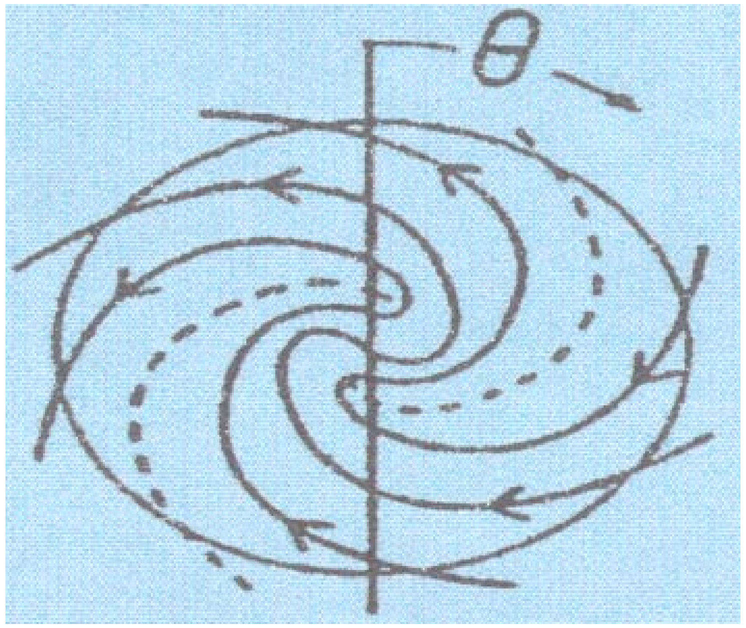

Disk field:
bisymmetrical spiral

Near solar system:
3μG (regular) ± 3μG (random)

Lamor radius (proton):
1pc = 3.2 ly at 3×10^{15} eV
1kpc at 3×10^{18} eV

Transition from galactic to extra-galactic CRs

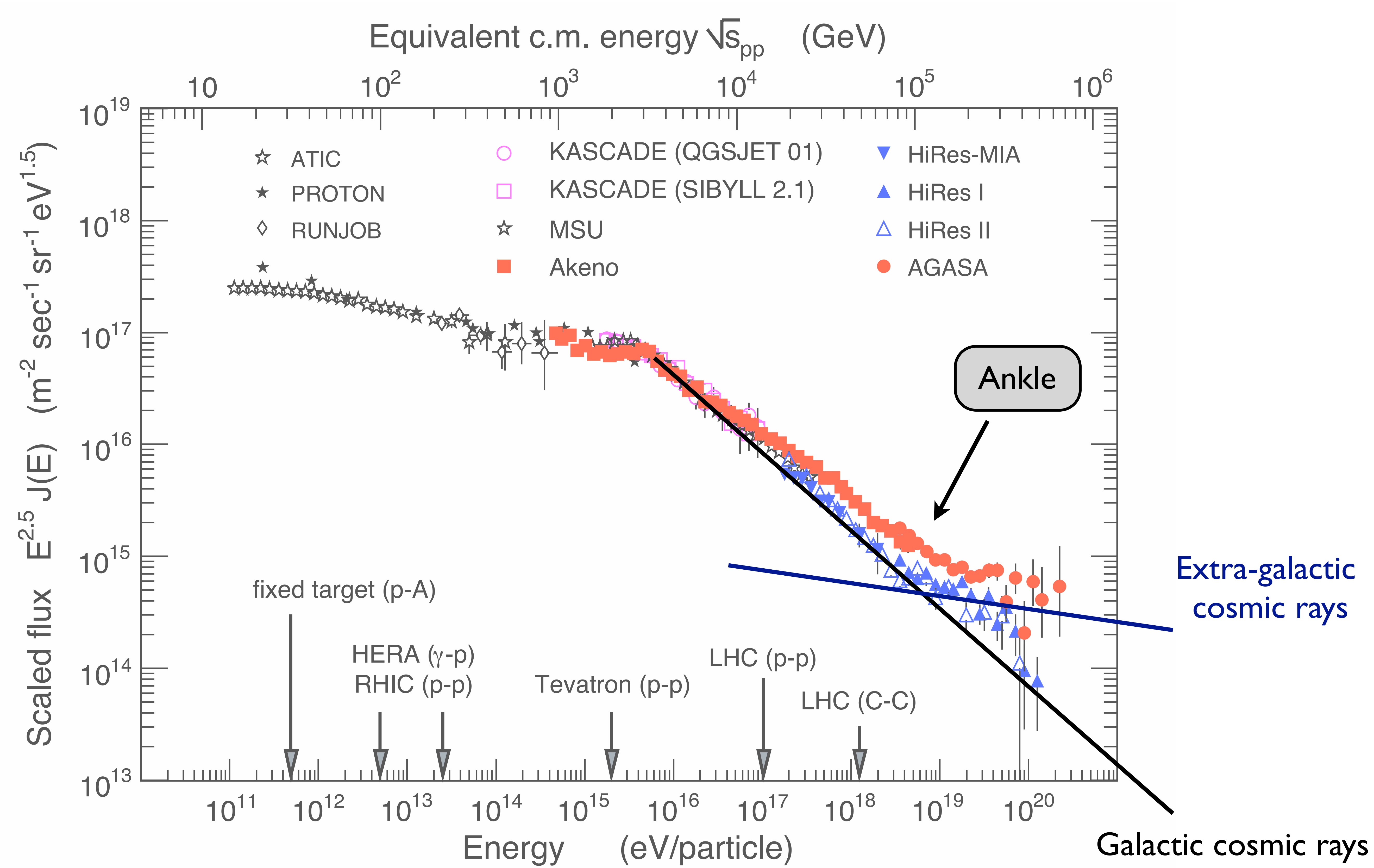

Acceleration: general source constraints

M. Hillas, 1984:

$$E_{\max} \simeq Ze\beta BR$$

shock velocity

mag. field strength

size of acc. region

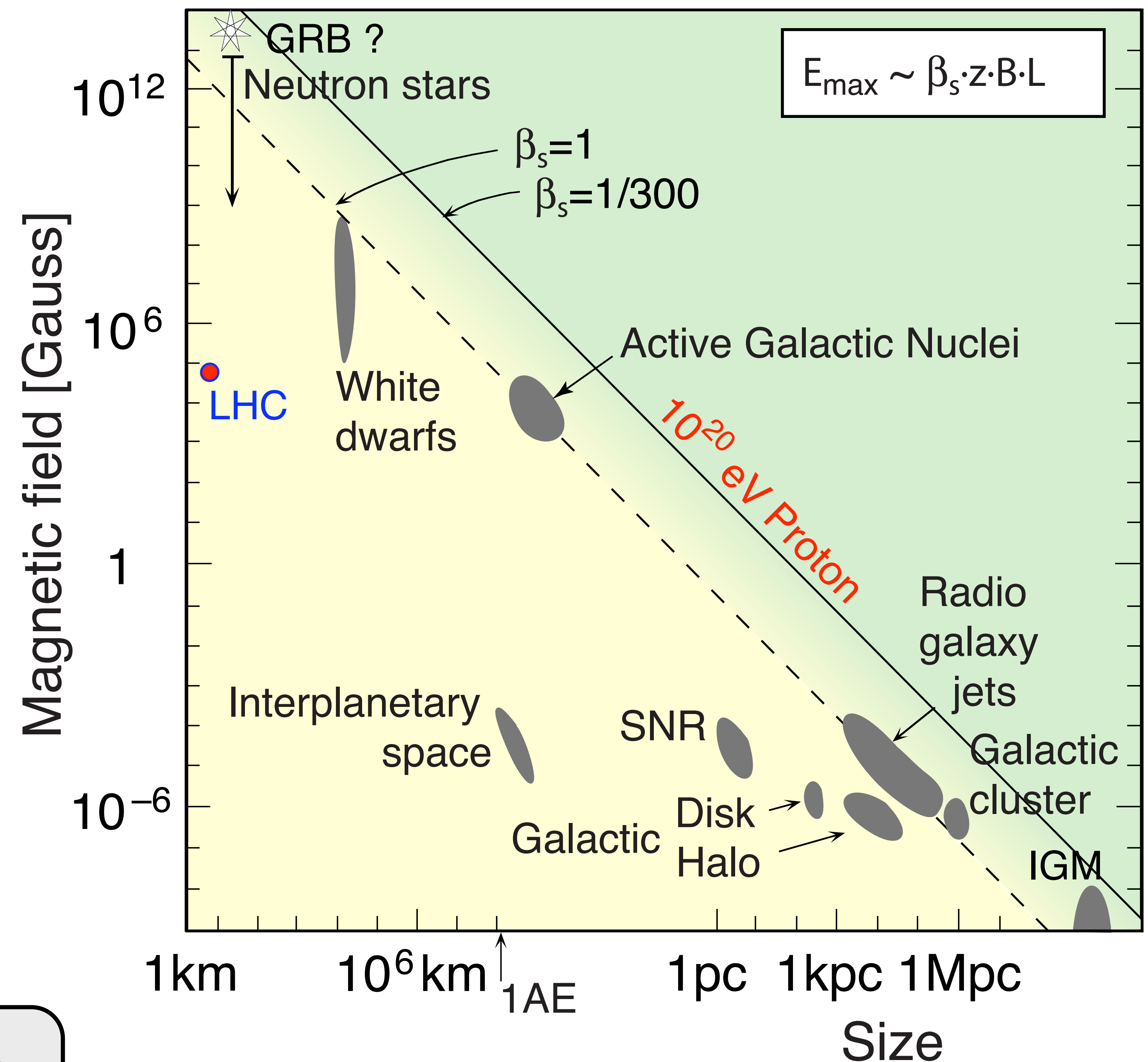

Additional constraints from energy losses in acceleration region !

Core of Galaxy NGC 4261

Hubble Space Telescope

Wide Field / Planetary Camera

Ground-Based Optical/Radio Image

HST Image of a Gas and Dust Disk

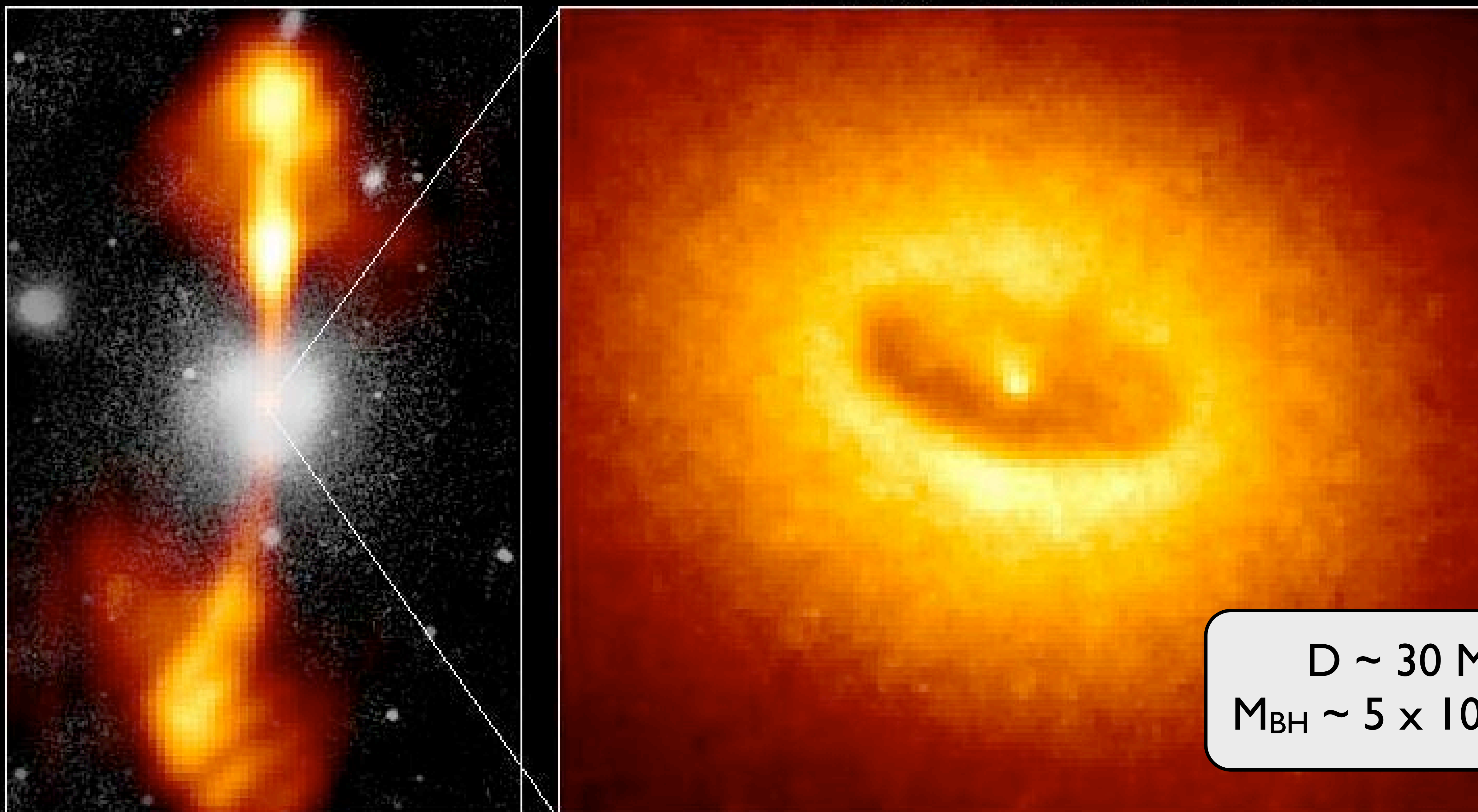

$D \sim 30$ Mpc

$M_{BH} \sim 5 \times 10^8\ M_{solar}$

380 Arc Seconds
88,000 LIGHT-YEARS

1.7 Arc Seconds
400 LIGHT-YEARS

Background radiation

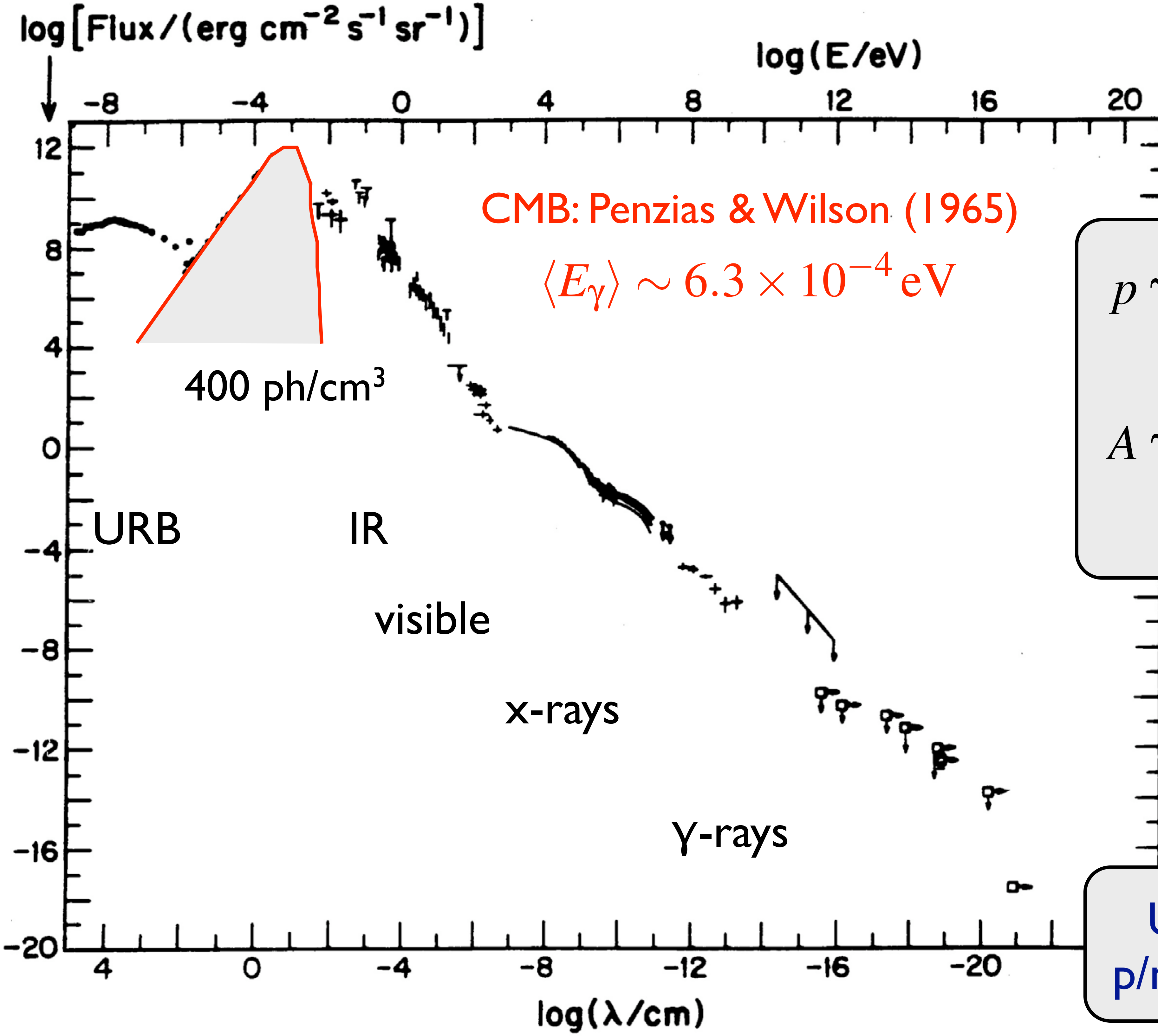

$$p\,\gamma_{CMB} \rightarrow p\,\pi^0$$
$$\rightarrow n\,\pi^+$$
$$A\,\gamma_{CMB} \rightarrow (A-1)\,N$$
$$\rightarrow (A-2)\,2N$$

Greisen, Zatsepin & Kuzmin (1966)

Universe opaque for p/n & nuclei E > 10^{20} eV

Energy loss due to propagation

Proton propagation

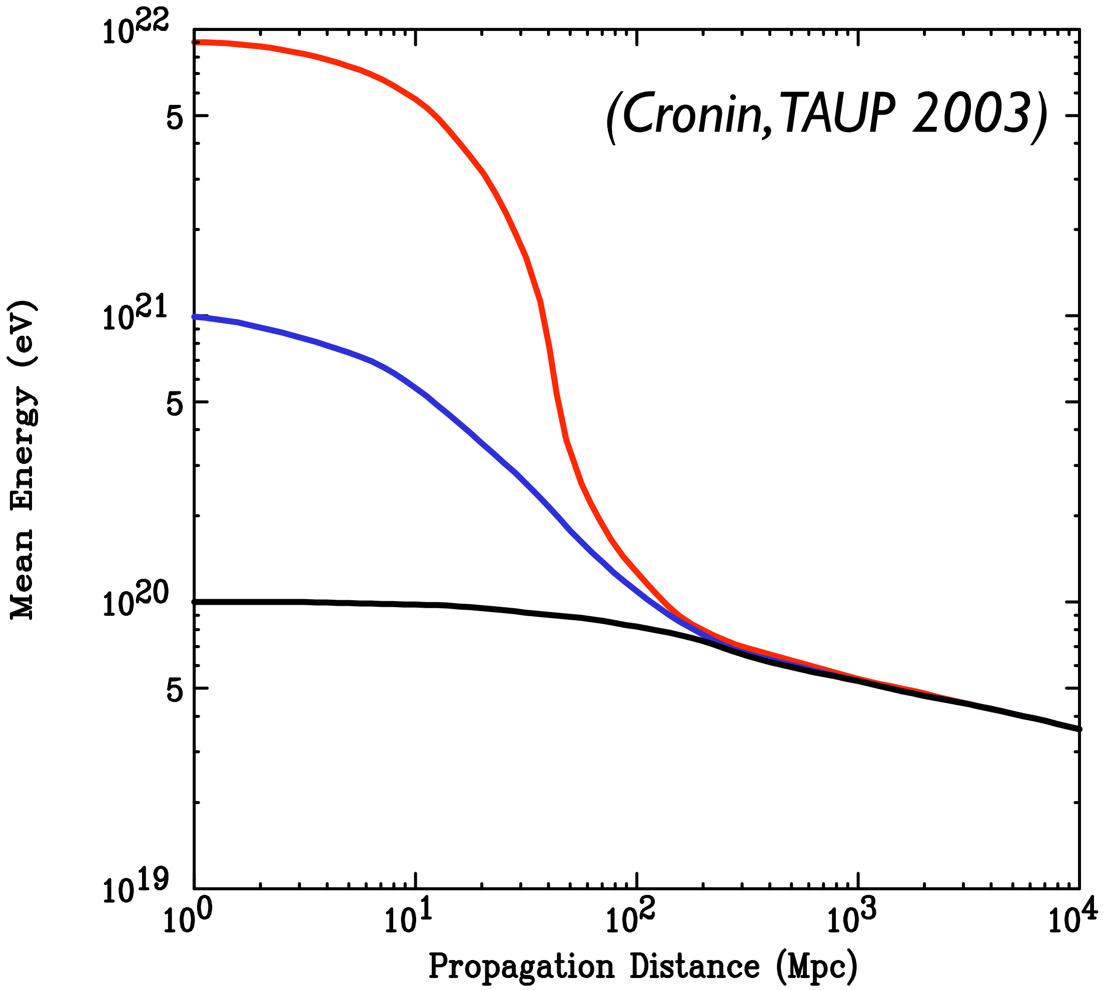

$$\frac{dE}{dl} = -\frac{E}{\chi_{Loss}}$$

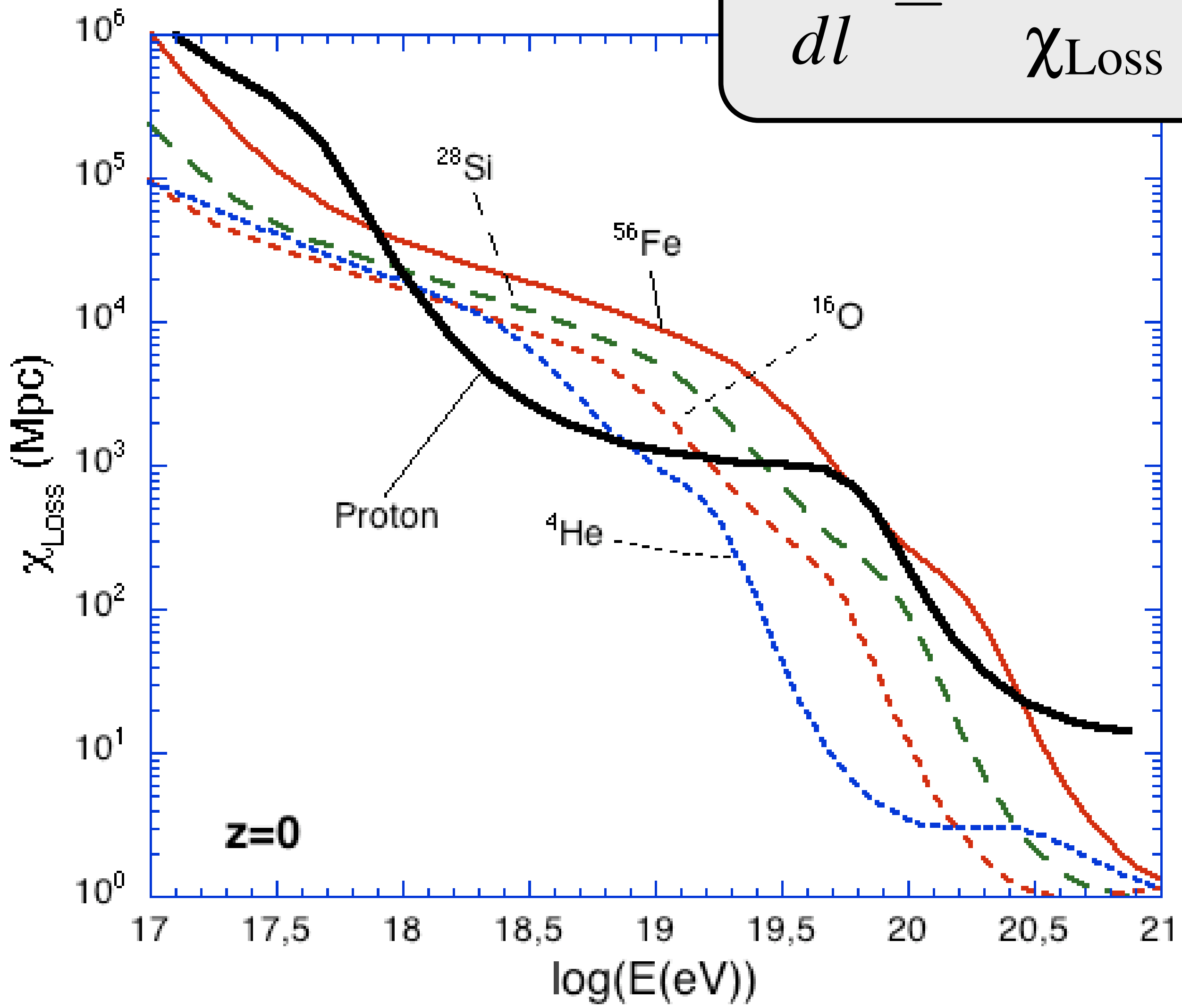

(Allard et al., JCAP 2006)

GZK suppression for all particles

Comparison AGASA vs. HiRes (E^3 scaled)

(AGASA, PRL 81,1998 & ICRC 2003)

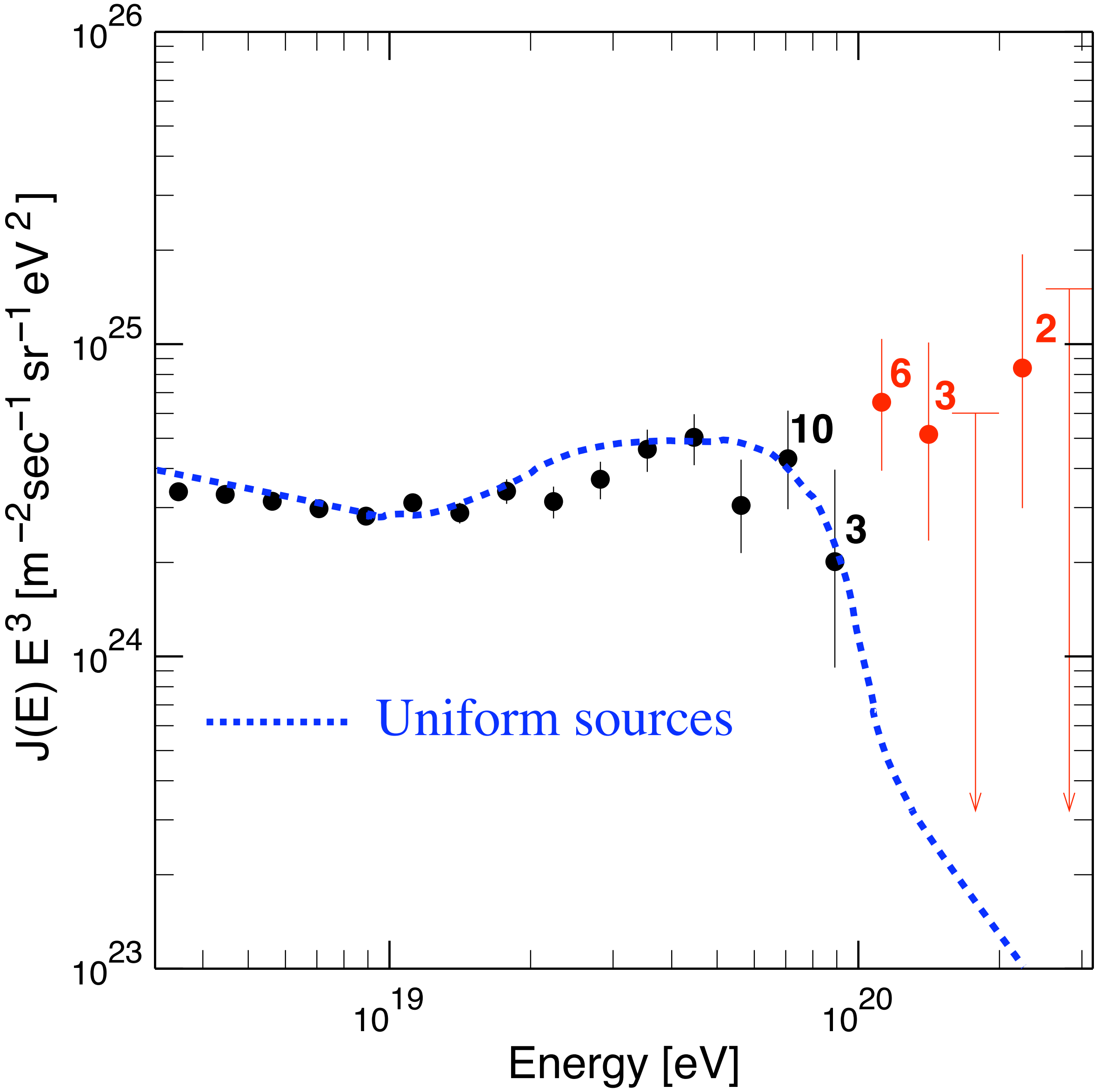

Inconsistent with Greisen-Zatsepin-Kuzmin (GZK) cutoff ?

(HiRes mono, PRL 92, 2004)

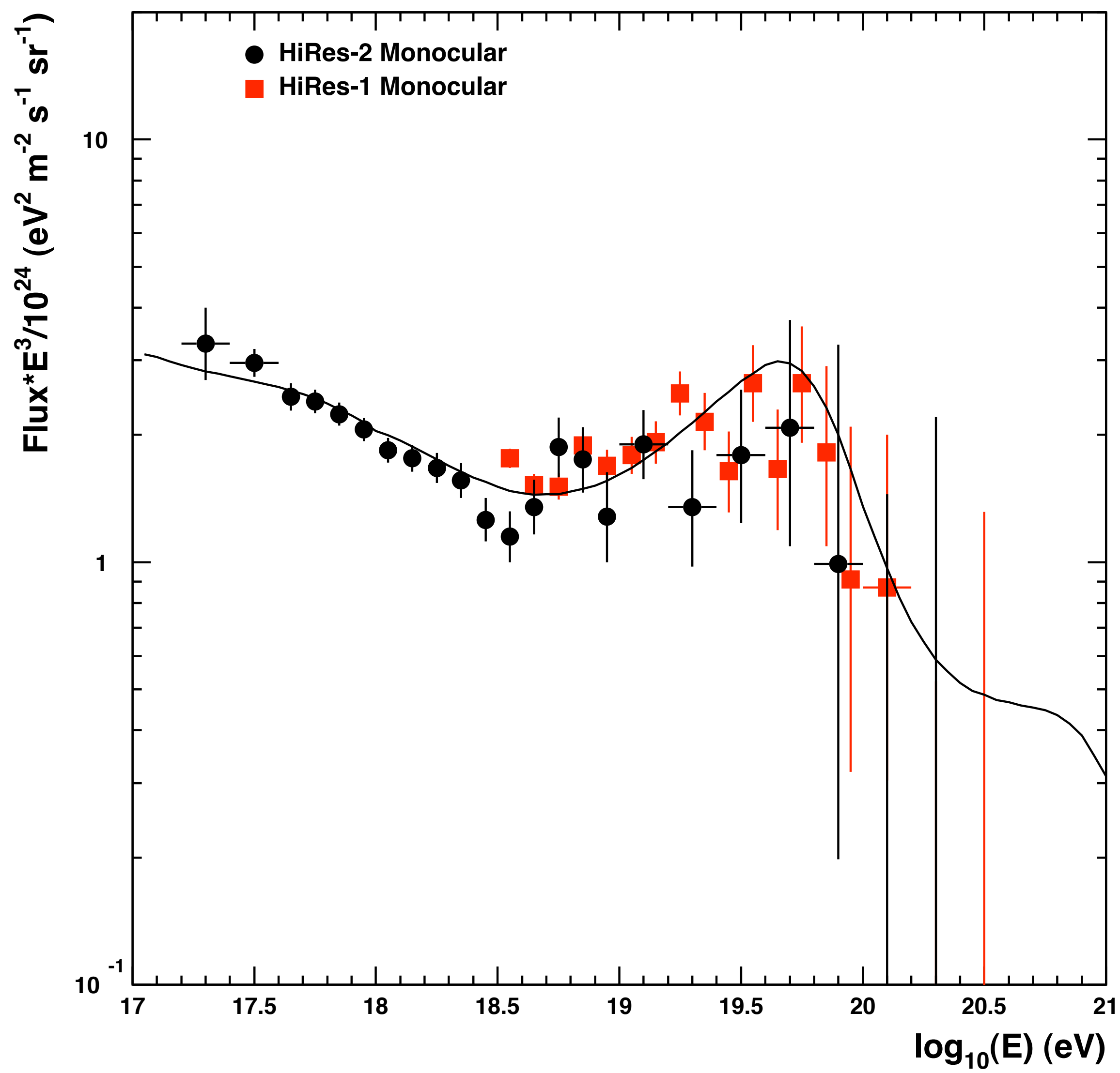

Consistent with GZK cutoff ?

Top-down source scenarios

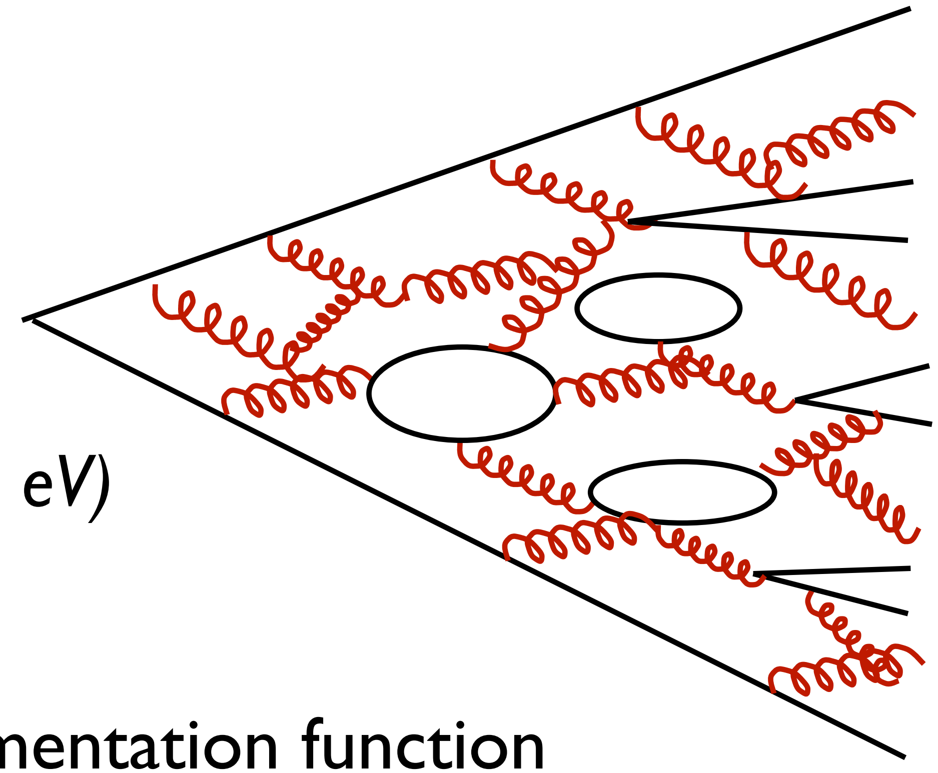

$(M_X \sim 10^{23} - 10^{24}$ eV$)$

Fragmentation function

$$\frac{dN_h}{dx} \sim x^{-3/2}(1-x)^2$$

X particles from:

- topological defects
- monopoles
- cosmic strings
- cosmic necklaces
- .....

QCD: ~ $E^{-1.5}$ energy spectrum

QCD+SUSY: ~ $E^{-1.9}$ spectrum

Top-down: SHDM flux predictions

(Aloisio, Berezinsky, Kachelrieß, 2004)

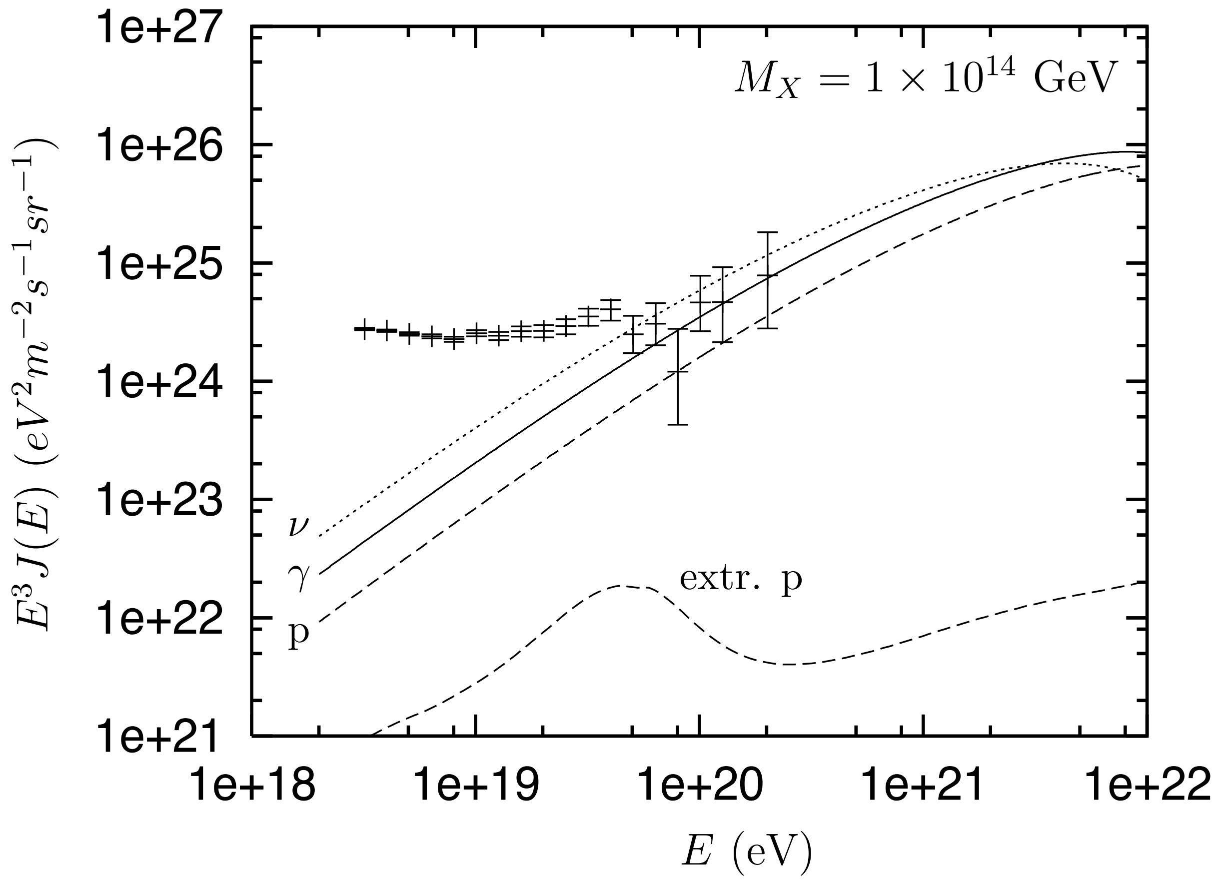

Model:

- 5×10^4 overdensity in halo
- lifetime 10^{17} - 10^{28} s

Comparison with AGASA data

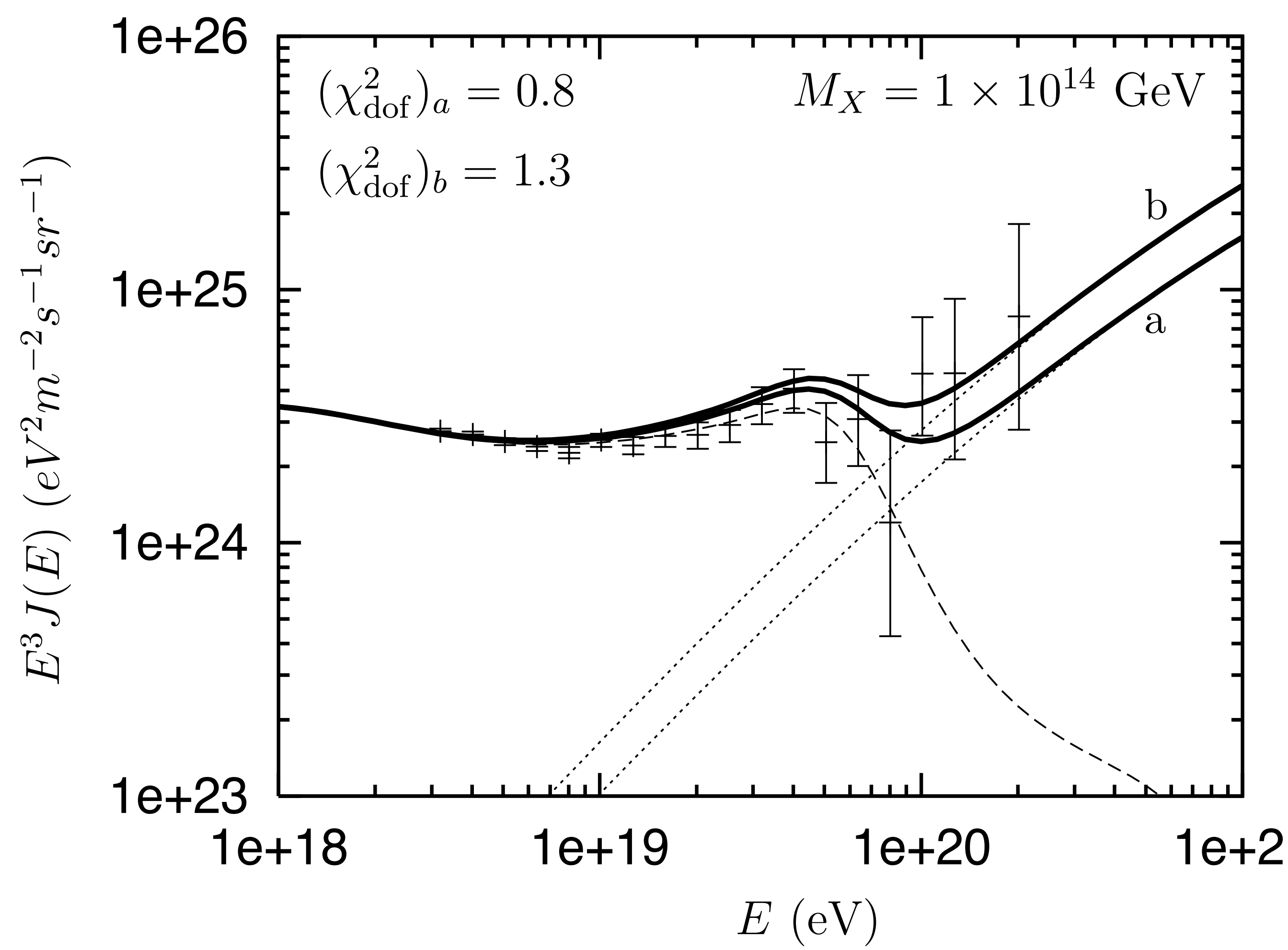

Predictions:

- no GZK cutoff
- large γ-ray and ν fluxes
- anisotropy (~ 10%)
- small-scale clustering (?)

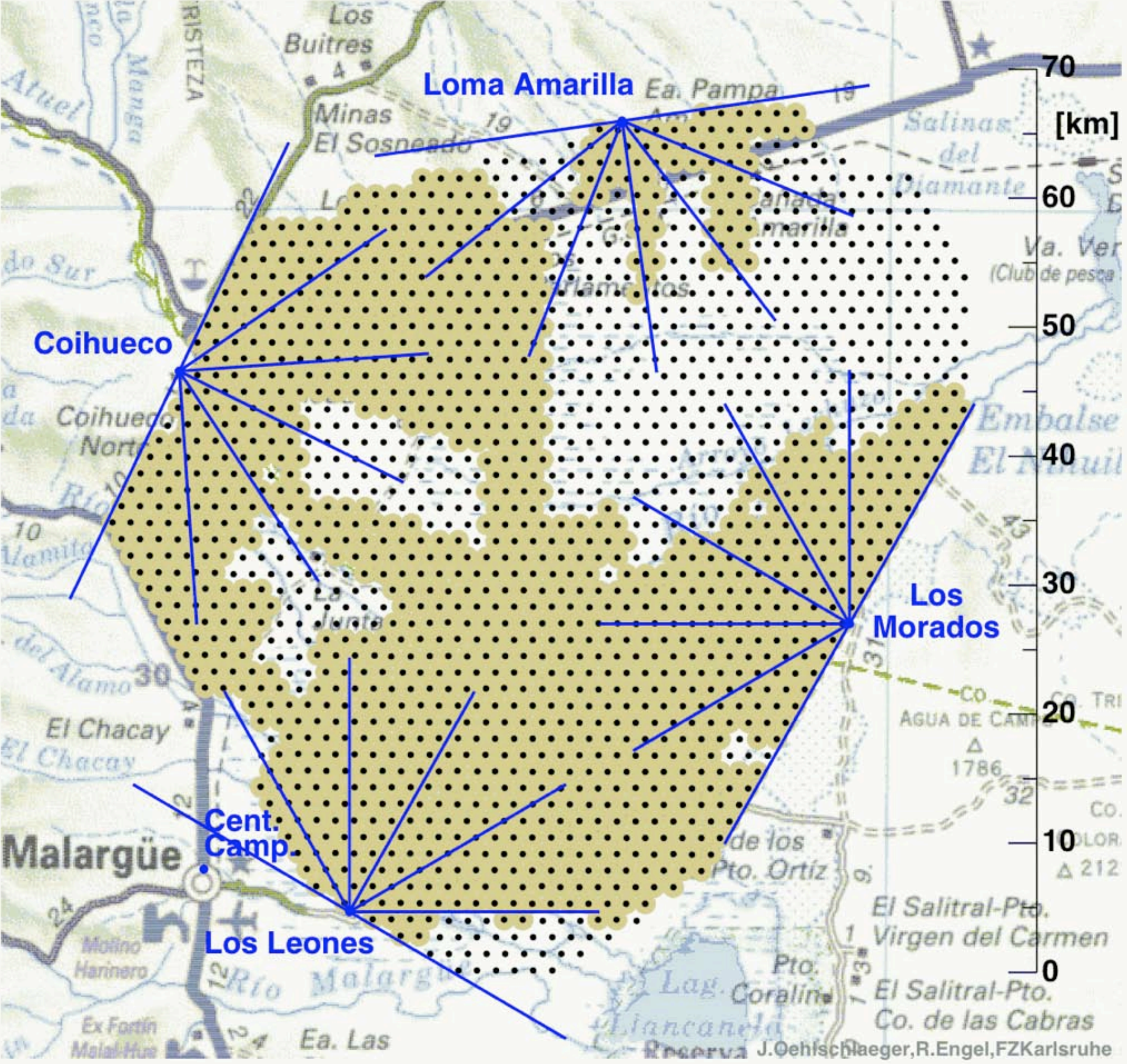

Southern Pierre Auger Observatory

Malargue, Argentina

Area ~3000 km^2,
1600 surface detectors,
24 telescopes

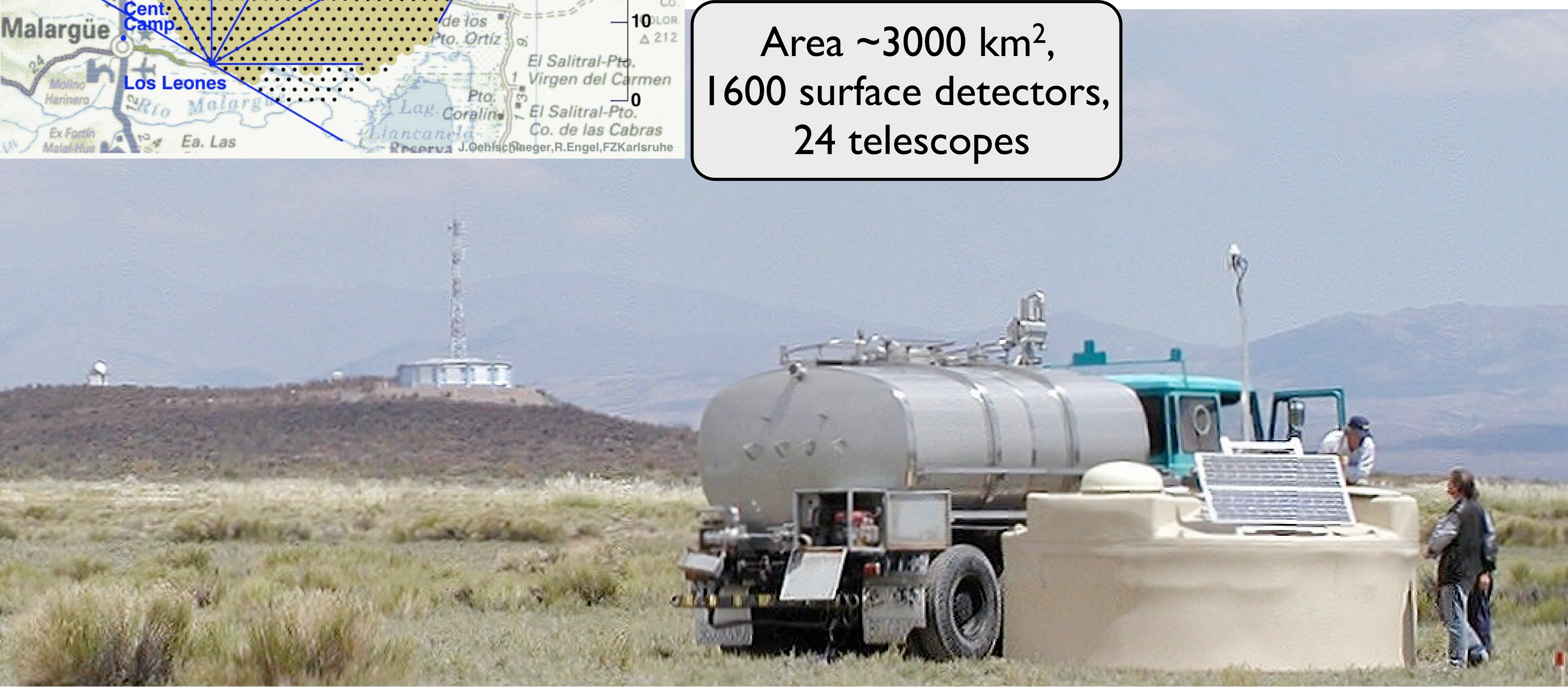

UHECRs and photoproduction

- **Propagation:**
  photoproduction at particle production threshold on nuclei up to Fe, photodissociation of nuclei

- **Acceleration:**
  photoproduction up to $\sqrt{s} \sim 100$ GeV on nuclei up to Fe, photodissociation of nuclei

- **Extensive air showers:**
  photoproduction up to $\sqrt{s} \sim 400.000$ GeV on light nuclei of atmosphere, muon production in photon-induced showers

Monte Carlo models needed for simulation even if no theory/phenomenology or data available

Simulation concepts: energy ranges

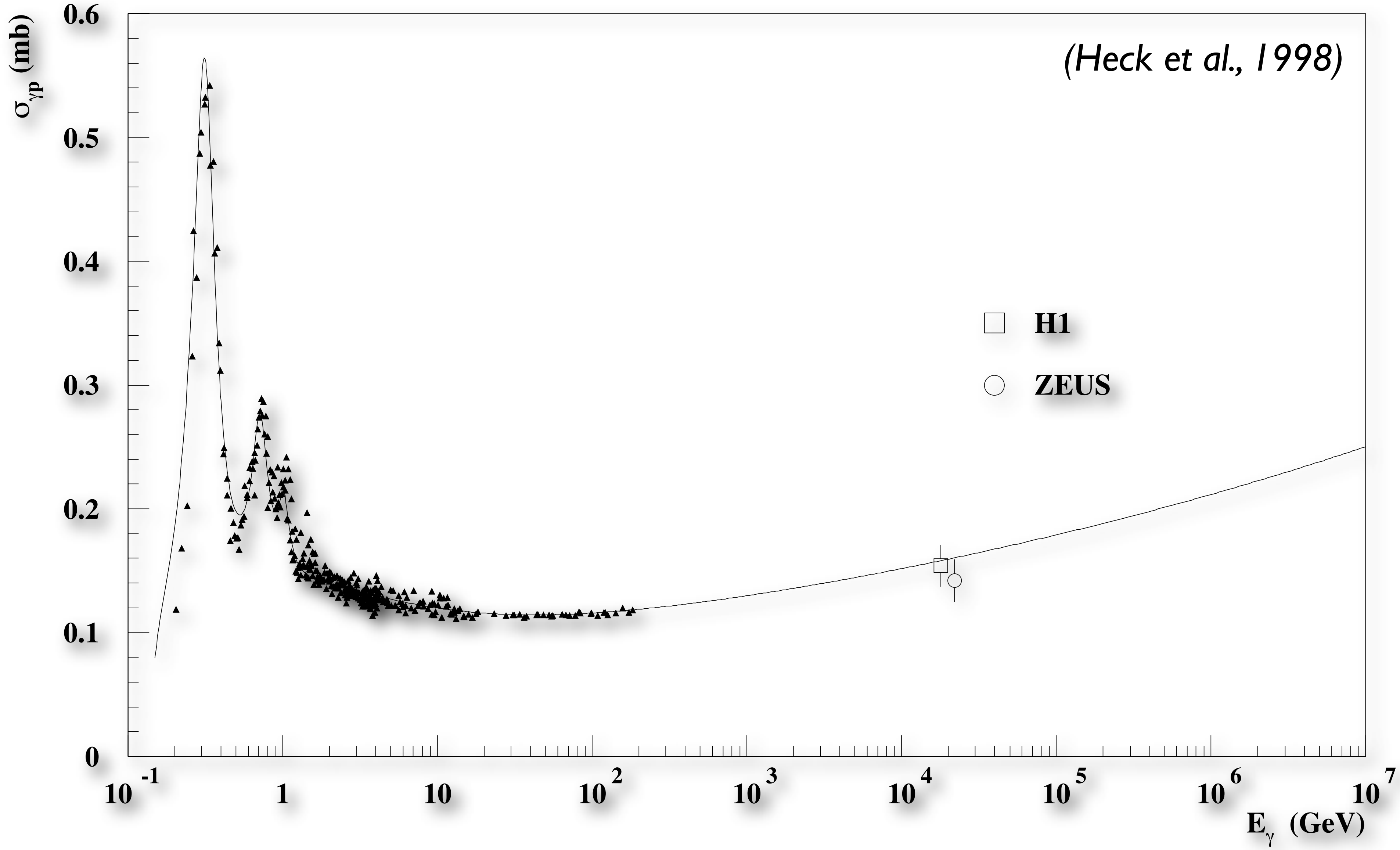

Resonances

Regge region

Parton region

???

Low energy region
(resonances)

Example: Monte Carlo code SOPHIA

SOPHIA (Mücke et al. CPC124, 2000)

Direct pion production

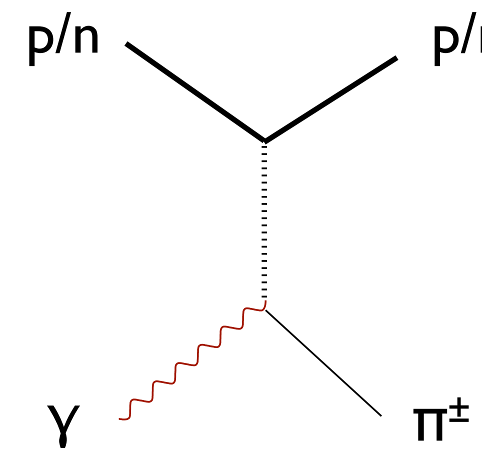

Resonance production
(s channel)

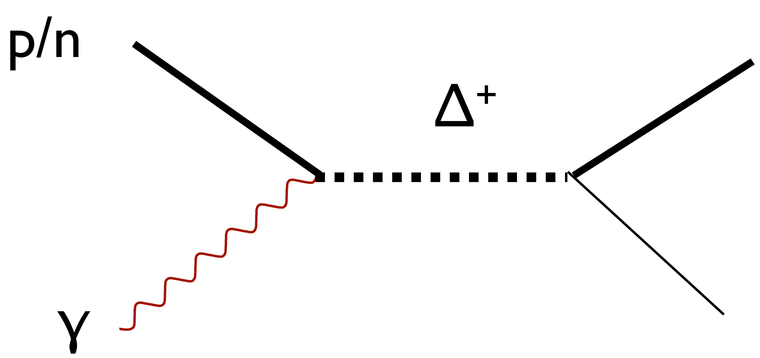

$$\sigma_{\mathrm{bw}}(s;M,\Gamma,J)=\frac{s}{(s-m_{\mathrm{N}}^2)^2}\,\frac{4\pi b_\gamma(2J+1)s\Gamma^2}{(s-M^2)^2+s\Gamma^2}$$

Multiparticle production

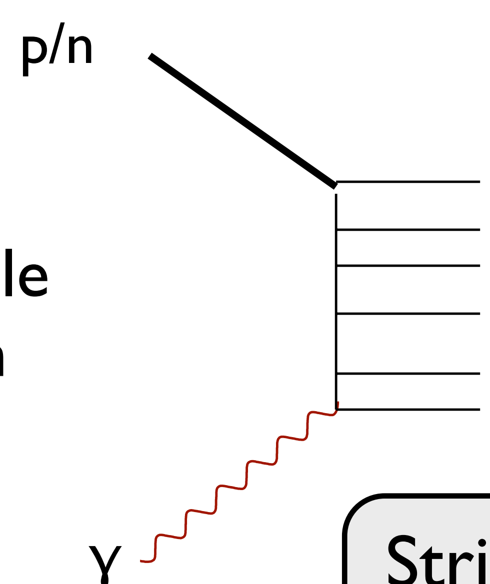

String model

Elastic scattering

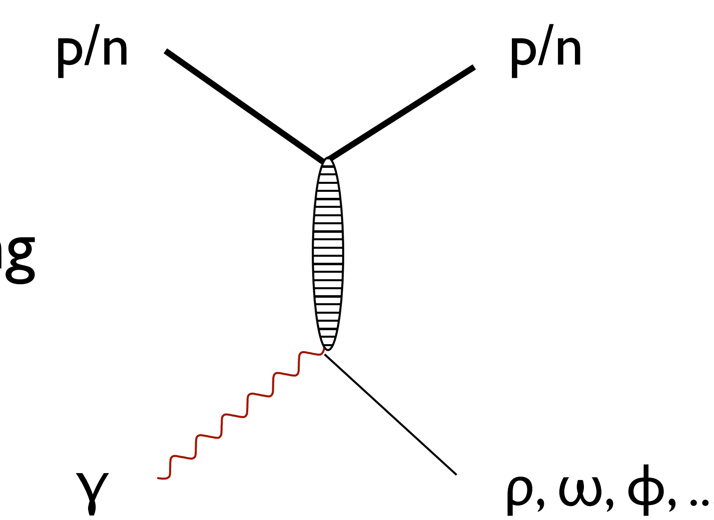

Description of total cross section

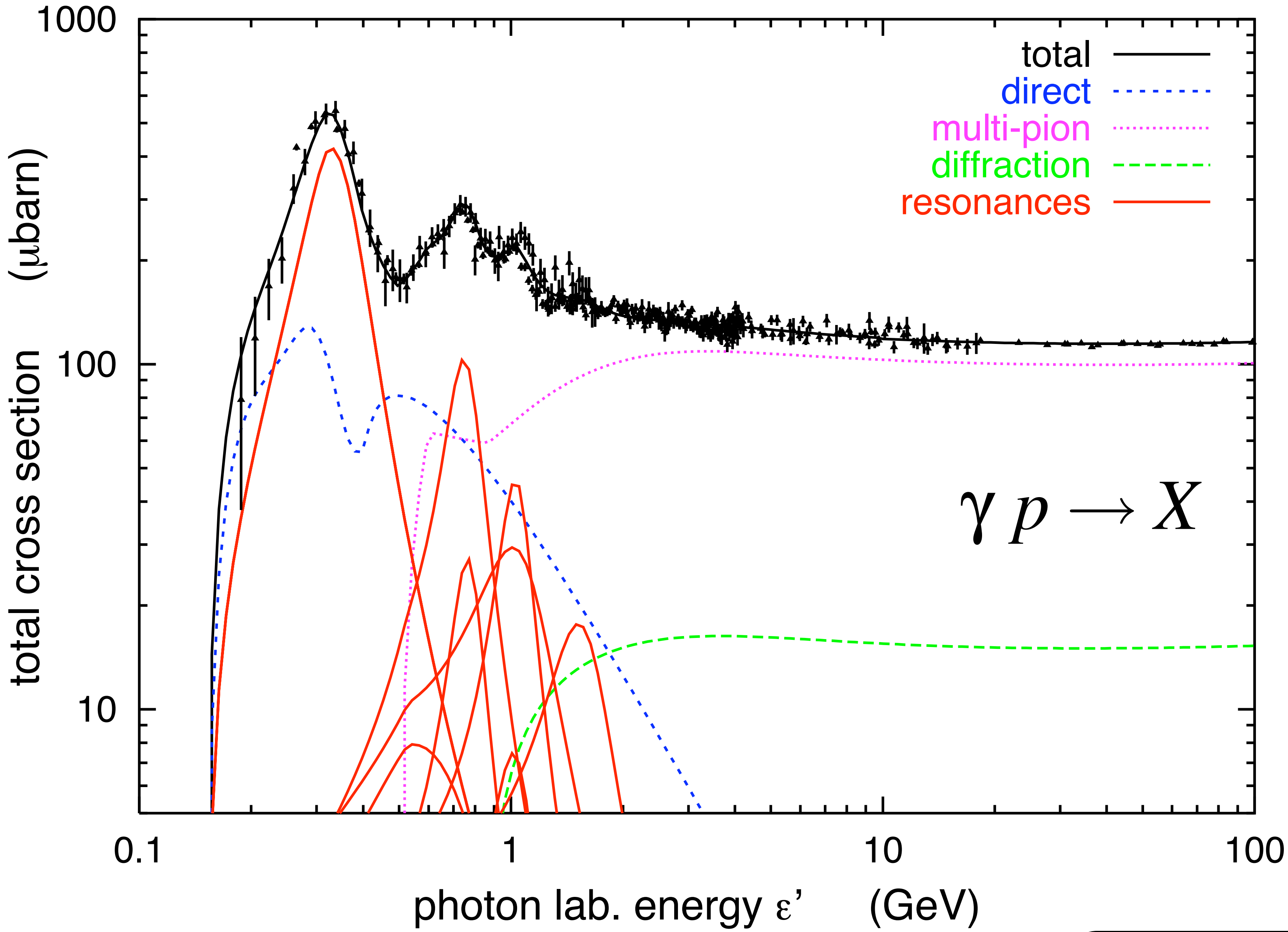

- PDG: 9 resonances, decay channels, angular distributions
- Regge parametrization at higher energy
- Direct contribution: fit to difference to data

Many measurements available, still approximations necessary

SOPHIA (Mücke et al. CPC124, 2000)

Description of final states

Baryon resonances and their physical parameters implemented in SOPHIA (see text). Superscripts $^+$ and ^{0} in the parameters refer to $p\gamma$ and $n\gamma$ excitations, respectively. The maximum cross section, $\sigma_{\max} = 4m_N^2 M^2 \sigma_0/(M^2 - m_N^2)^2$, is also given for reference

Resonance	M	Γ	$10^3 b_\gamma^+$	σ_0^+	$\sigma_{\max}^+$	$10^3 b_\gamma^0$	σ_0^0	$\sigma_{\max}^0$
$\Delta(1232)$	1.231	0.11	5.6	31.125	411.988	6.1	33.809	452.226
$N(1440)$	1.440	0.35	0.5	1.389	7.124	0.3	0.831	4.292
$N(1520)$	1.515	0.11	4.6	25.567	103.240	4.0	22.170	90.082
$N(1535)$	1.525	0.10	2.5	6.948	27.244	2.5	6.928	27.334
$N(1650)$	1.675	0.16	1.0	2.779	7.408	0.0	0.000	0.000
$N(1675)$	1.675	0.15	0.0	0.000	0.000	0.2	1.663	4.457
$N(1680)$	1.680	0.125	2.1	17.508	46.143	0.0	0.000	0.000
$\Delta(1700)$	1.690	0.29	2.0	11.116	28.644	2.0	11.085	28.714
$\Delta(1905)$	1.895	0.35	0.2	1.667	2.869	0.2	1.663	2.875
$\Delta(1950)$	1.950	0.30	1.0	11.116	17.433	1.0	11.085	17.462

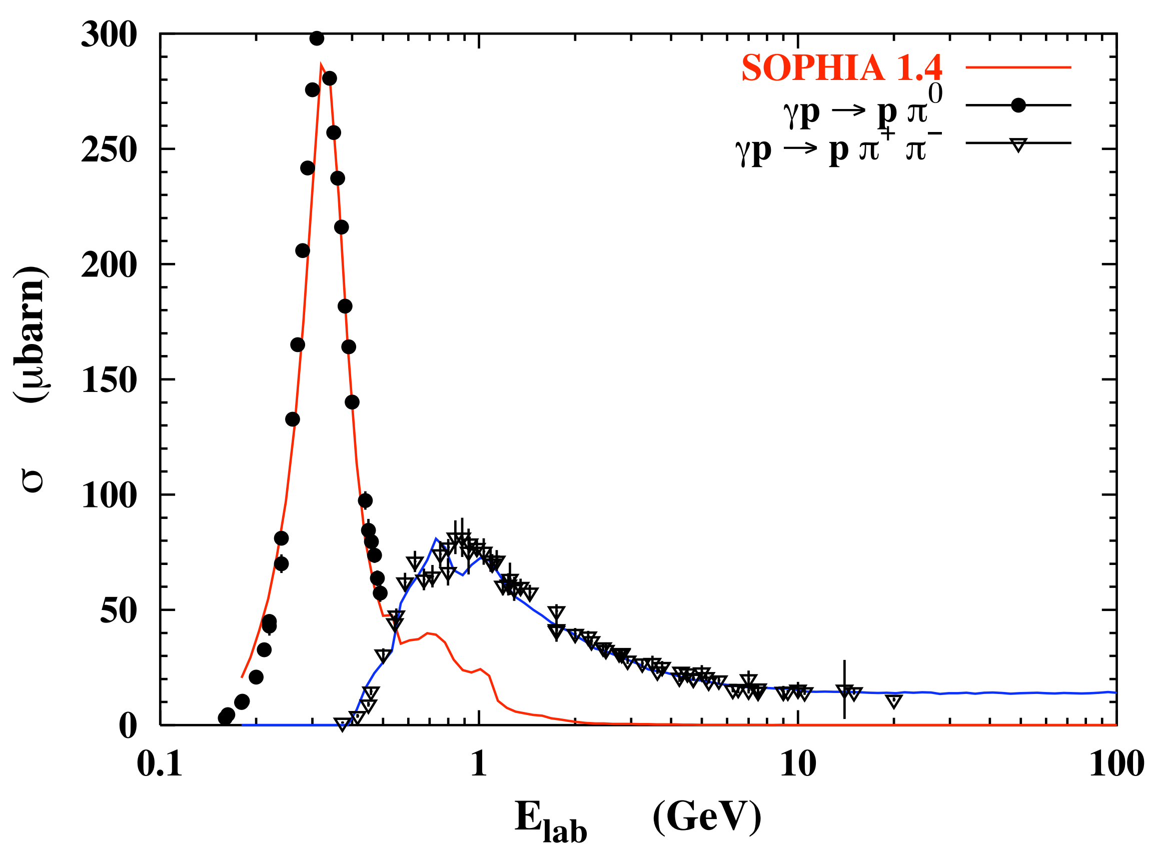

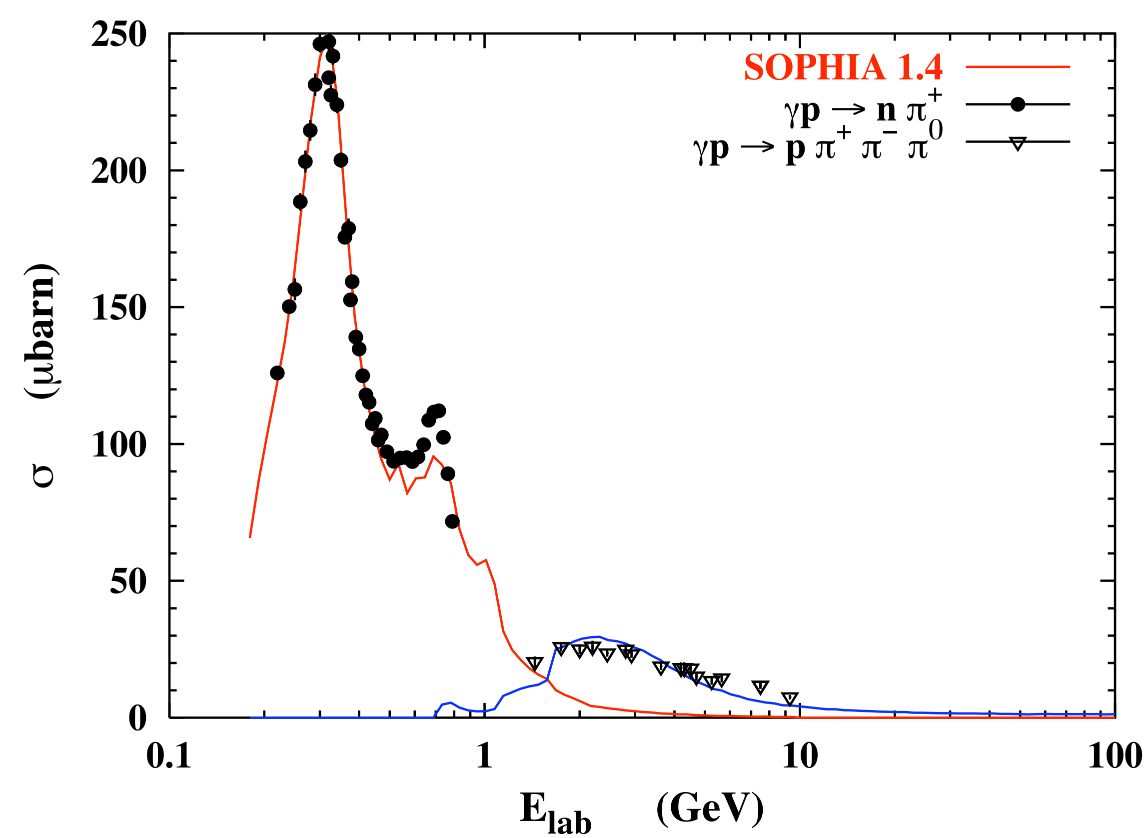

Example: INC Monte Carlo model

(Ilinov, Pshenichnov et al., NPA616, 1997)

Decay channels of 6 baryon resonances and multiparticle channels

Explicit generation of kinematics of multiparticle final states (isobar model)

Interaction with nuclei, used in RELDIS

Others:
PEANUT (FLUKA)

Channels of elementary γN interactions taken into account in the INC model

γp-interaction	γn-interaction
$\gamma p \to \pi^+ n$	$\gamma n \to \pi^- p$
$\gamma p \to \pi^0 p$	$\gamma n \to \pi^0 n$
$\gamma p \to \pi^- \Delta^{++}$	$\gamma n \to \pi^- \Delta^+$
$\gamma p \to \pi^0 \Delta^+$	$\gamma n \to \pi^0 \Delta^0$
$\gamma p \to \pi^+ \Delta^0$	$\gamma n \to \pi^+ \Delta^-$
$\gamma p \to \eta p$	$\gamma n \to \eta n$
$\gamma p \to \omega p$	$\gamma n \to \omega n$
$\gamma p \to \rho^0 p$	$\gamma n \to \rho^0 n$
$\gamma p \to \rho^+ n$	$\gamma n \to \rho^- p$
$\gamma p \to \pi^+ \pi^- p$	$\gamma n \to \pi^+ \pi^- n$
$\gamma p \to \pi^0 \pi^+ n$	$\gamma n \to \pi^0 \pi^- p$
$\gamma p \to \pi^0 \pi^0 \pi^0 p$	$\gamma n \to \pi^0 \pi^0 \pi^0 n$
$\gamma p \to \pi^+ \pi^- \pi^0 p$	$\gamma n \to \pi^+ \pi^- \pi^0 n$
$\gamma p \to \pi^+ \pi^0 \pi^0 n$	$\gamma n \to \pi^- \pi^0 \pi^0 p$
$\gamma p \to \pi^+ \pi^+ \pi^- n$	$\gamma n \to \pi^+ \pi^- \pi^- p$
$\gamma p \to i\pi N$ $(4 \leqslant i \leqslant 8)$ (35 channels)	$\gamma n \to i\pi N$ $(4 \leqslant i \leqslant 8)$ (35 channels)

INC: Description of final states

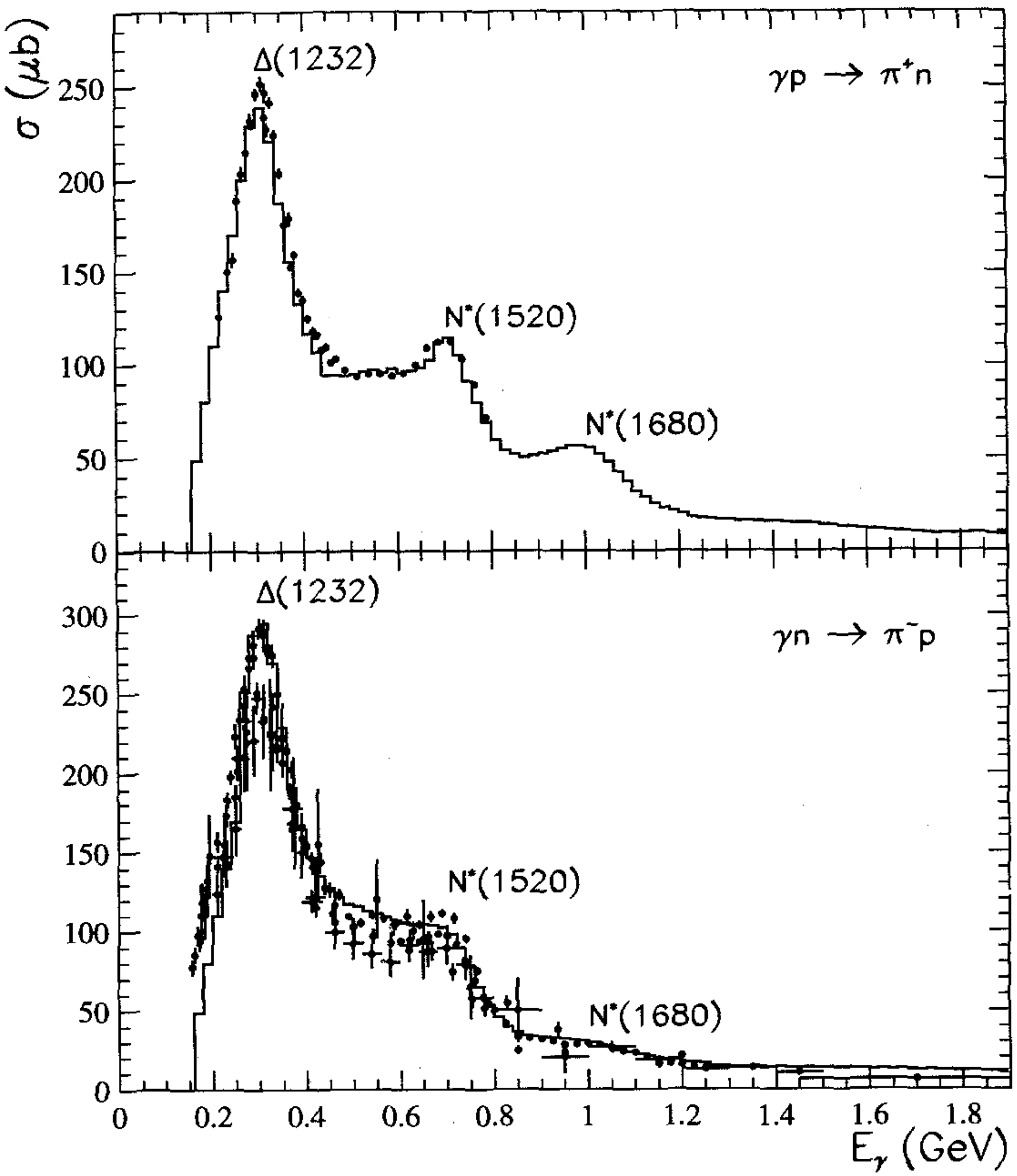

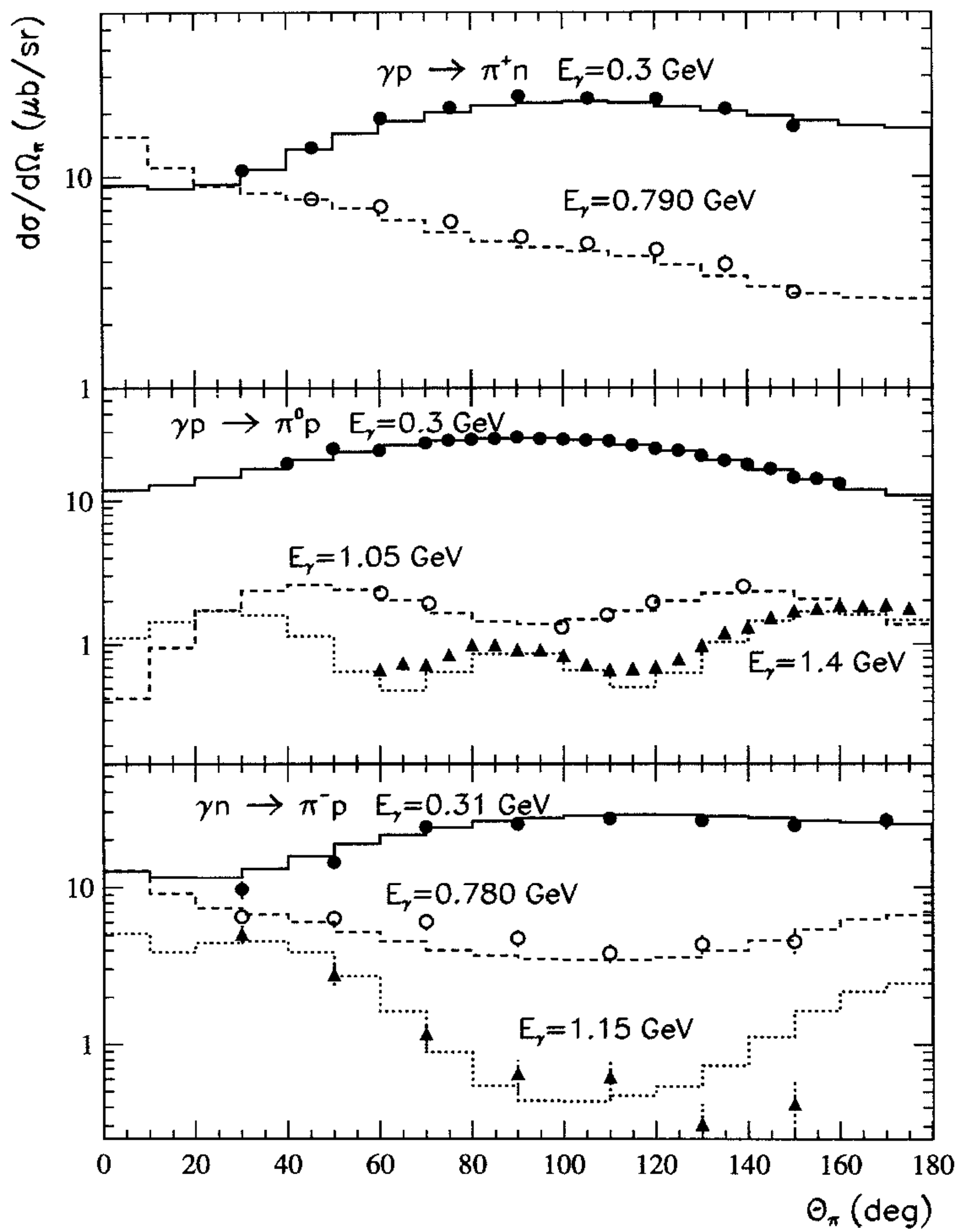

(Ilinov, Pshenichnov et al., NPA616, 1997)

Interaction with nuclei

Purely electromagnetic excitations:

- $E_\gamma \leq 20$ MeV: E and M transitions, Giant Dipole resonance, selection according to quantum numbers
- $50 \leq E_\gamma \leq 150$ MeV: mainly photon absorption by p and p-n pair
- evaporation: neutron, quasi-deuteron and alpha-particle emission

Hadronic interactions (particle production):

- $150 \leq E_\gamma \leq$ few GeV: single nucleon absorption of photon
- intra-nuclear cascade of secondaries (formation time)
- evaporation, fission, multifragmentation

Available code packages

- RELDIS (RElativistic ELectromagnetic DISsociation) *I. Pshenichnov*
- FLUKA (FLUktuierende KAskade) *A. Ferrari et al. & G.I. Smirnov*

Effective em. dissociation cross section

Product of equivalent photon flux dn/dE_γ and cross section for dissociation

Simulation with RELDIS

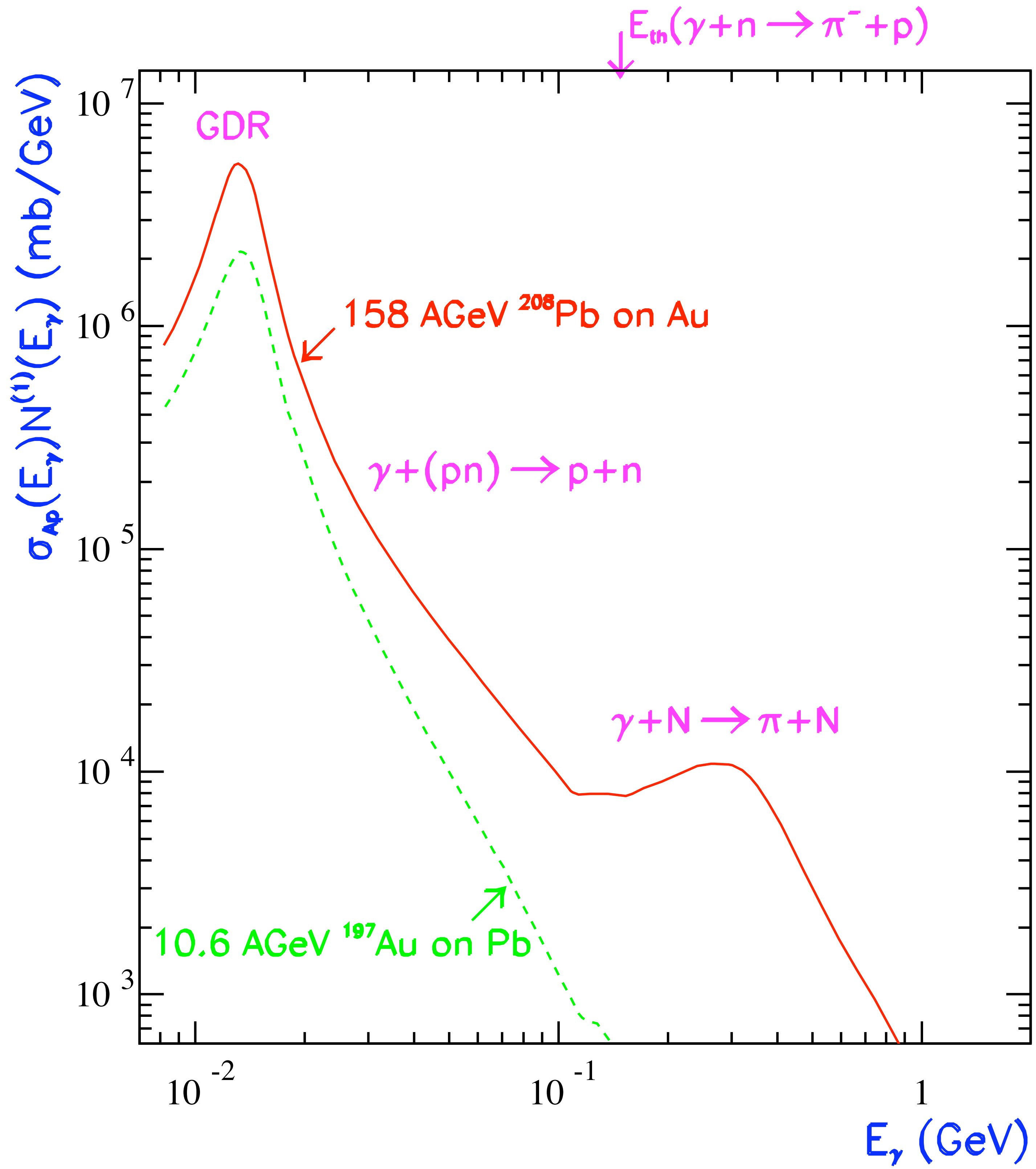

(Pshenichnov 2002)

Example: photo-dissociation of nuclei

Saclay & Livermore data

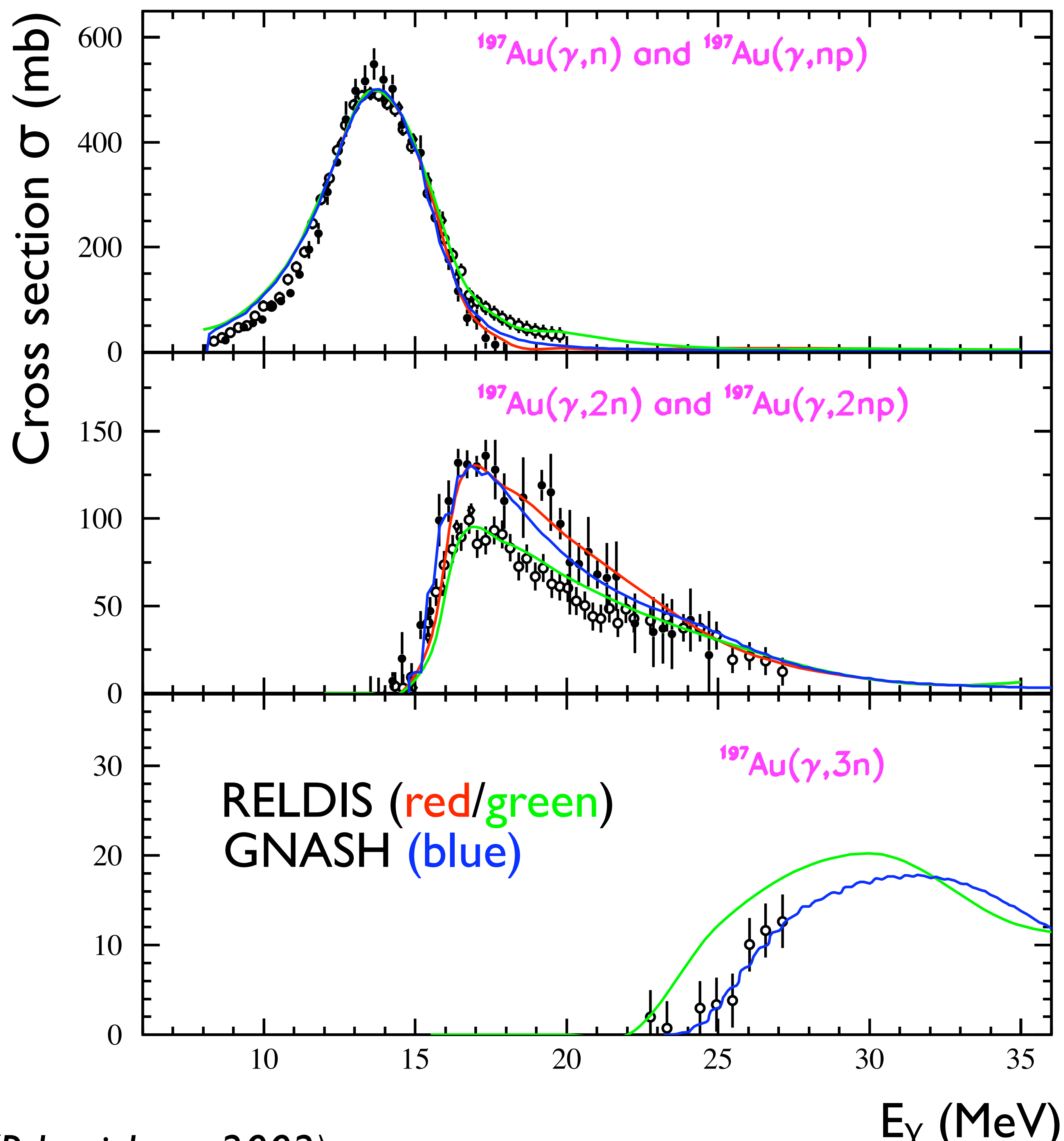

(Pshenichnov 2002)

Projectile: 30 AGeV Pb, different targets

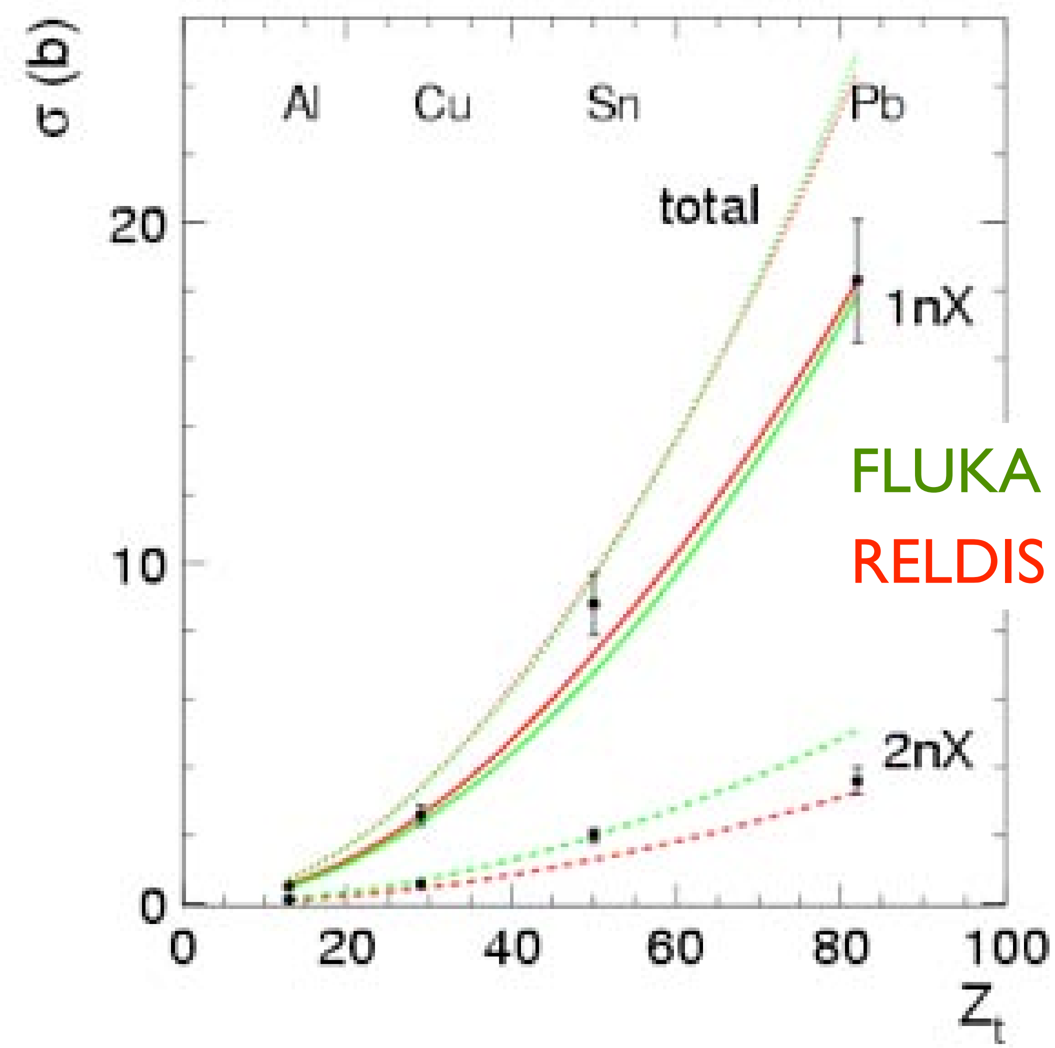

(Smirnov, 2005)

Intermediate energy region
(Reggeons, topologies)

Vector meson dominance model

Lifetime of hadronic fluctuation of real photon

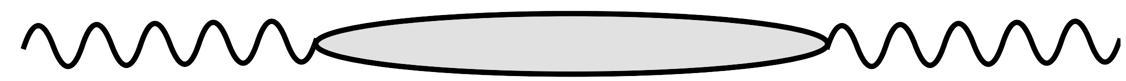

$$t_{\text{fluc}} \sim 1/\Delta E \sim \frac{2k_\gamma}{M^2+Q^2}$$

Approximation (low energy):

$$A^{(T)}_{\gamma h\to X}(s,t,q^2,\dots) = \sum_{V=\rho,\omega,\phi}\left(\frac{e}{f_V}\right)\frac{m_V^2}{m_V^2-q^2-i\Gamma_V m_V}\,A^{(T)}_{Vh\to X}(s,t,\dots)$$

$$A^{(L)}_{\gamma h\to X}(s,t,q^2,\dots) = \sum_{V=\rho,\omega,\phi}\left(\frac{e}{f_V}\right)\left(\frac{-q^2\xi_V}{m_V^2}\right)^{\frac{1}{2}}\frac{m_V^2}{m_V^2-q^2-i\Gamma_V m_V}\,A^{(T)}_{Vh\to X}(s,t,\dots)$$

$$\frac{e^2}{f_\rho^2}\approx 0.0036,\quad \frac{e^2}{f_\omega^2}\approx 0.00031,\quad \frac{e^2}{f_\phi^2}\approx 0.00055$$

Very successful at low Q^2

Generalized vector dominance model

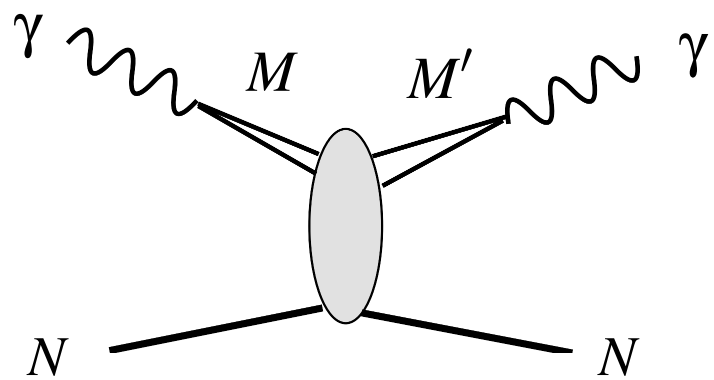

- Sum over all hadronic states
- Non-diagonal terms
- Many parameters (assumptions needed)

Neglecting off-diagonal transitions:

$$D(M^2) = \frac{R_{e^+e^-}(M^2)}{12\pi^2 M^2}$$

$$\sigma_{\gamma^\star N}(s,Q^2) = 4\pi\alpha_{\rm em}\int_{M_0^2}^{M_1^2} dM^2 D(M^2)\left(\frac{M^2}{M^2+Q^2}\right)^2\left(1+\epsilon\frac{Q^2}{M^2}\right)\sigma_{VN}(s,Q^2,M^2)$$

$$\sigma_{VN}(s,Q^2,M^2) = \frac{\widetilde{\sigma}_{VN}(s,Q^2)}{M^2+Q^2+C^2}$$

(RE, Ranft, Roesler, PRD55, 1997)

Confinement: color flow topologies

Partons only asymptotically free !

Example:
meson propagation

time →

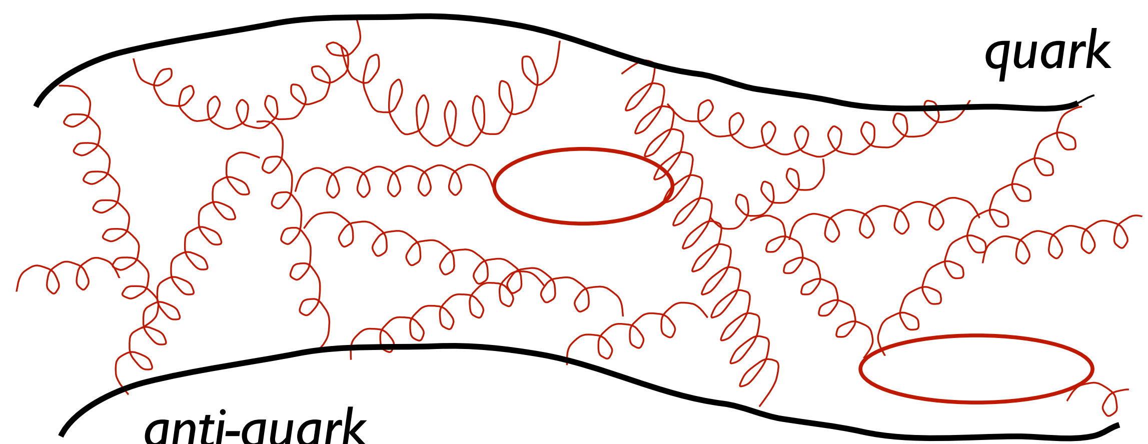

Scattering process:

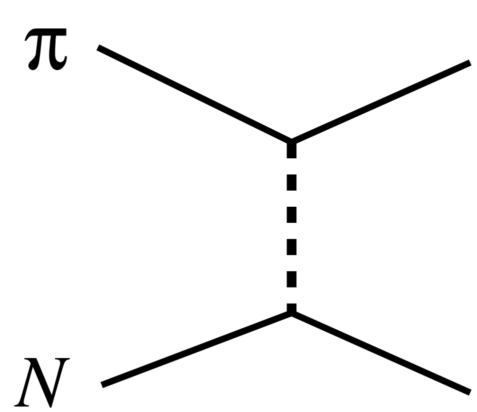

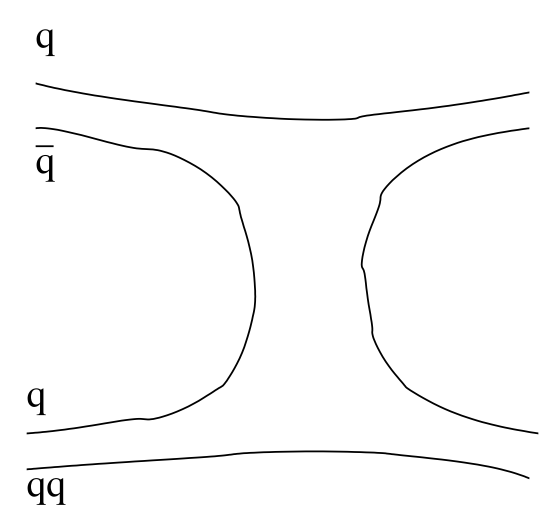

(´t Hooft, Veneziano, Witten, ... 1974)

Unitarity cuts (optical theorem)

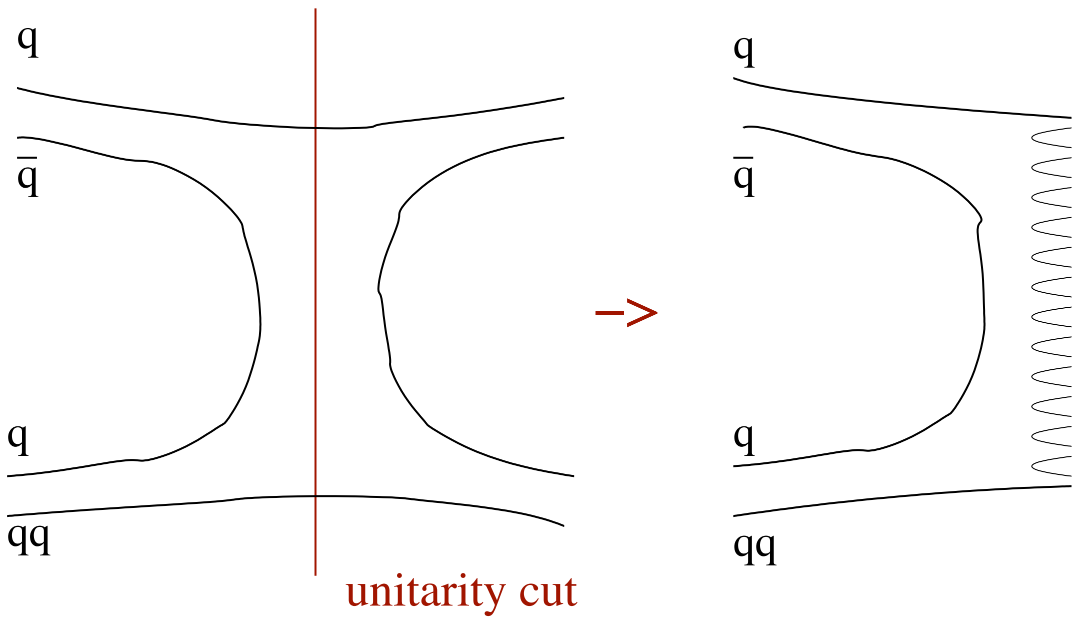

(Capella et al. PR 1994, Kaidalov et al.)

Unitarity cut of Reggeon exchange: chain of hadrons

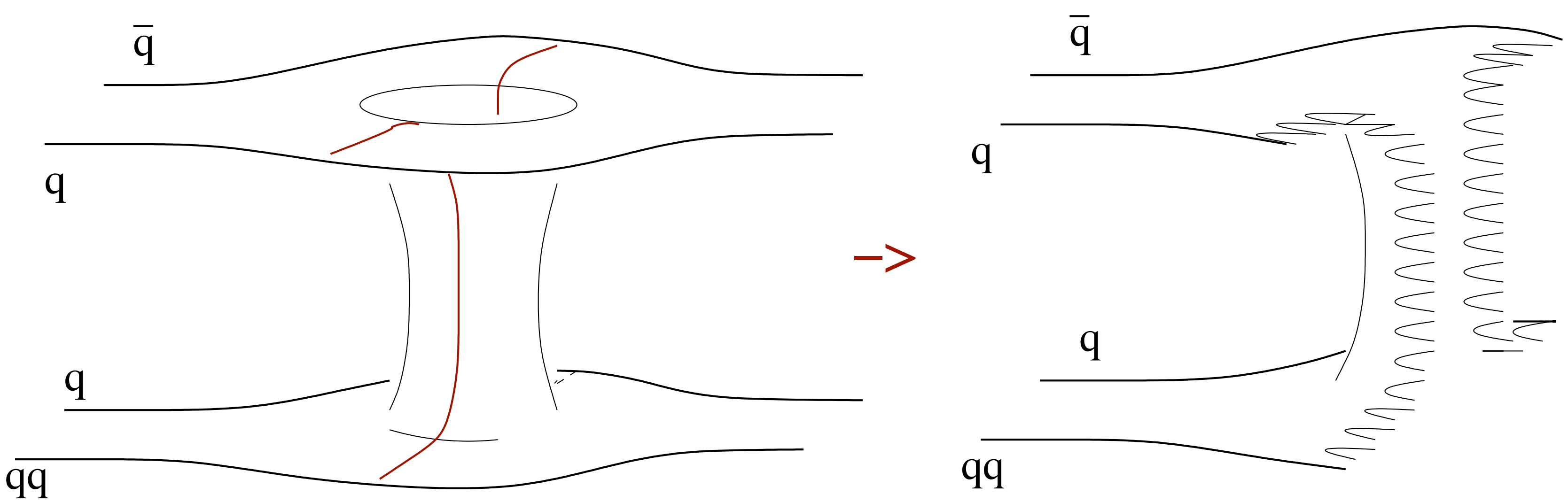

Pomeron exchange: two strings of hadrons

Splitting functions (Regge asymptotics)

$$f_{\mathrm{nuc}}^{\mathrm{DPM}}(x) \sim x_q^{-1/2}(1-x_q)^{3/2}$$

$$f_{\mathrm{mes}}^{\mathrm{DPM}}(x) \sim x_q^{-1/2}(1-x_q)^{1/2}$$

Fragmentation & two-string model

Example:
q-qbar pair produced
in e^+e^- annihilation

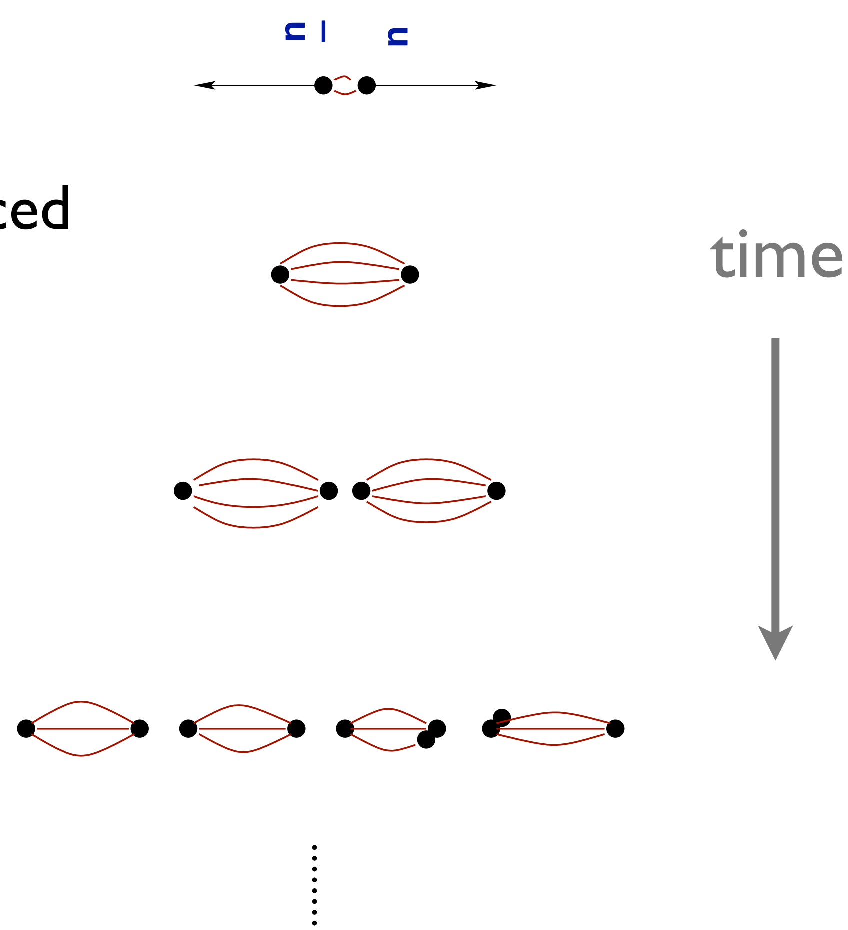

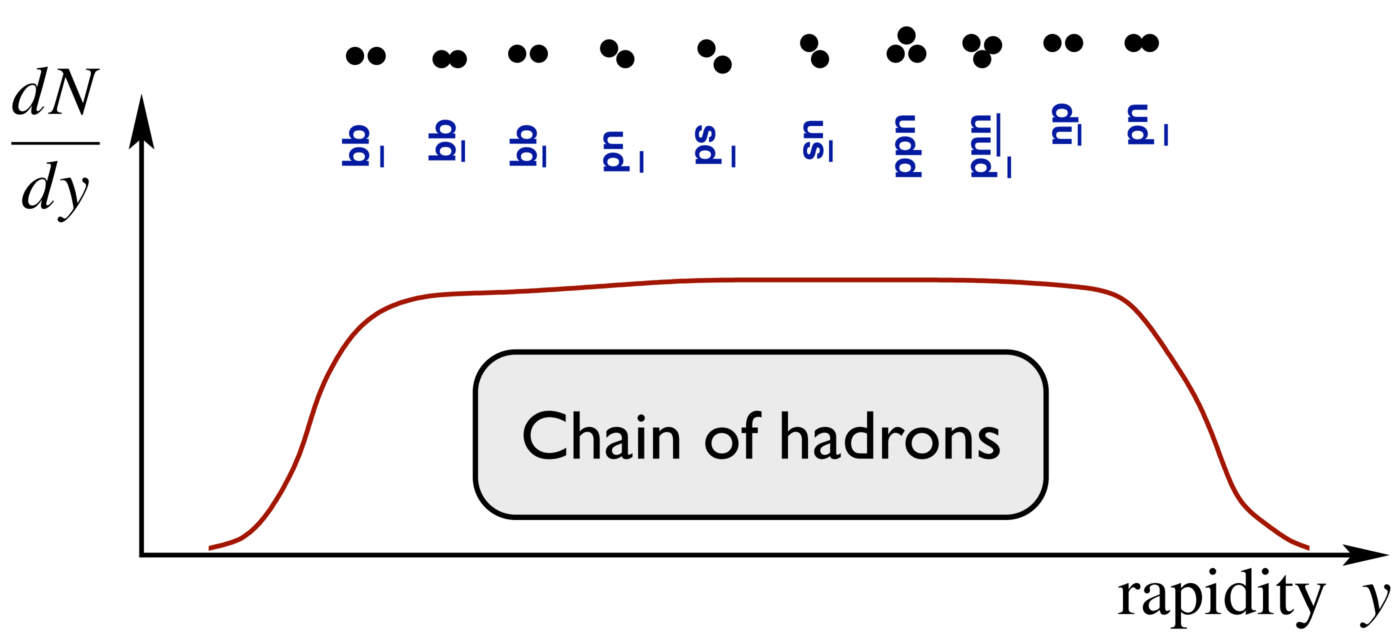

Most important final
state topology

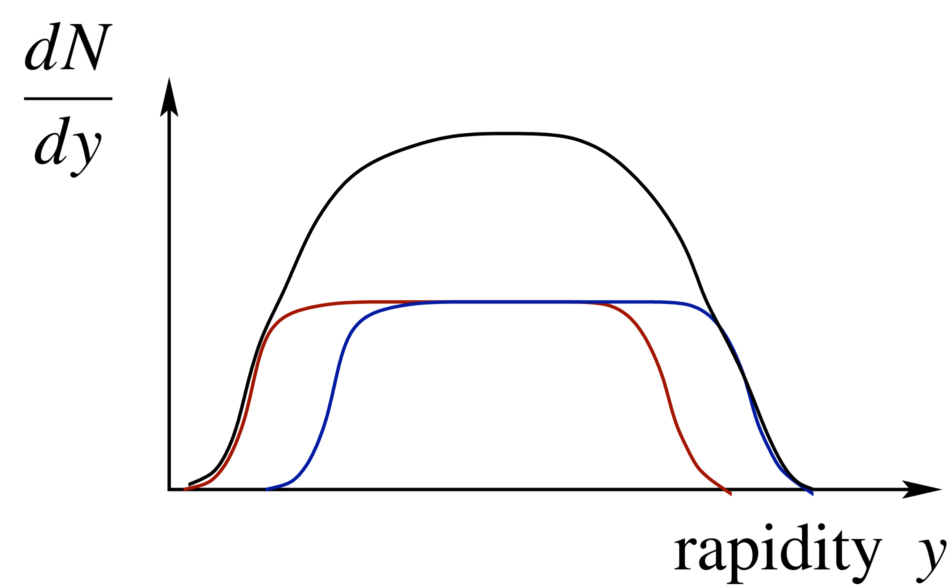

PHOJET (RE, Ranft)
DPMJET (Roesler, RE, Ranft)

PYTHIA (Sjöstrand)

NA22 European Hybrid Spectrometer data

(Roesler, 2006)

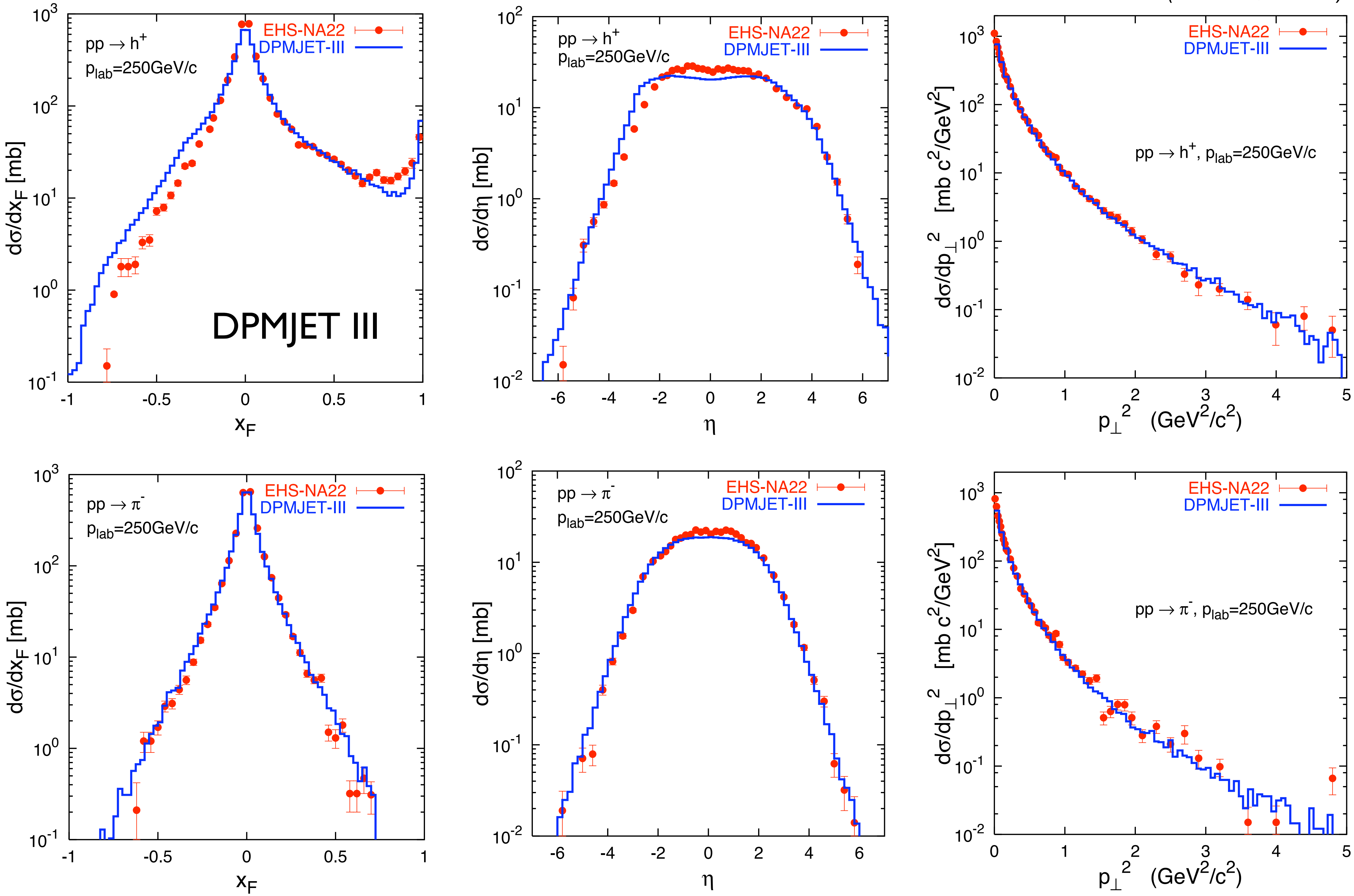

Multiplicity at low energy

DPMJET in p-p mode:
simulation of particle production from energy threshold on

proton - proton, $E_{lab} = 200\text{GeV}$

	Exp.	DPMJET-III
charged	7.69 ± 0.06	7.64
neg.	2.85 ± 0.03	2.82
p	1.34 ± 0.15	1.26
n	0.61 ± 0.30	0.66
π^+	3.22 ± 0.12	3.20
π^-	2.62 ± 0.06	2.55
K^+	0.28 ± 0.06	0.30
K^-	0.18 ± 0.05	0.20
Λ	0.096 ± 0.01	0.10
$\bar{\Lambda}$	0.0136 ± 0.004	0.0105

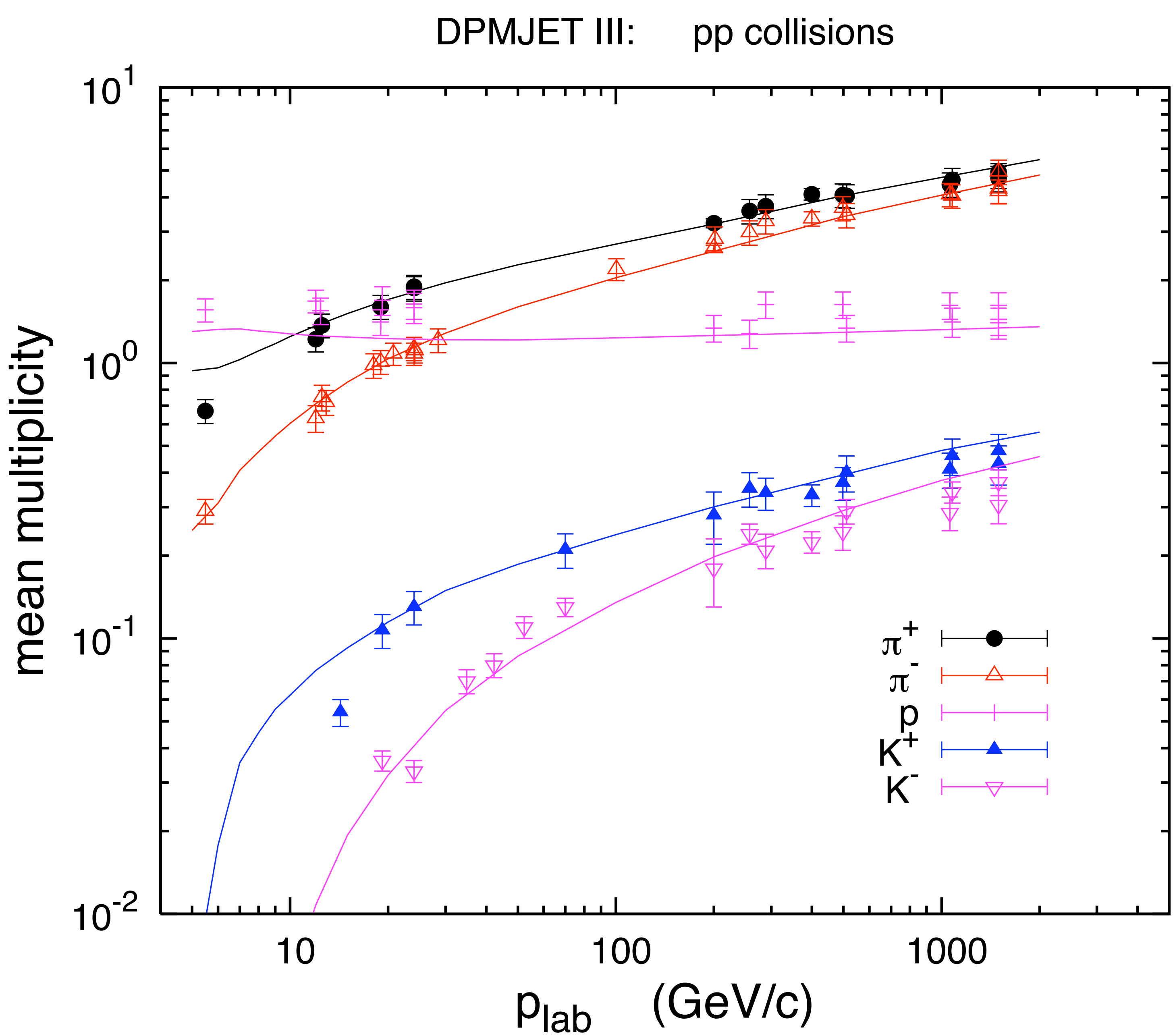

(Roesler, 2006)

New NA49 data (p-p and p-C, 158 GeV)

(Baznat, 2006)

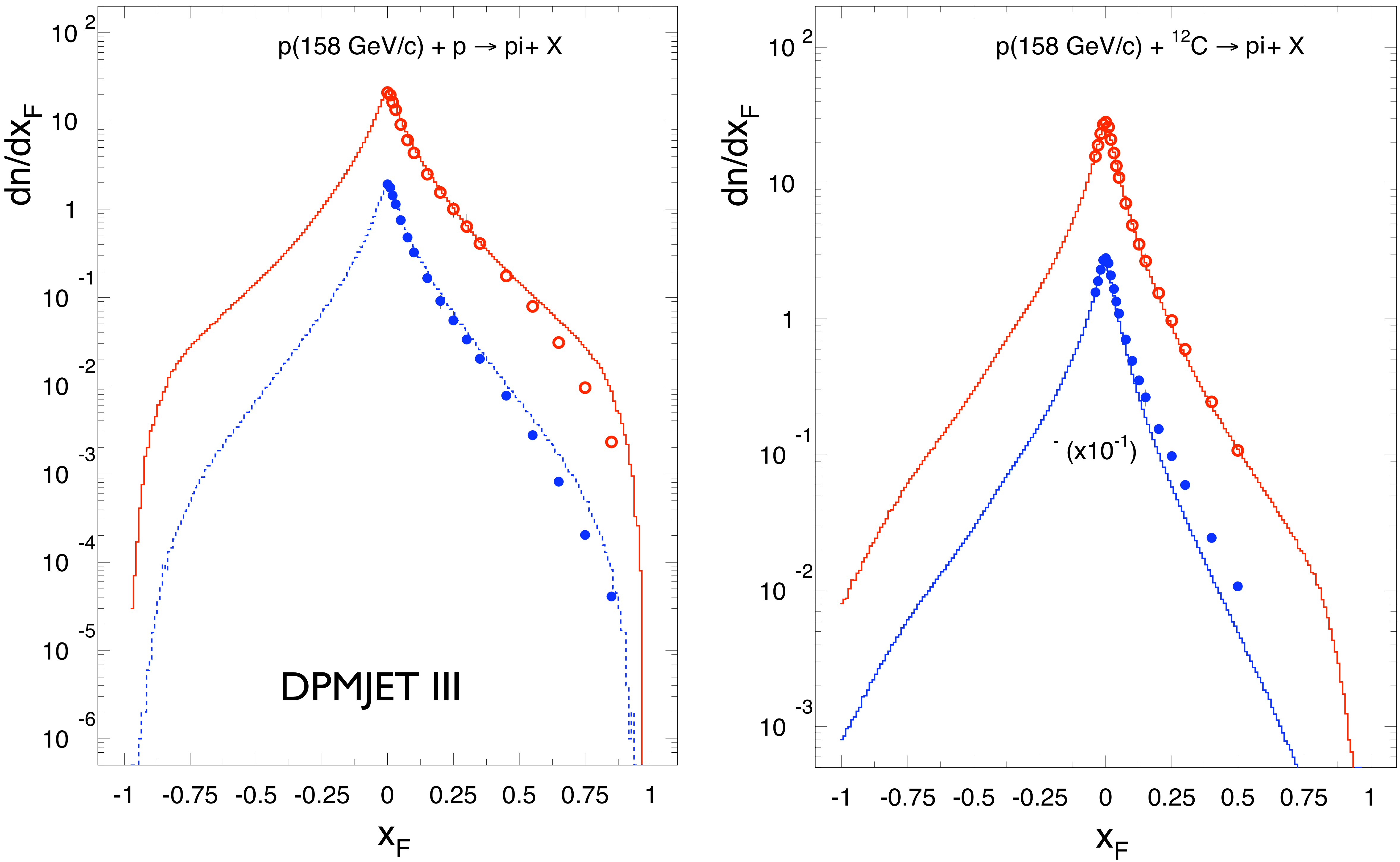

Photoproduction on hadrons

OMEGA Collab., E_γ = 110 ... 170 GeV

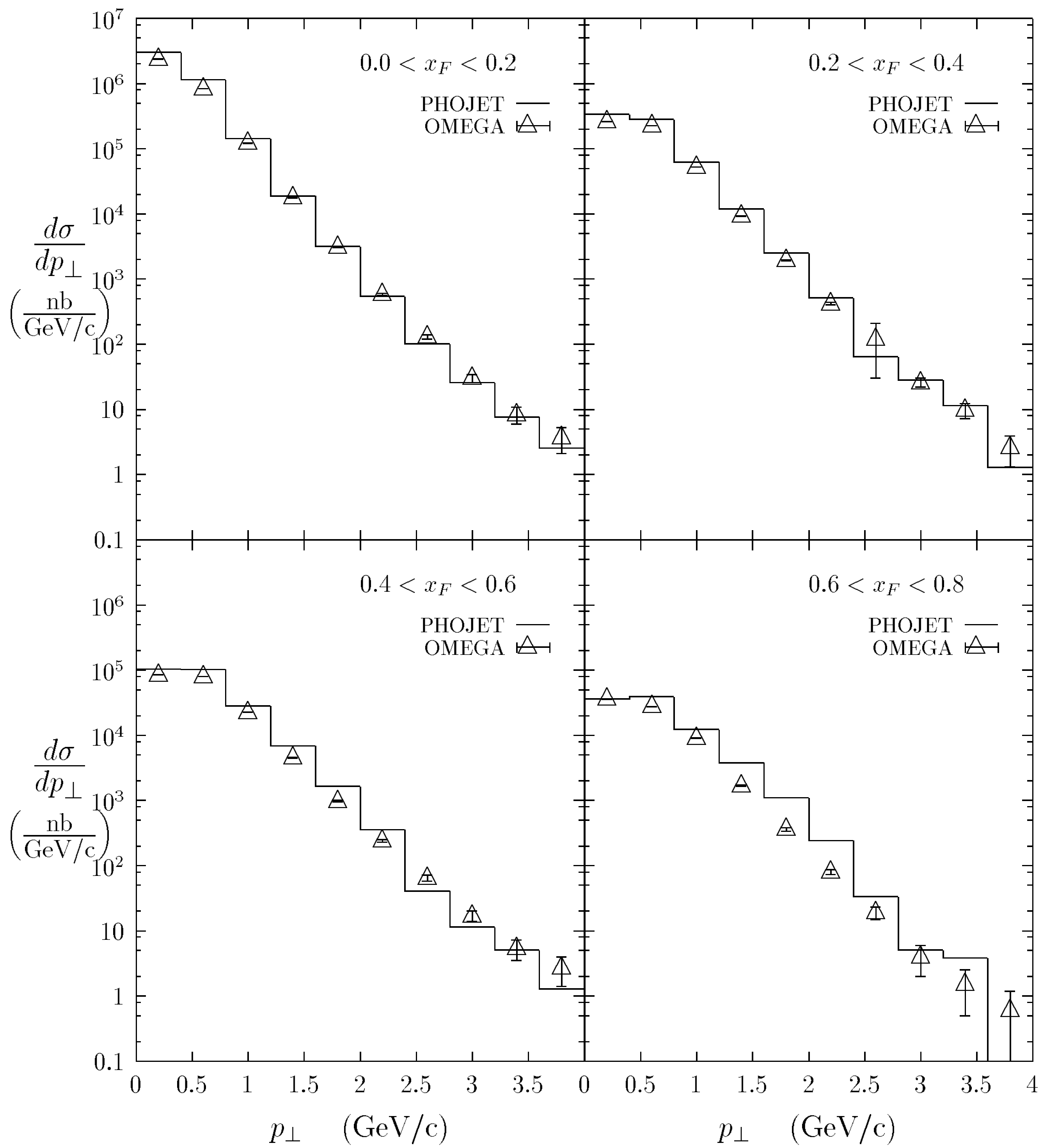

Virtual photons

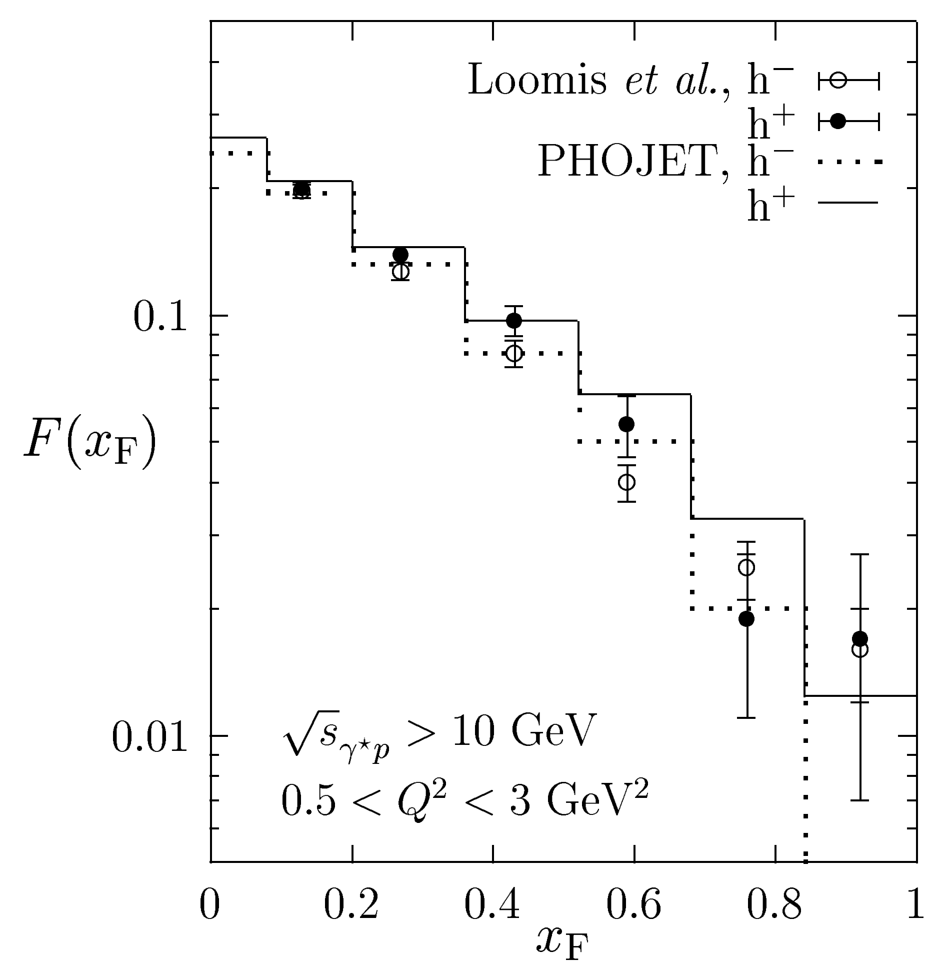

Note: PHOJET now part of DPMJET III

Glauber model of nuclear collisions

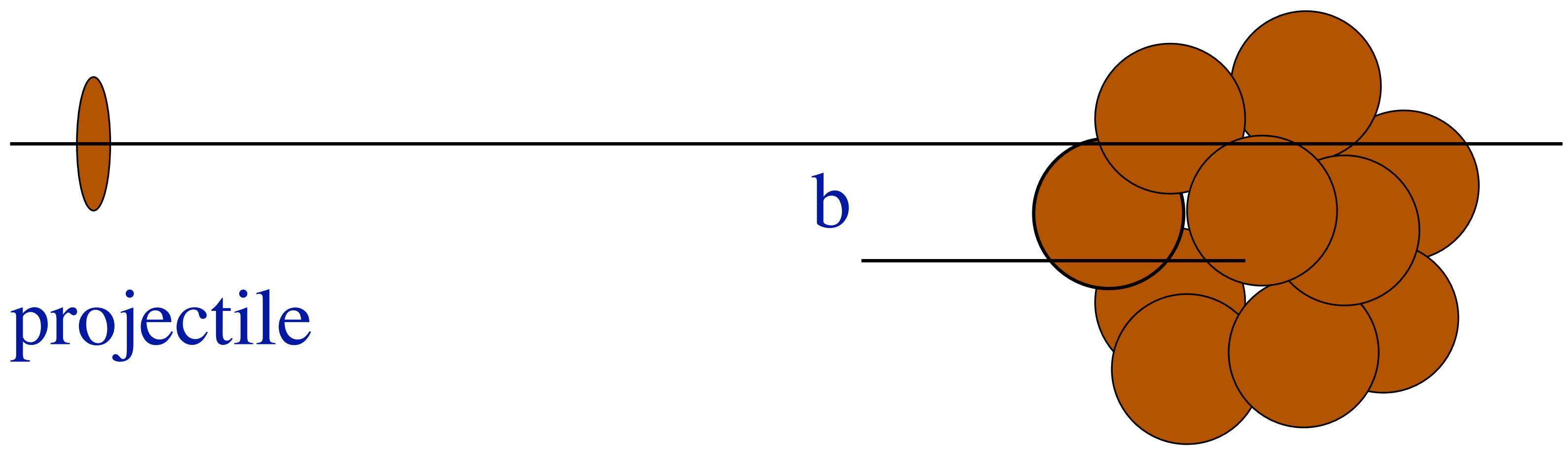

Standard Glauber approximation:

$$\sigma_{\text{inel}} = \int d^2\vec{b} \left[1 - \prod_{k=1}^{A} \left(1 - \sigma_{\text{tot}}^{NN} T_N(\vec{b} - \vec{s}_k) \right) \right] \approx \int d^2\vec{b} \left[1 - \exp\left\{ -\sigma_{\text{tot}}^{NN} T_A(\vec{b}) \right\} \right]$$

$$\sigma_{\text{prod}} \approx \int d^2\vec{b} \left[1 - \exp\left\{ -\sigma_{\text{ine}}^{NN} T_A(\vec{b}) \right\} \right]$$

DPMJET: Pauli blocking intranuclear cascade with formation zone

Fixed-target hadron-nucleus data (i)

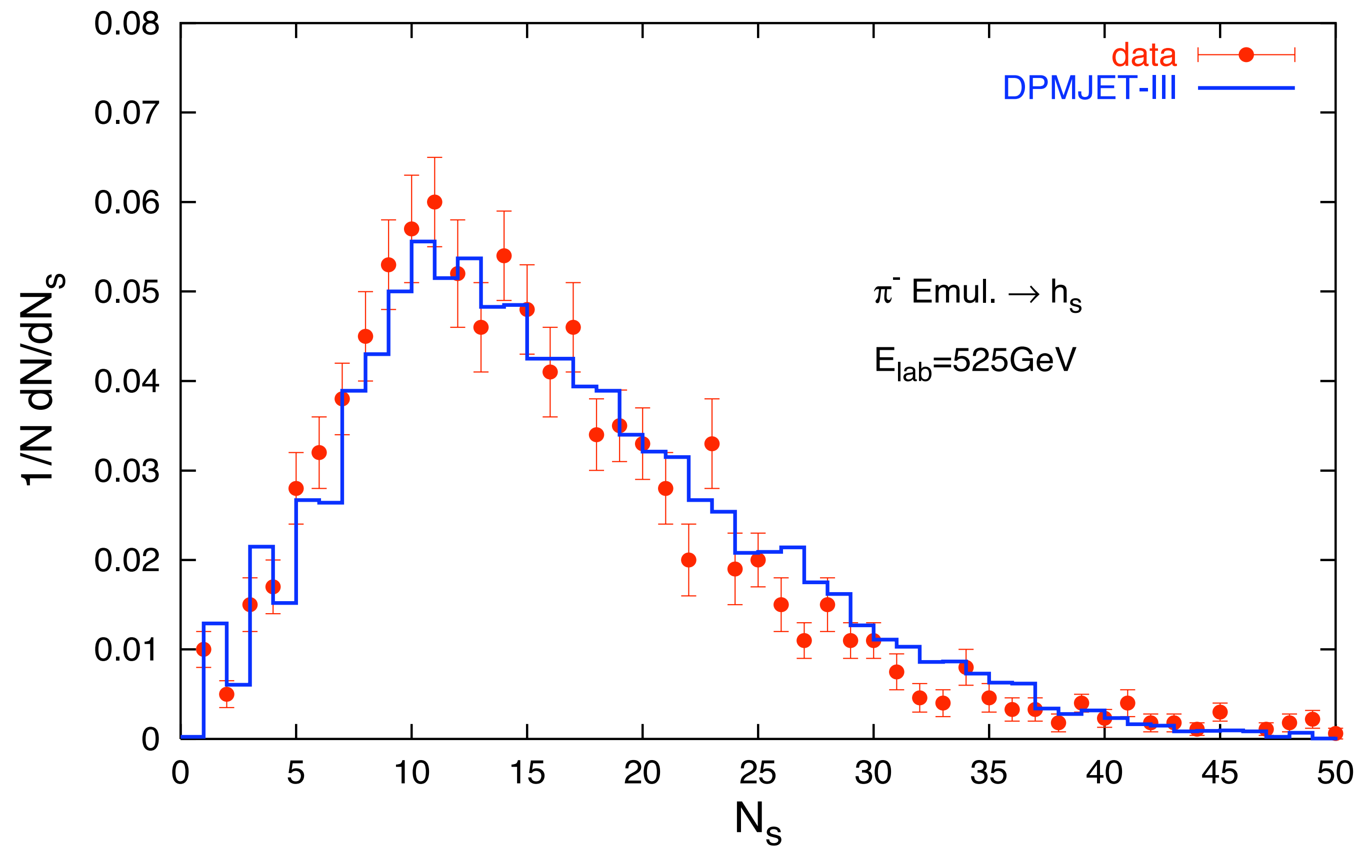

(Roesler, 2006)

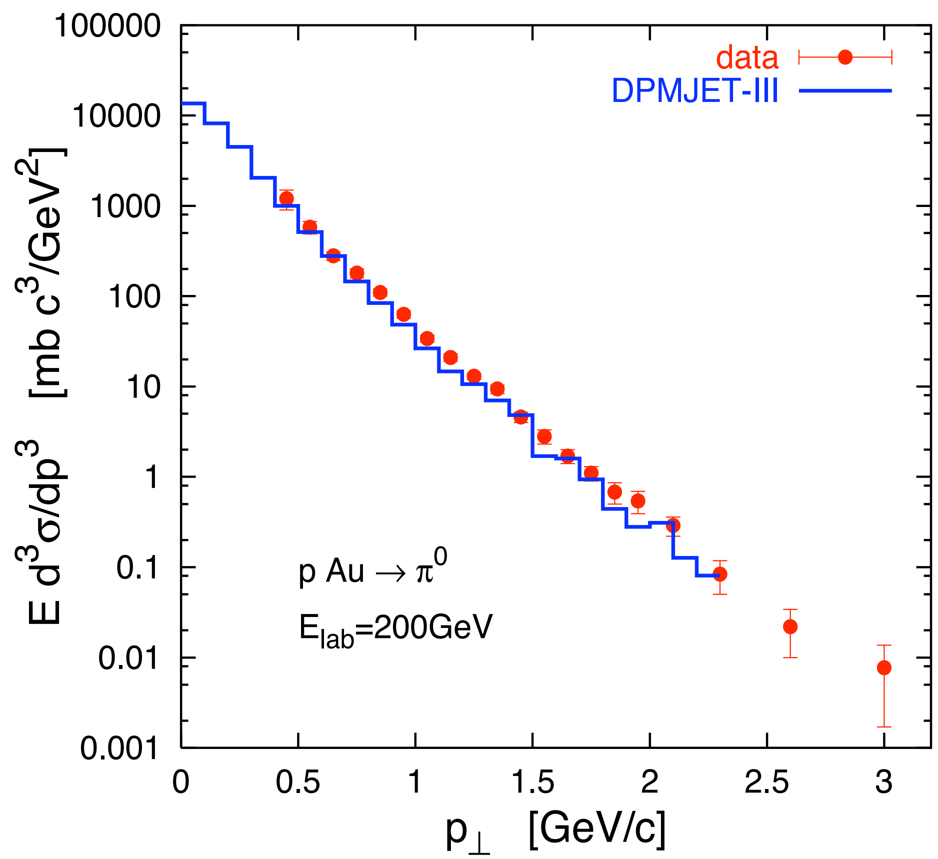

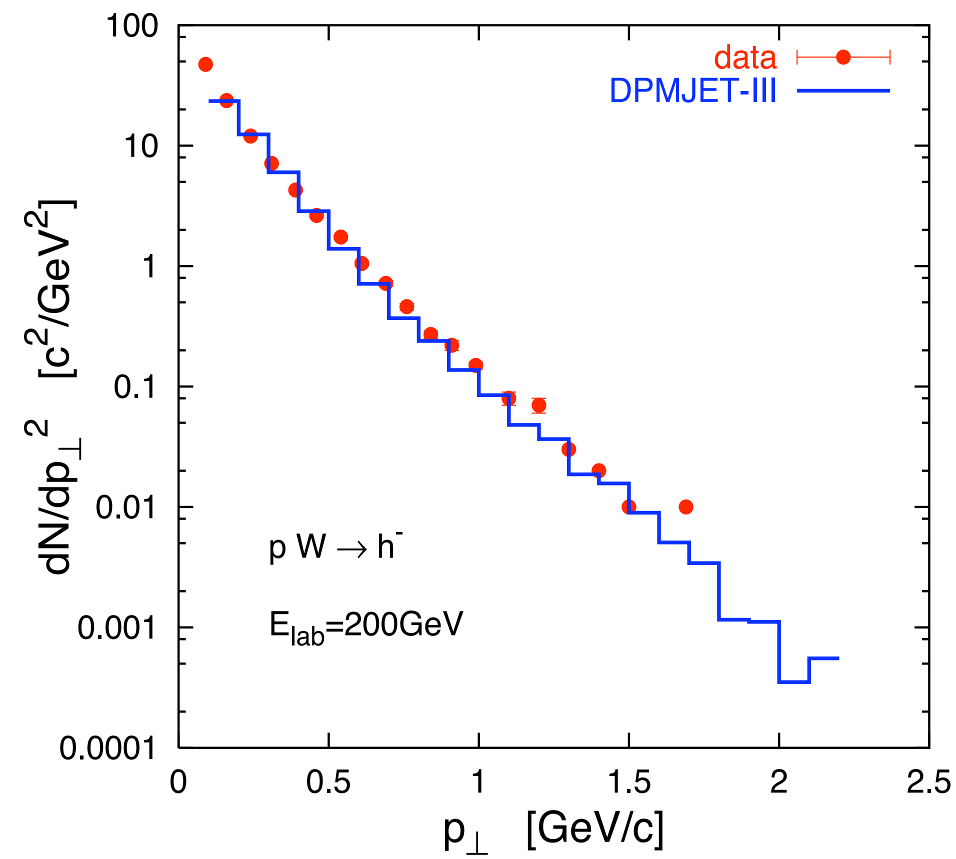

Fixed-target hadron-nucleus data (ii)

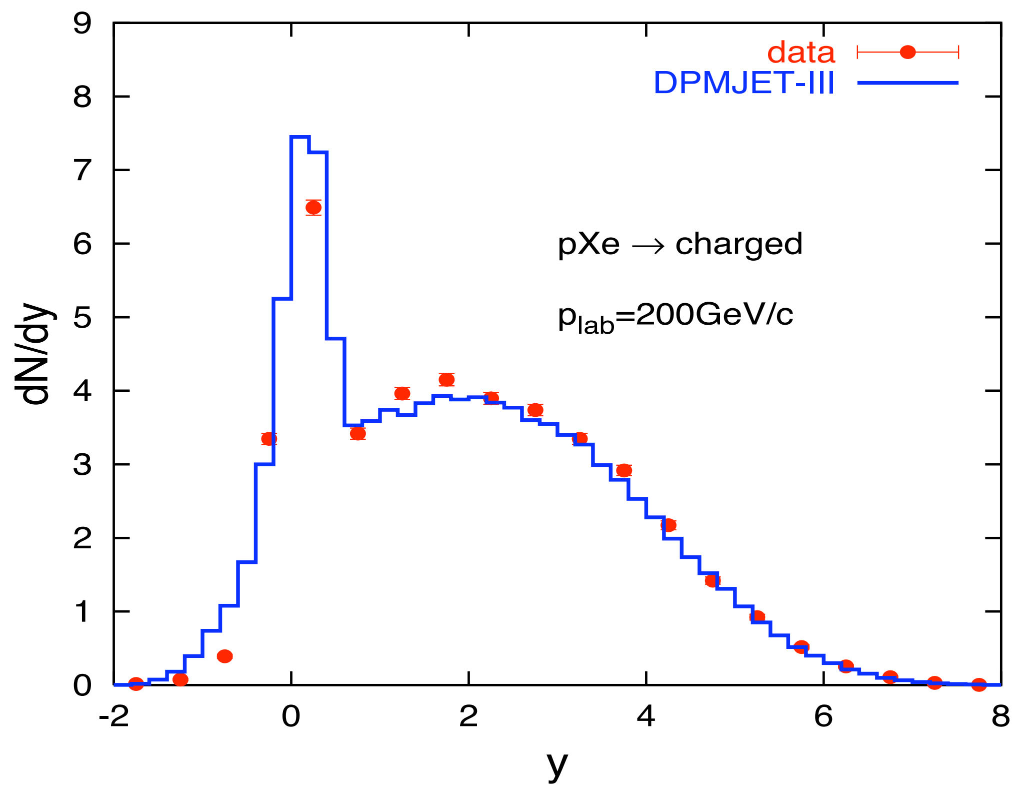

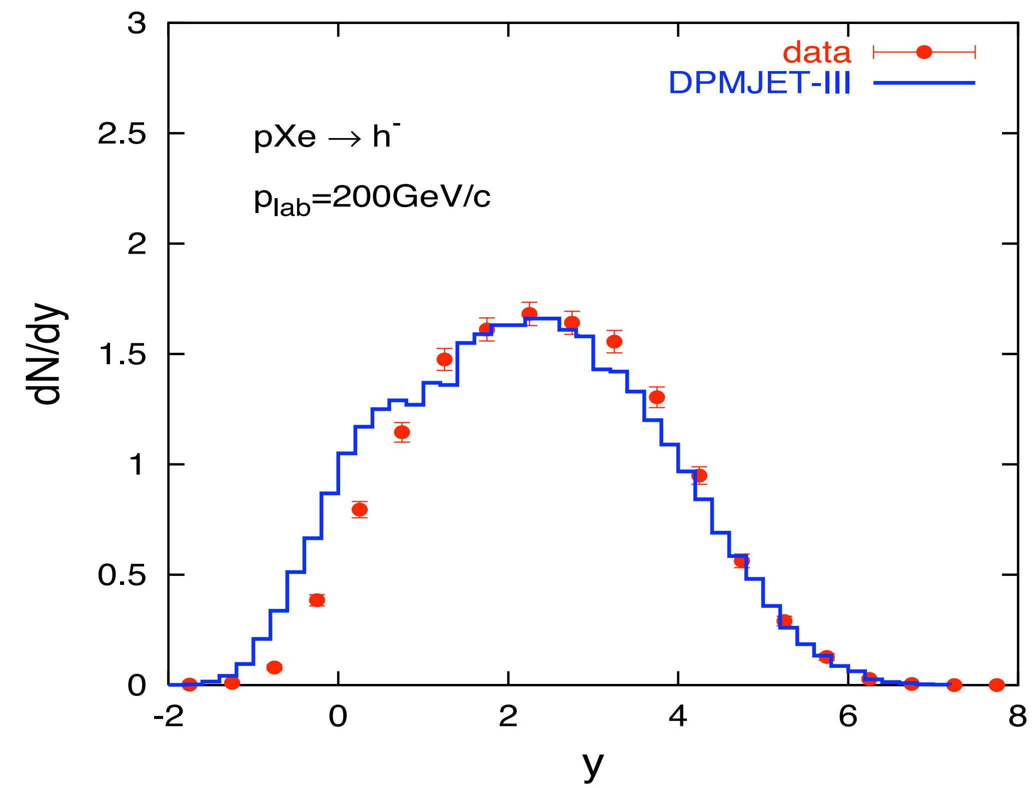

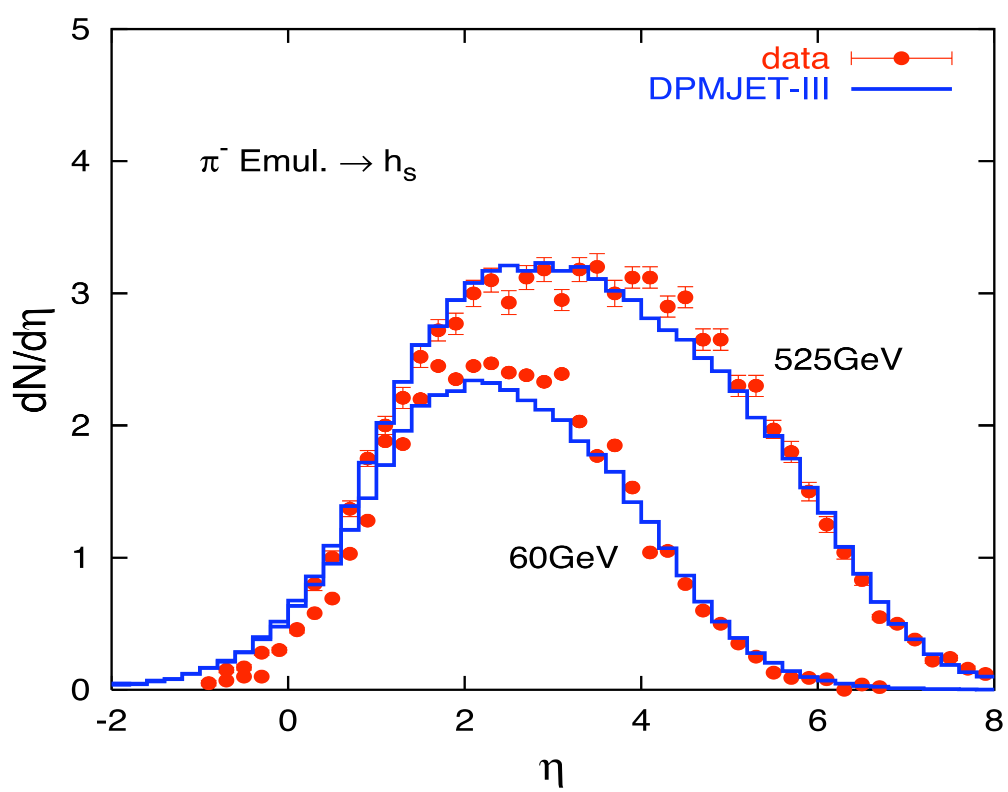

(Roesler, 2006)		Exp.	DPMJET-III
14.6 GeV	p Al	1.57 ±0.23	1.52
	p Au	2.15 ±0.33	1.92
200 GeV	p S	5.0 ± 0.2	4.98
	p Xe	6.84 ±0.13	6.67
360 GeV	p Al	6.8 ±0.6	5.87
	p Au	8.9 ±0.4	8.77

Fixed-target nucleus-nucleus data

(Roesler, 2006)

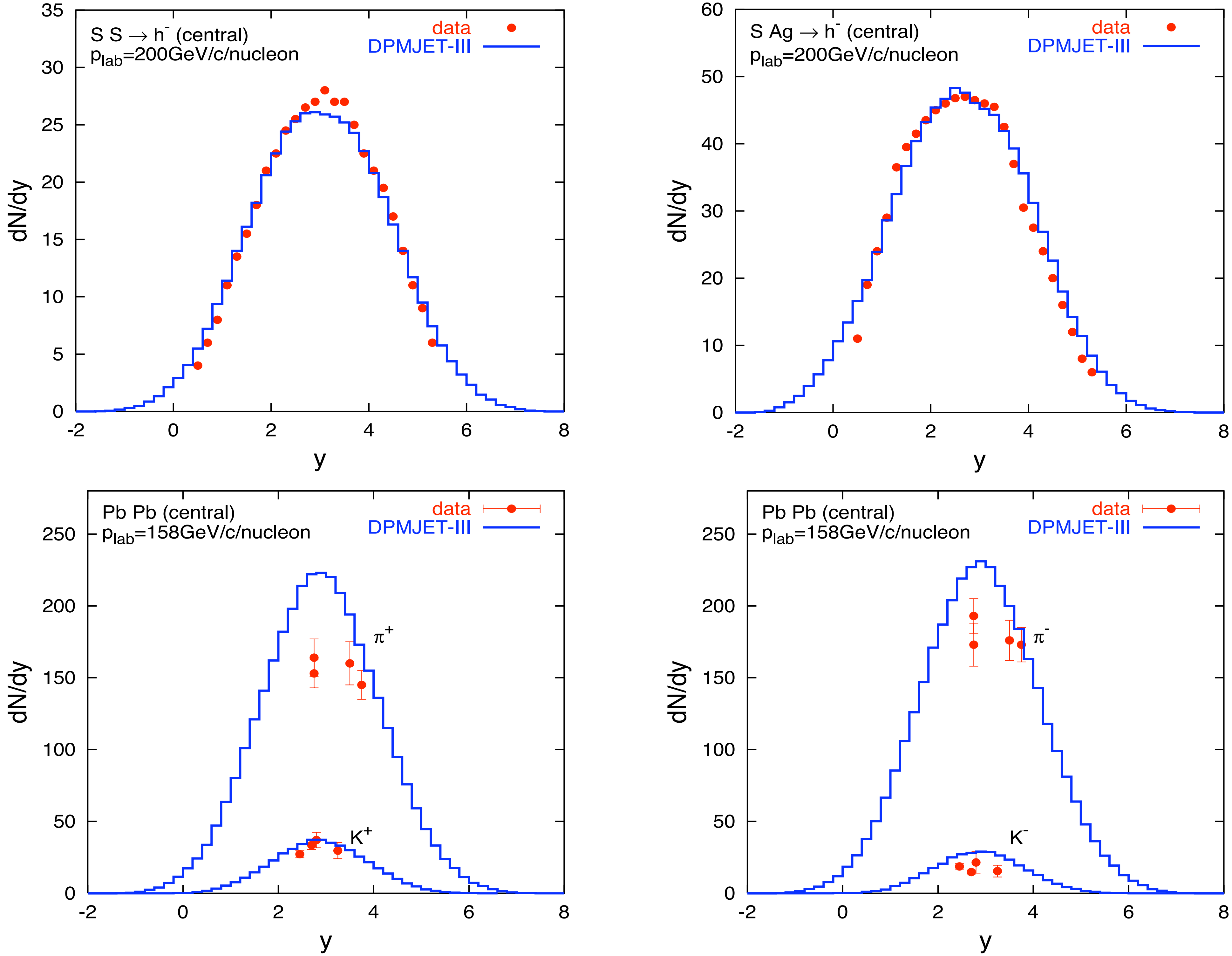

Photon-nucleus scattering

Straightforward application of GVDM (DPMJET III)

$$\sigma_{\gamma^\star A}(s,Q^2)=4\pi\alpha_{\rm em}\int_{M_0^2}^{M_1^2} dM^2 D(M^2)\left(\frac{M^2}{M^2+Q^2}\right)^2\left(1+\epsilon\frac{Q^2}{M^2}\right)\sigma_{VA}(s,Q^2,M^2)$$

$$\Gamma(s,Q^2,M^2,\vec{b})=\frac{\sigma_{VN}(s,Q^2,M^2)}{4\pi B(s,Q^2,M^2)}\left(1-i\frac{{\rm Re}f(0)}{{\rm Im}f(0)}\right)\exp\left(\frac{-\vec{b}^2}{2B(s,Q^2,M^2)}\right)$$

$$B(s,Q^2,M^2)=2\left[B_0^2+\alpha'_{\mathbb{P}}\ln\left(\frac{s}{M^2+Q^2}\right)\right],$$

$$B_0^2=\left(2+\frac{m_\rho^2}{M^2+Q^2}\right){\rm GeV}^{-2},\qquad \alpha'_{\mathbb{P}}=0.25{\rm GeV}^{-2}$$

$$\sigma_{VA}^{\rm inel}(s,Q^2,M^2)=\int d^2b\int\prod_{j=1}^{A}d^3r_j\rho_A(\vec{r}_j)\left(1-\left|\prod_{i=1}^{A}[1-\Gamma(s,Q^2,M^2,\vec{b}_i)]\right|^2\right)$$

DPMJET: cross sections

Coherence length

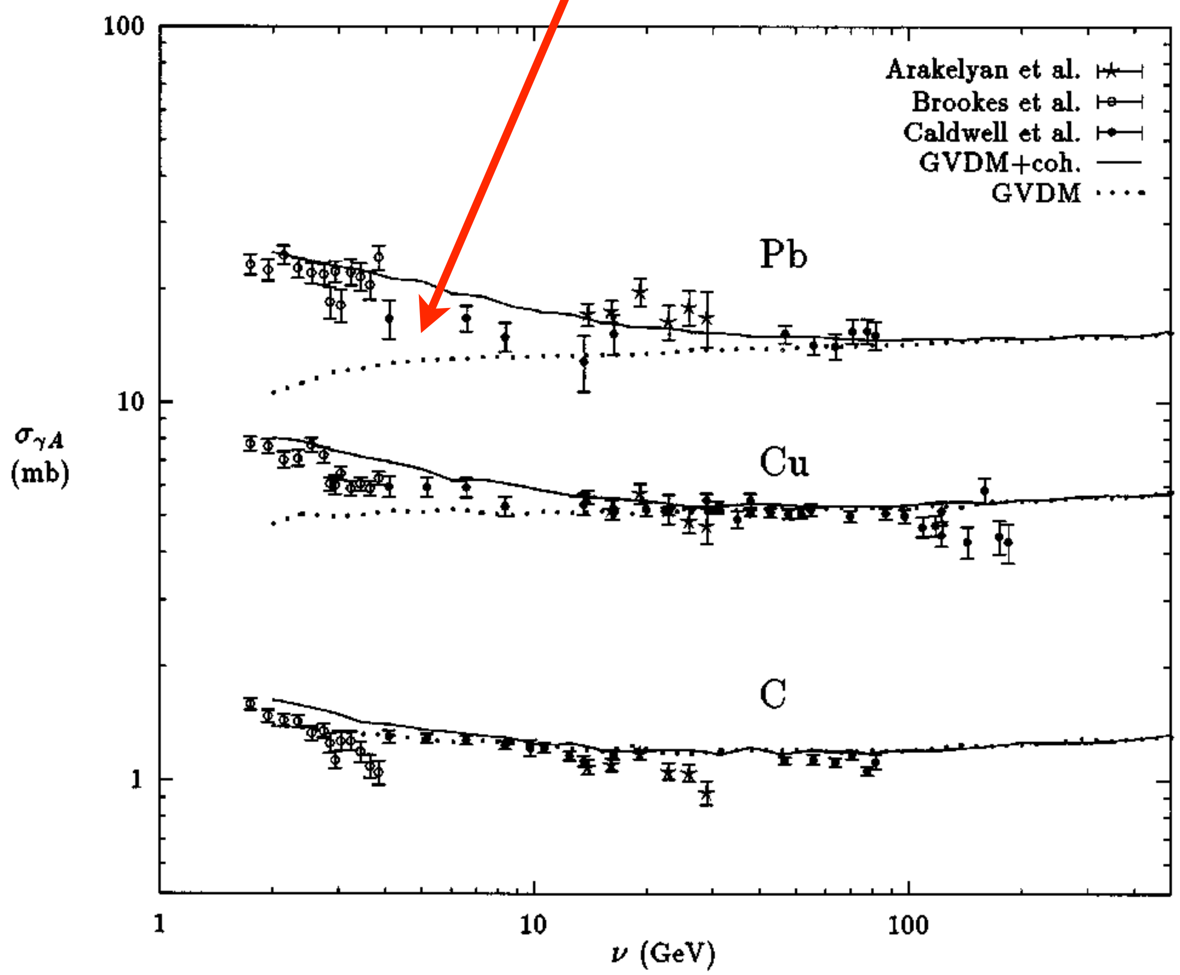

Photoproduction cross section

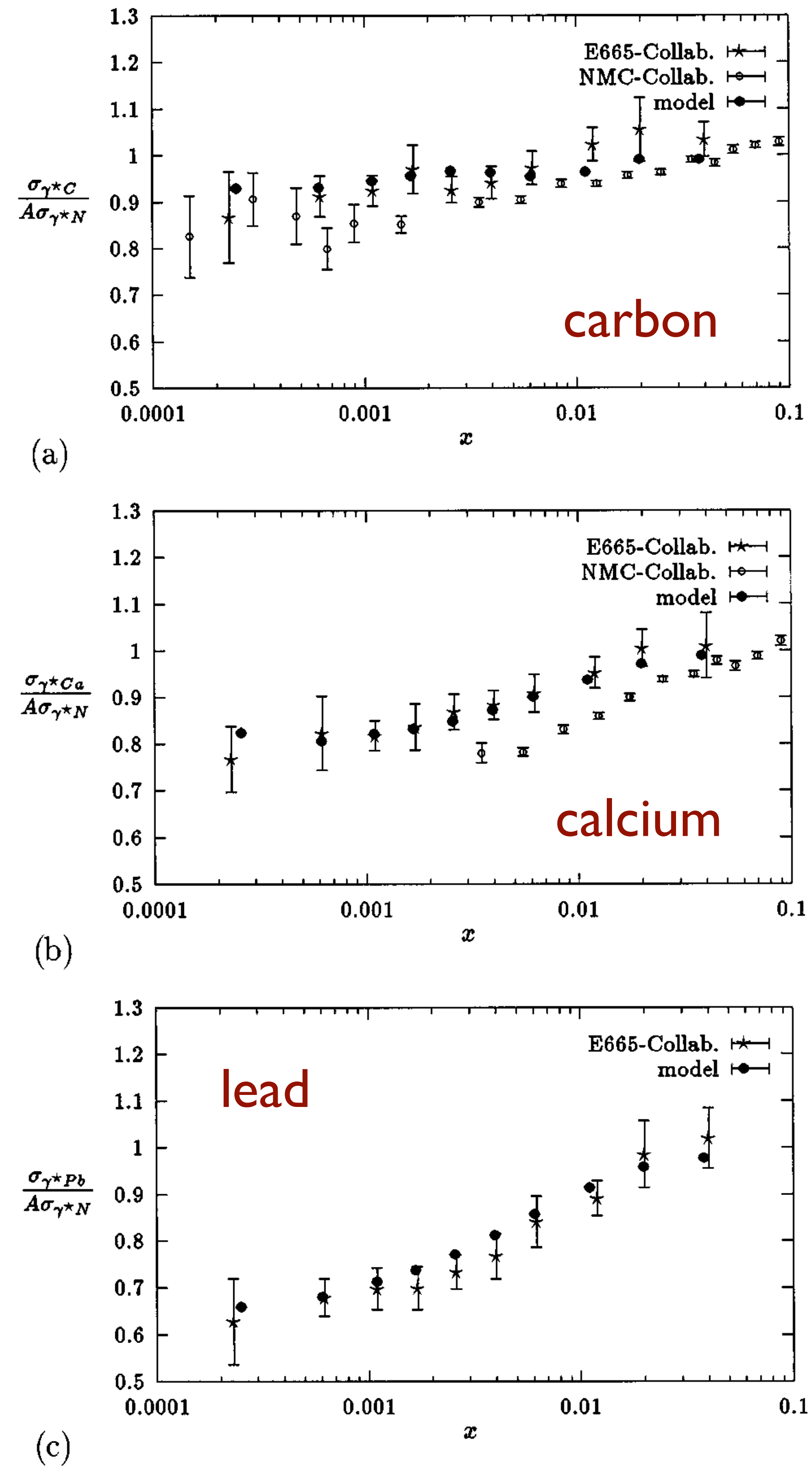

$0.15 \leq Q^2 \leq 8\ \mathrm{GeV}^2$

(RE, Ranft, Roesler, PRD55, 1997)

Inclusive photoproduction on nuclei

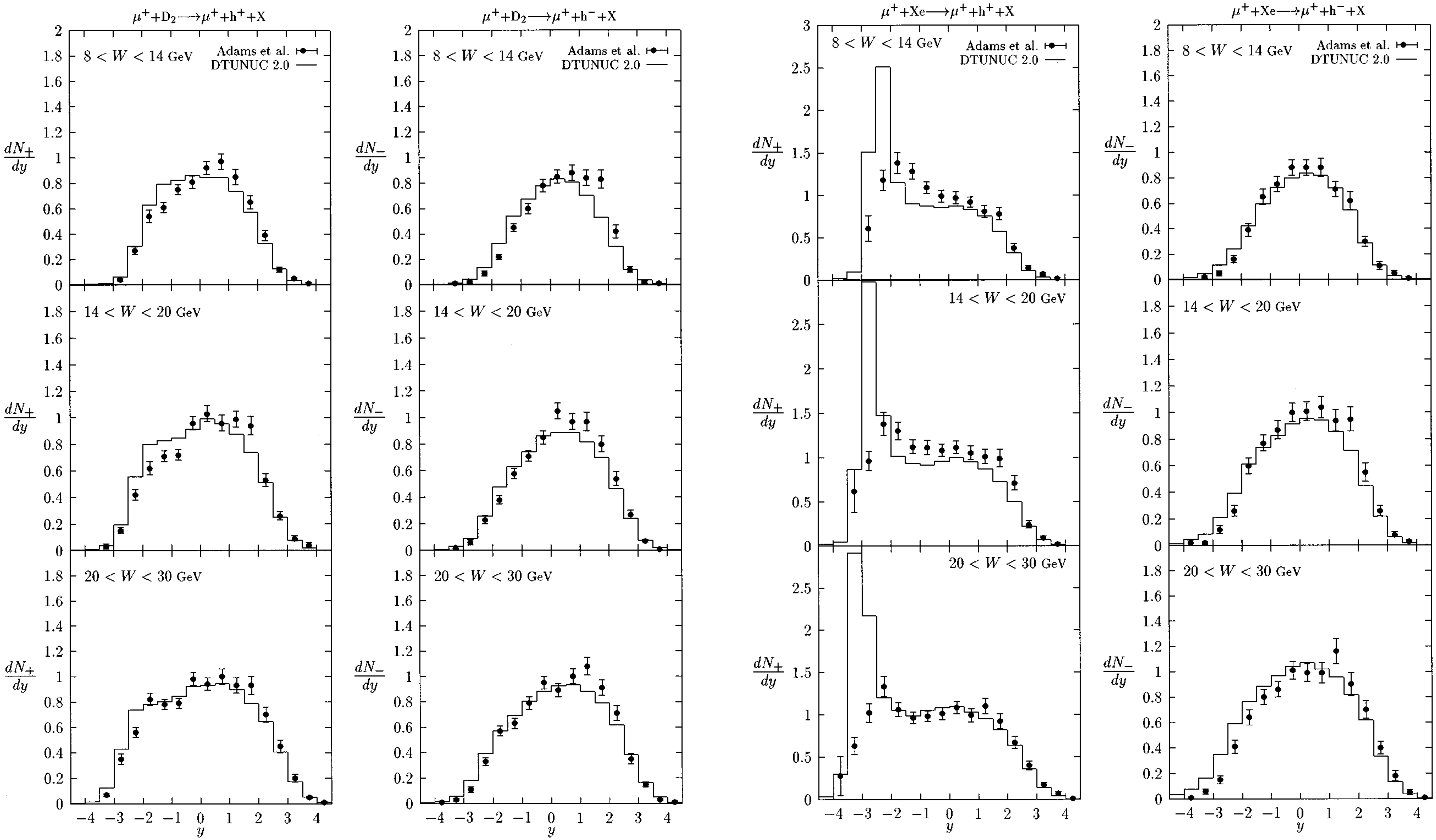

deuterium xenon

490 GeV muon beam

(Roesler, RE, Ranft, PRD57, 1998)

High energy region
(partons, perturbative QCD)

Partons and color flow configurations (i)

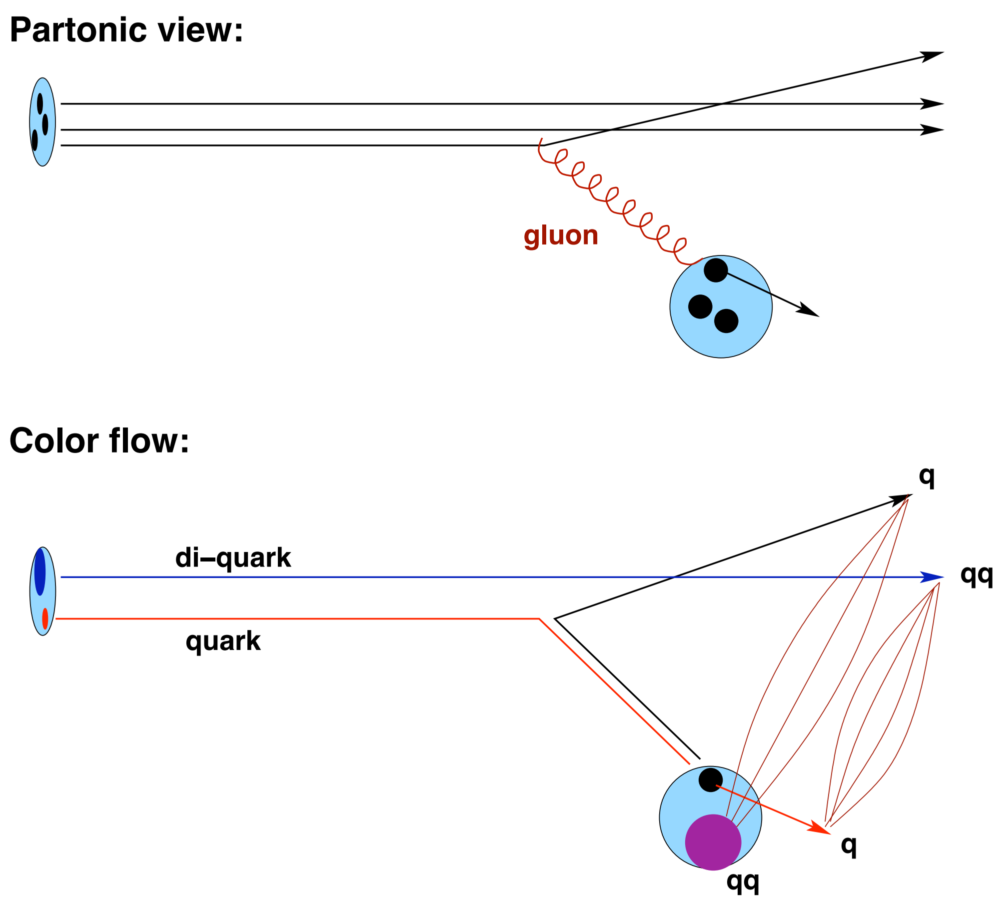

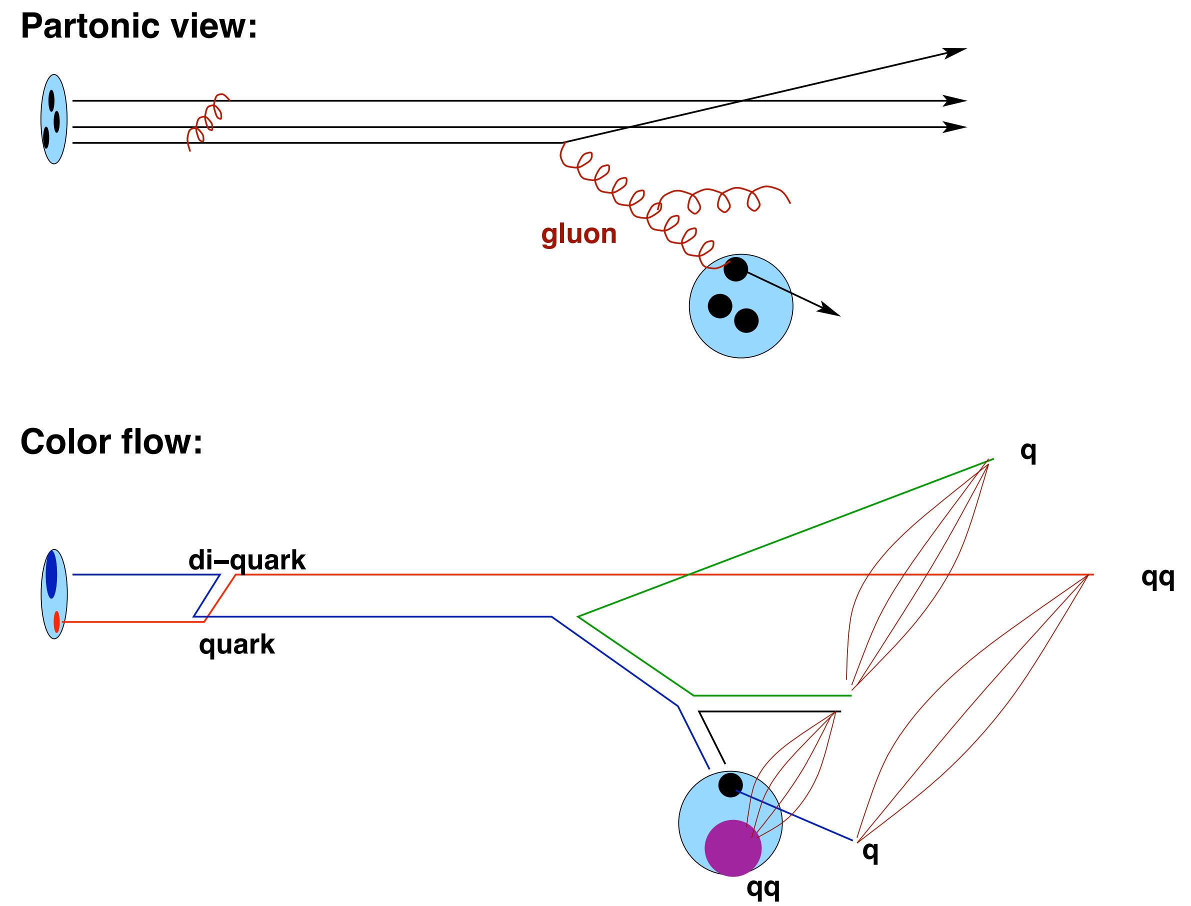

Large N_c approximation

One-gluon exchange:
pomeron topology

Initial and final state radiation:
no change of basic topology

Partons and color flow configuations (ii)

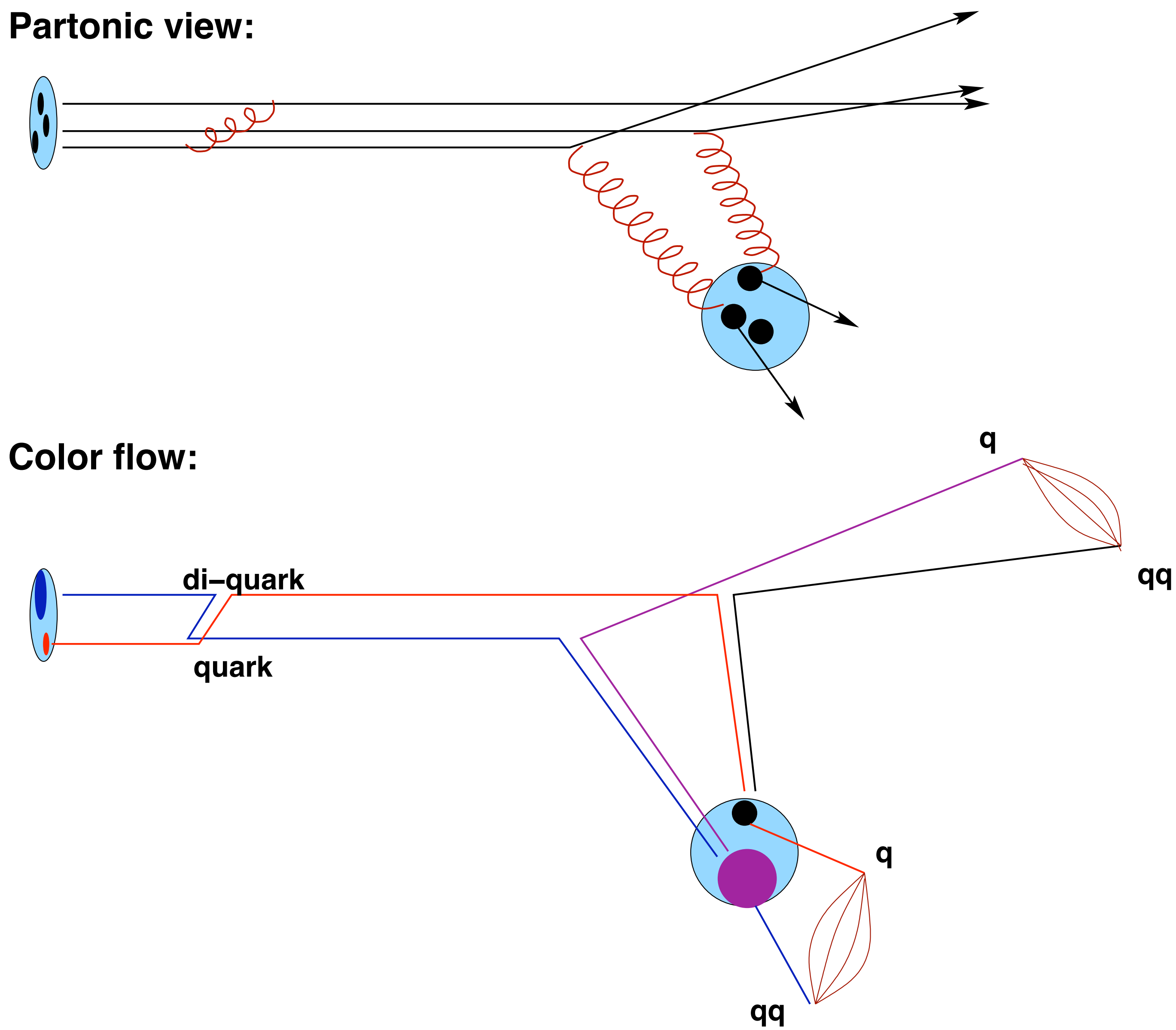

Two-gluon exchange: diffraction dissociation

DPMJET III: detailed color flow simulation for each event

QCD parton model: minijets

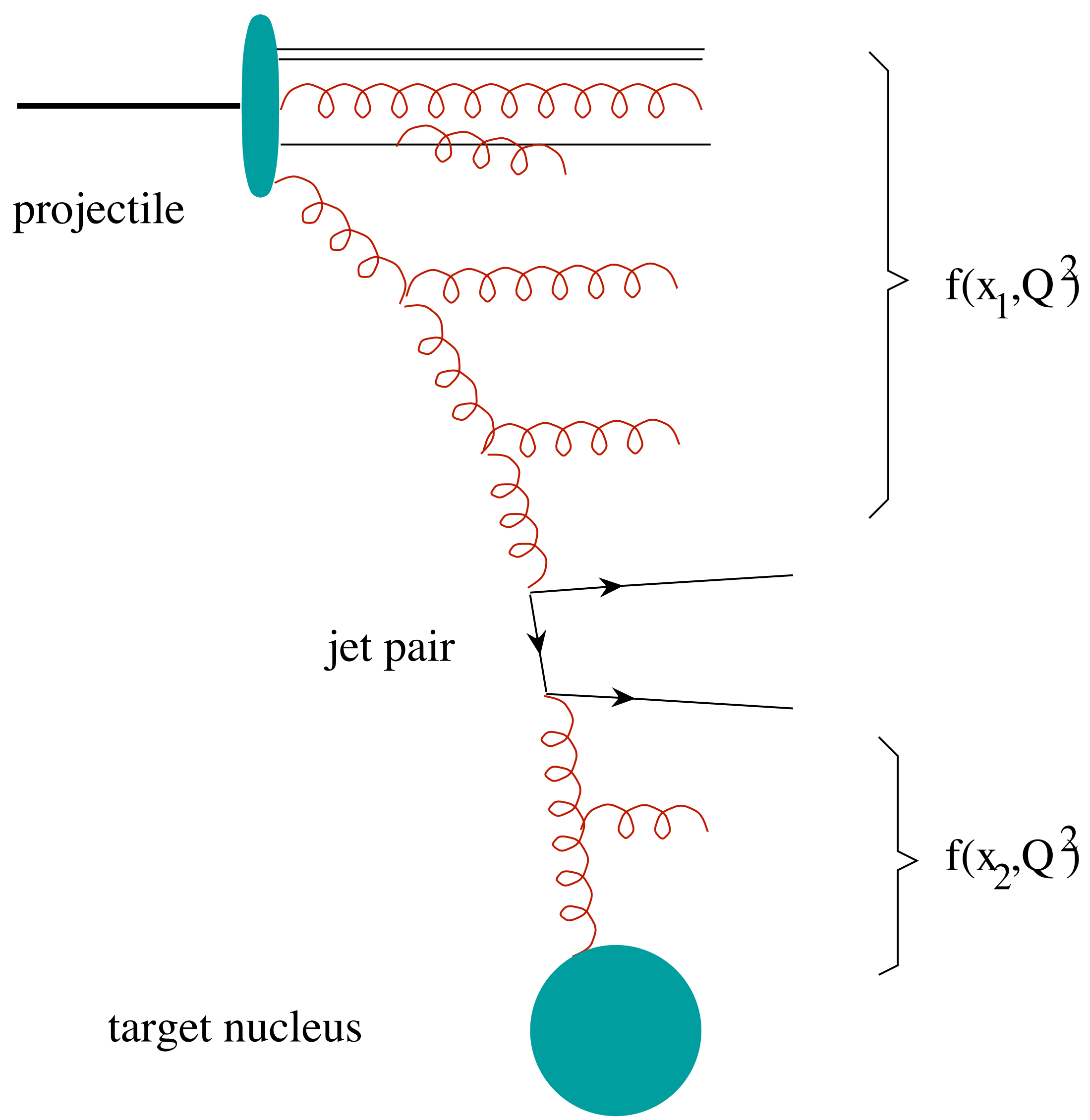

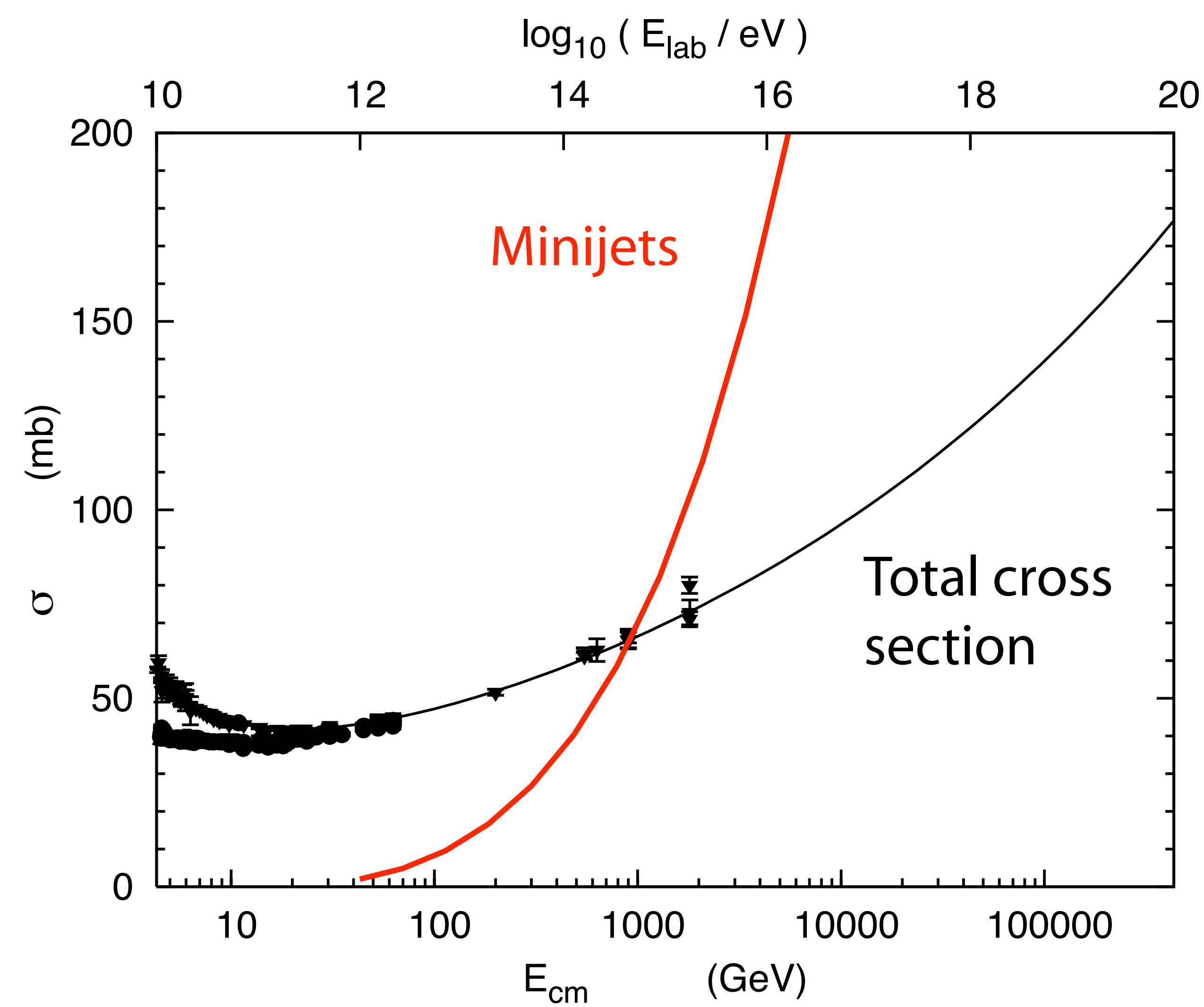

$$\sigma_{QCD} = \sum_{i,j,k,l} \frac{1}{1+\delta_{kl}} \int dx_1\, dx_2 \int_{p_\perp^{\rm cutoff}} dp_\perp^2\; f_i(x_1,Q^2)\; f_j(x_2,Q^2)\; \frac{d\sigma_{i,j\to k,l}}{dp_\perp}$$

Direct interactions of photons

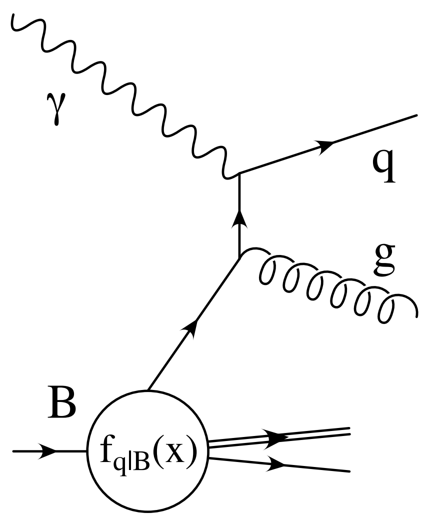

Gluon Compton scattering

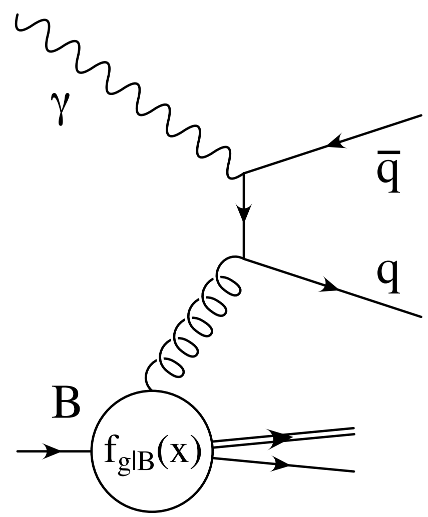

Boson-gluon fusion

LO, GRV parton densities

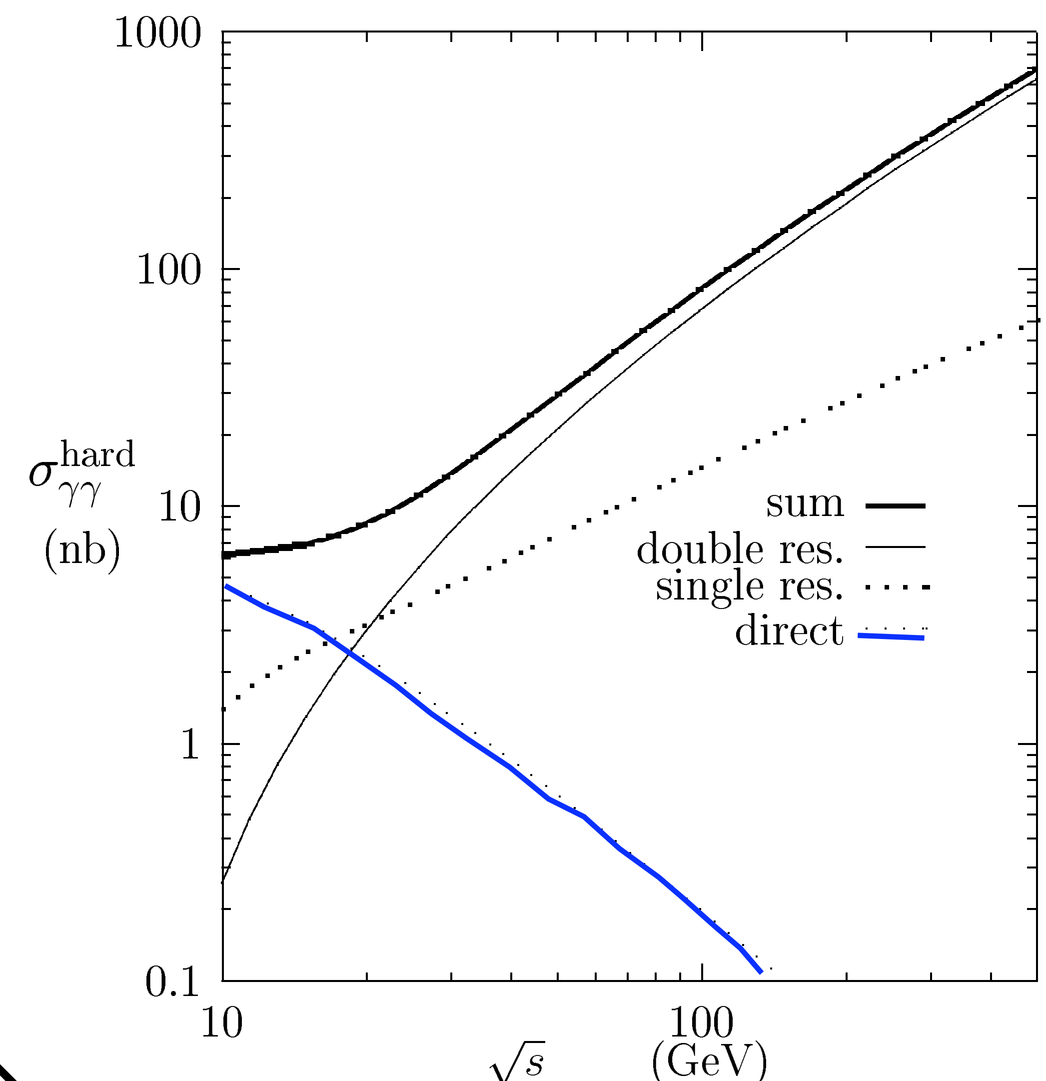

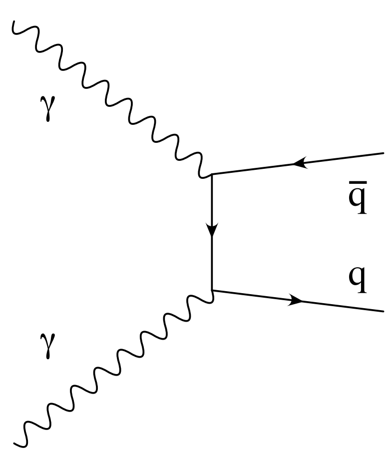

Box diagram

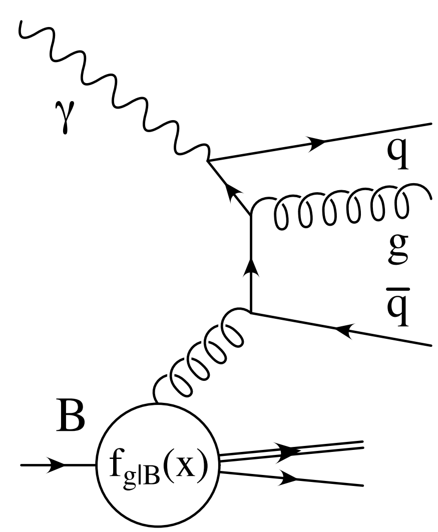

Anomalous contribution

ISR parton shower does not always end at soft scale

Problem: matching soft/hard contributions

$\sigma_{soft} \sim s^{0.1}$

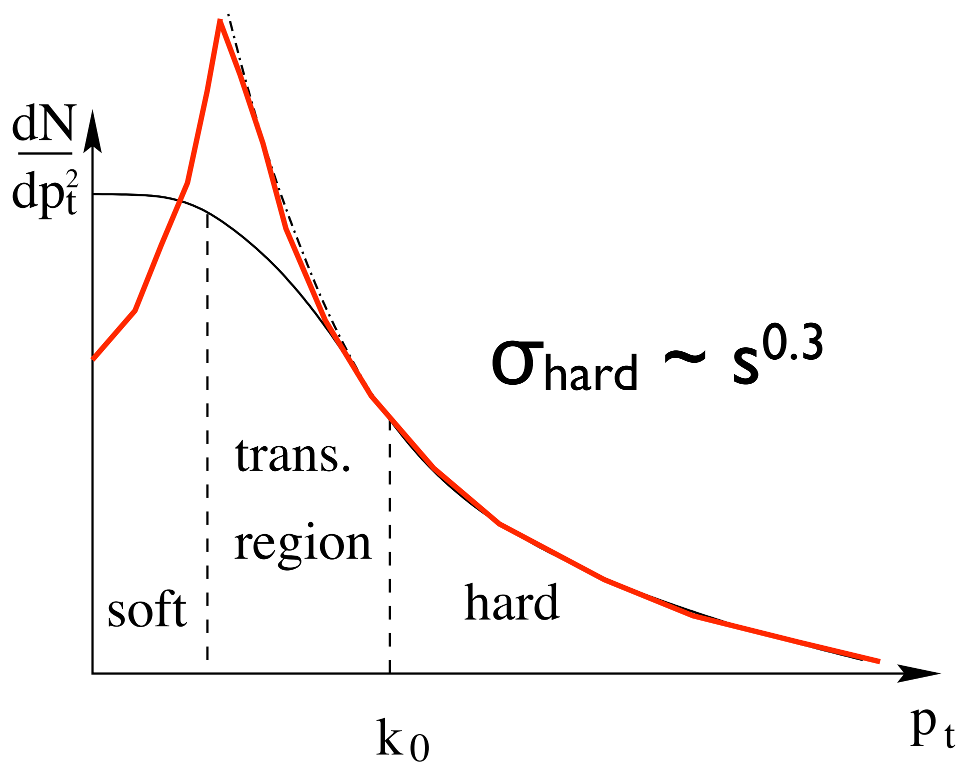

$\sigma_{hard} \sim s^{0.3}$

pt cutoff

CDF inclusive charged particle distribution

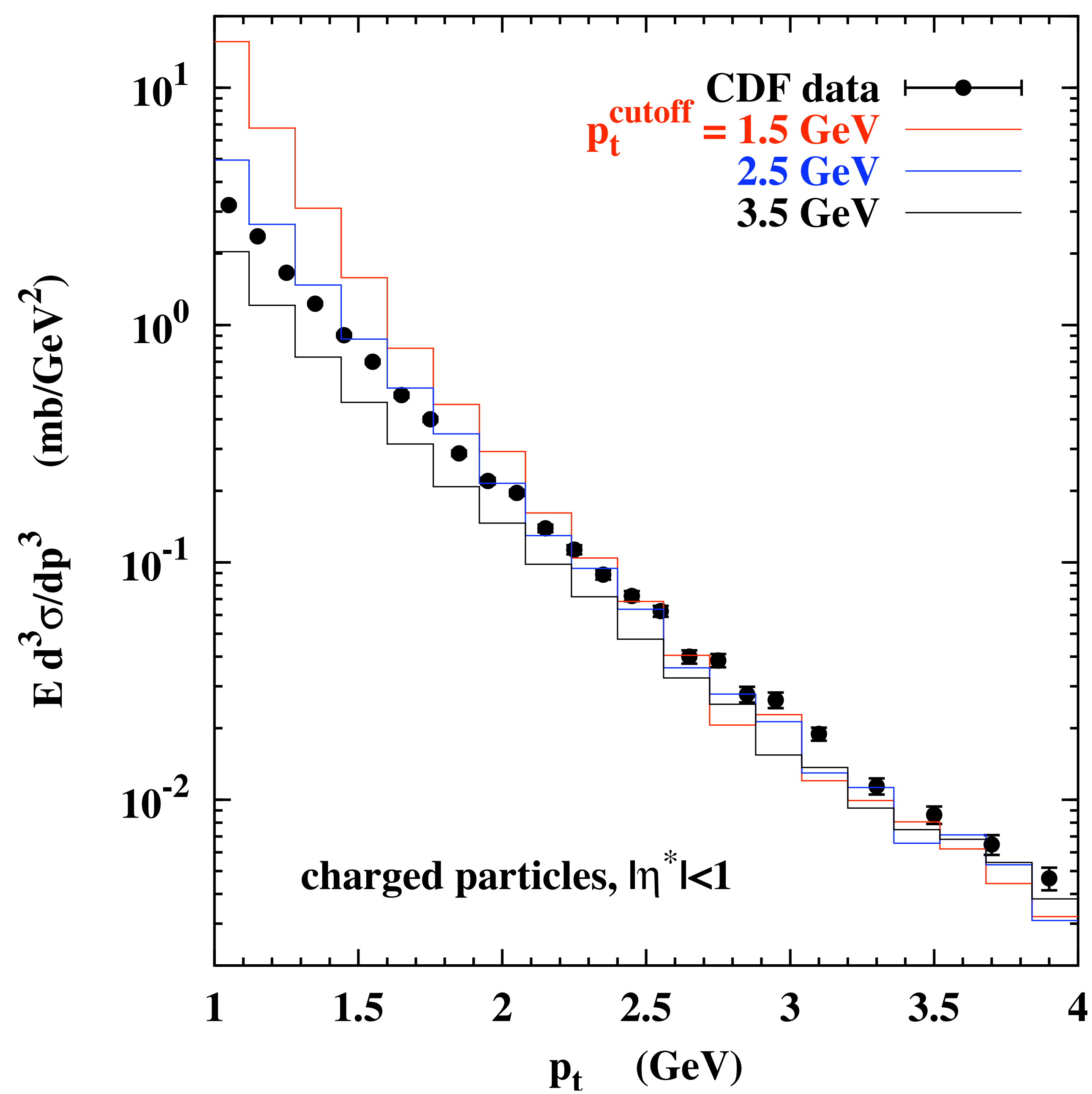

- Topologies similar
- Matching of p_t distribution of partons

Unitarization: eikonal-based model

Classic eikonal formula

$$\sigma_{\rm ine} = \int d^2\vec{b} \left(1 - \exp\left\{-\sigma_{\rm soft} A_{\rm soft}(s,\vec{b}) - \sigma_{\rm QCD} A_{\rm hard}(s,\vec{b})\right\}\right)$$

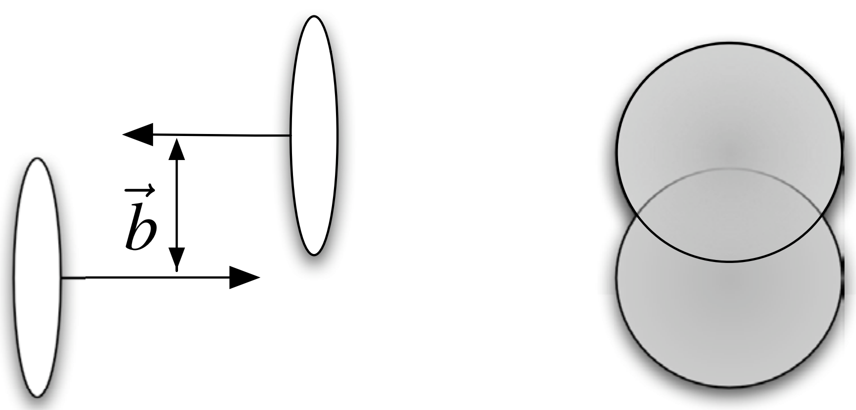

Overlap function

$$\langle n(\vec{b})\rangle = \sigma_{\rm QCD}\, A(s,\vec{b})$$

Independent interactions: Poisson distribution
(same result follows from AGK cutting rules)

$$P_n = \frac{\langle n(\vec{b})\rangle^n}{n!} \exp\left(-\langle n(\vec{b})\rangle\right)$$

AKG cutting rules

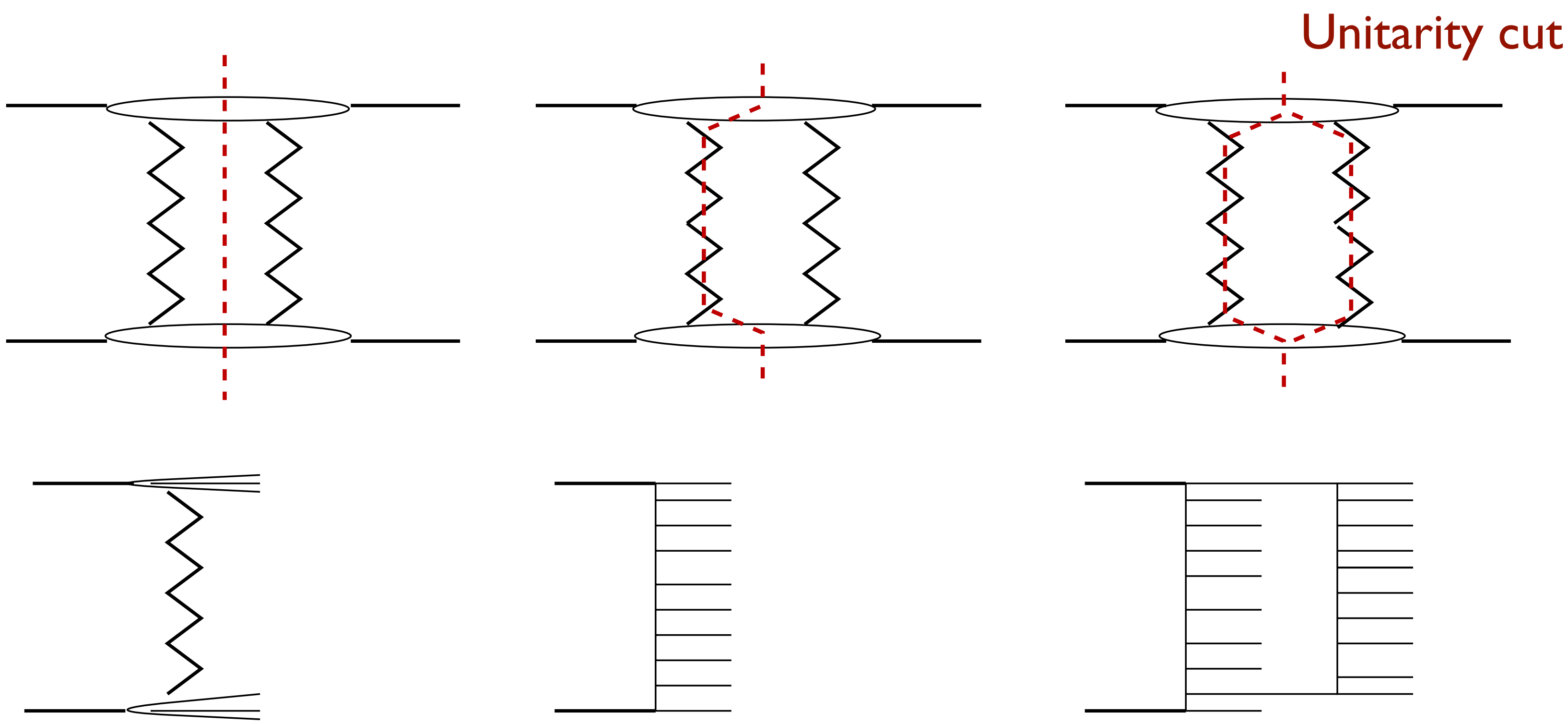

(Abramovskii, Gribov, Kancheli 1974)

Weights: *(-1)* *(+4)* *(-2)*

Other graphs explicitly calculated in DPMJET III

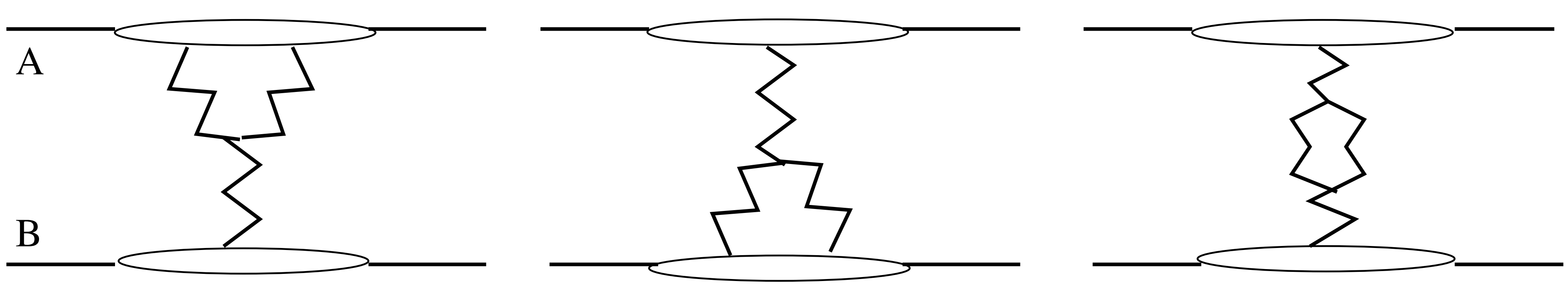

Miracles of model building or physics ?

Unjustified approximations (known not to be satisfied)

- Eikonal and Glauber approximations:
  - known to follow from planar graphs

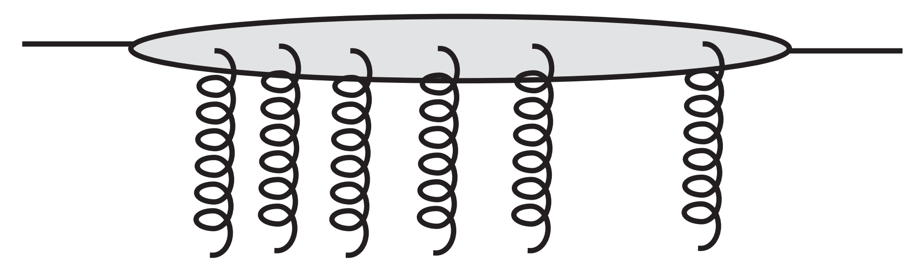

$$a^{(n)}(s,\vec{B}) = -\frac{i}{2}(i)^n \frac{1}{n!}\prod_{i=1}^{n}\left(2a^{(1)}(s,\vec{B})\right)$$

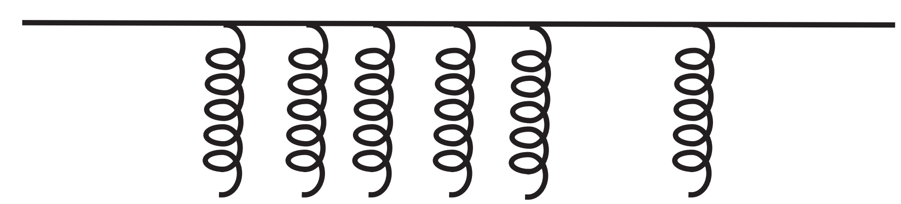

  - recoil (momentum transfer) neglected
  - inelastic intermediate states (off-diagonal terms)

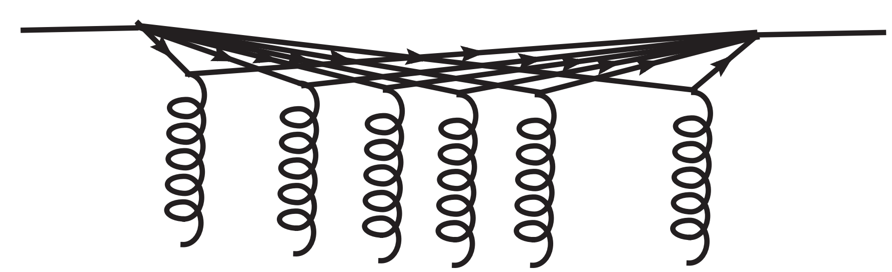

- No correlations between partons
- Universality of string fragmentation (soft/hard)

Comparison with collider data

Charged particle multiplicity distribution at 200 GeV cms.

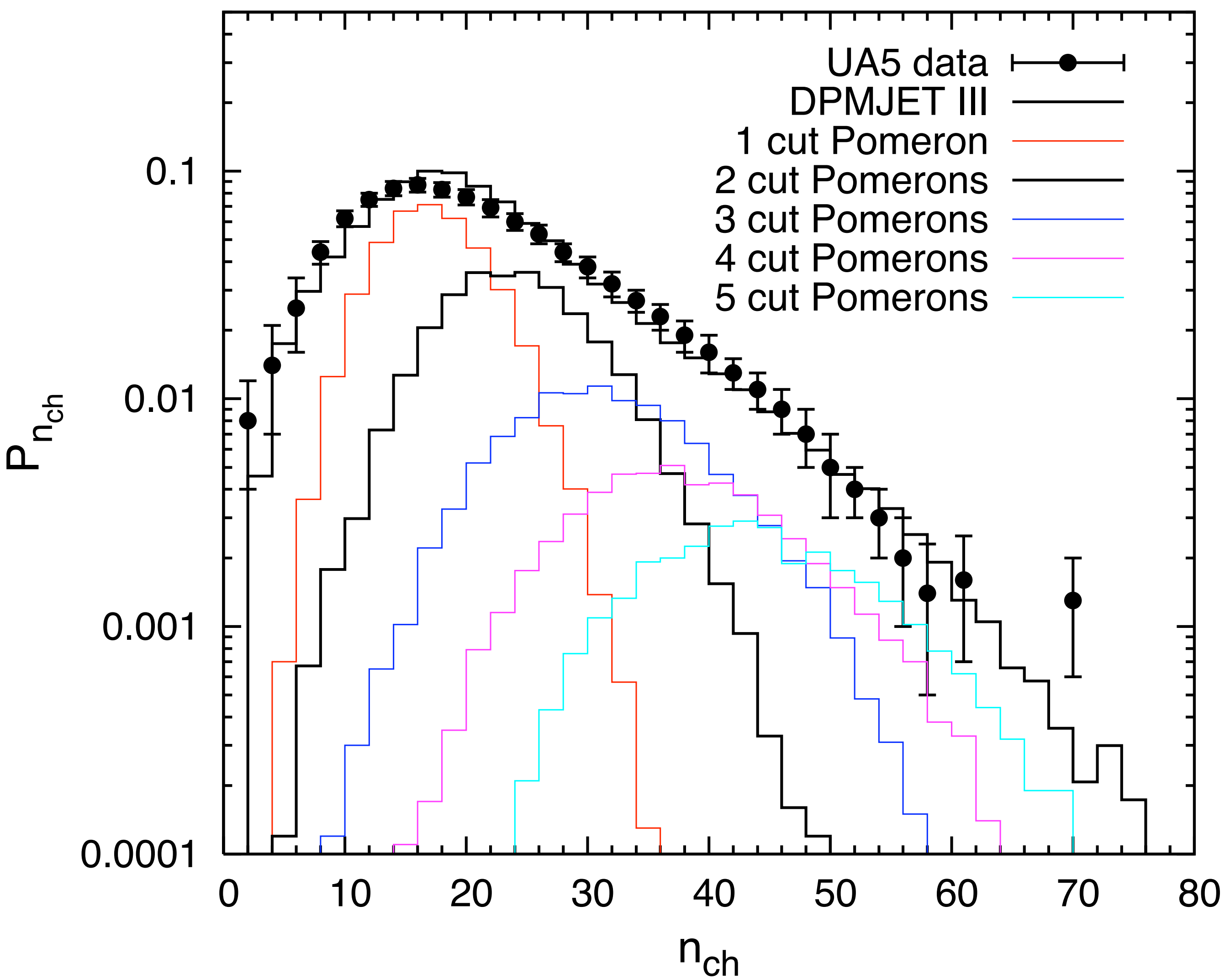

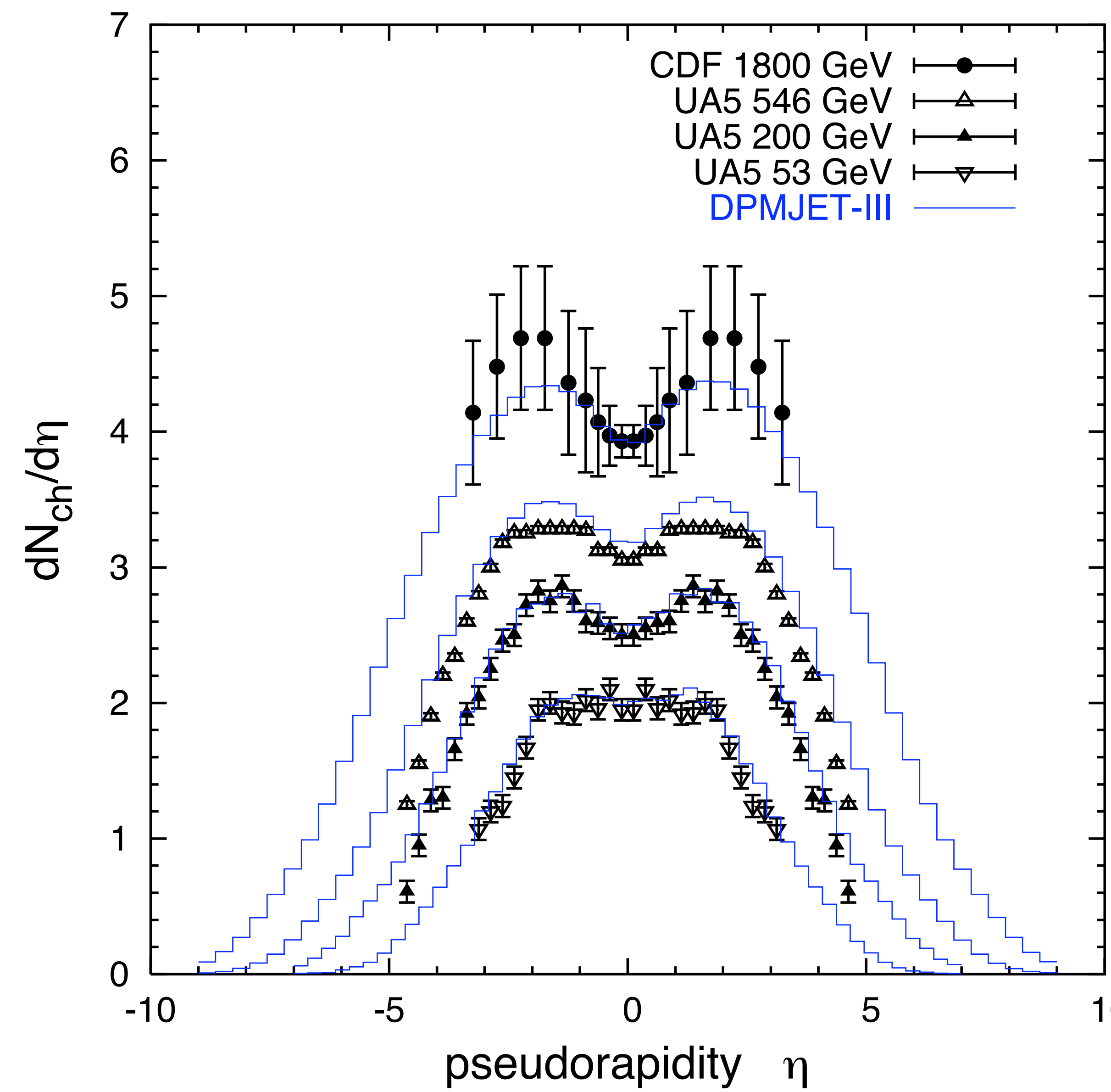

Charged particle pseudorapidity distributions

Photoproduction at HERA

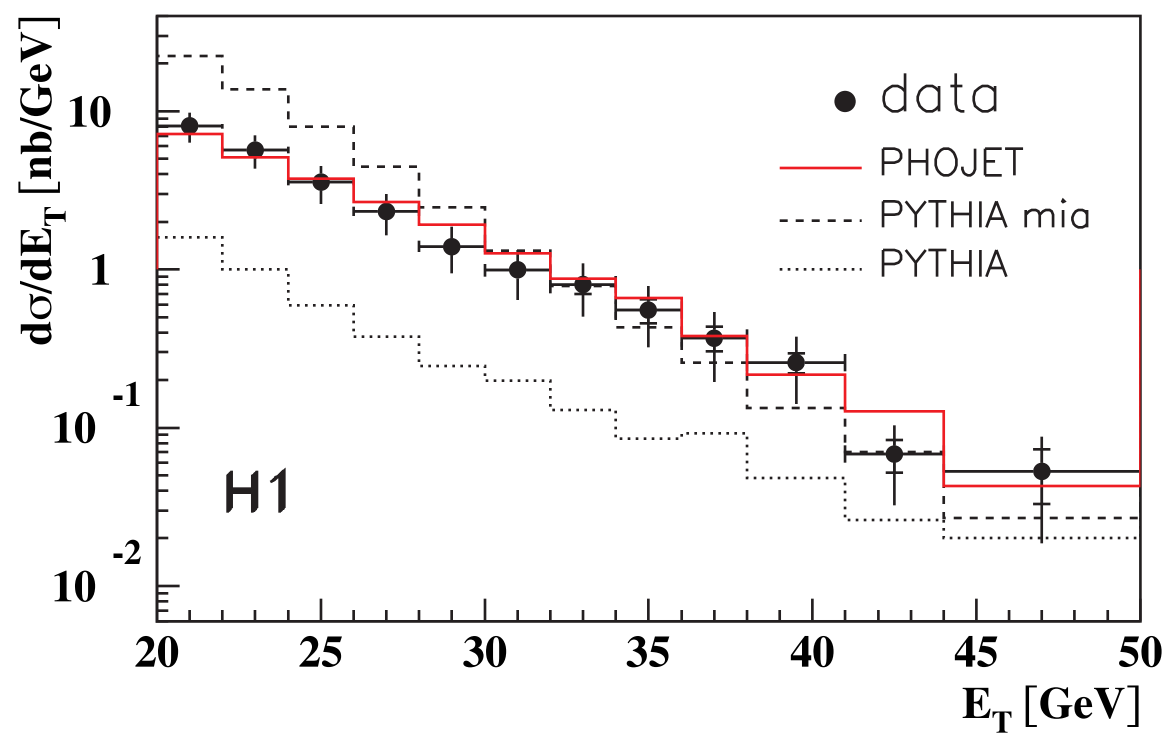

Jet and multiple interaction study by H1

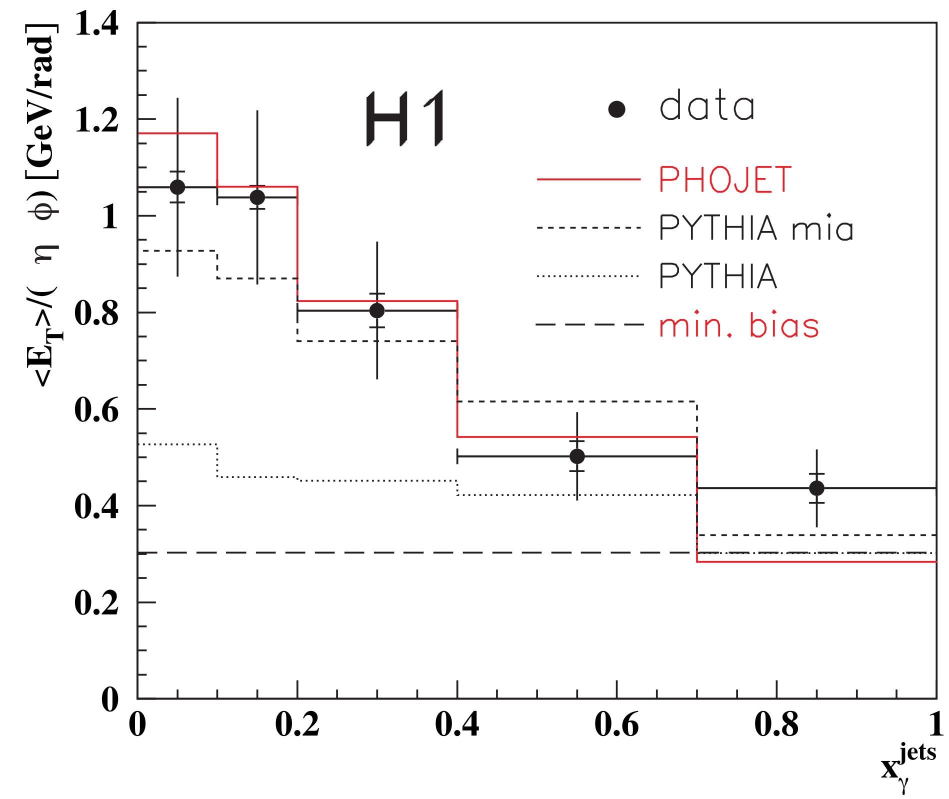

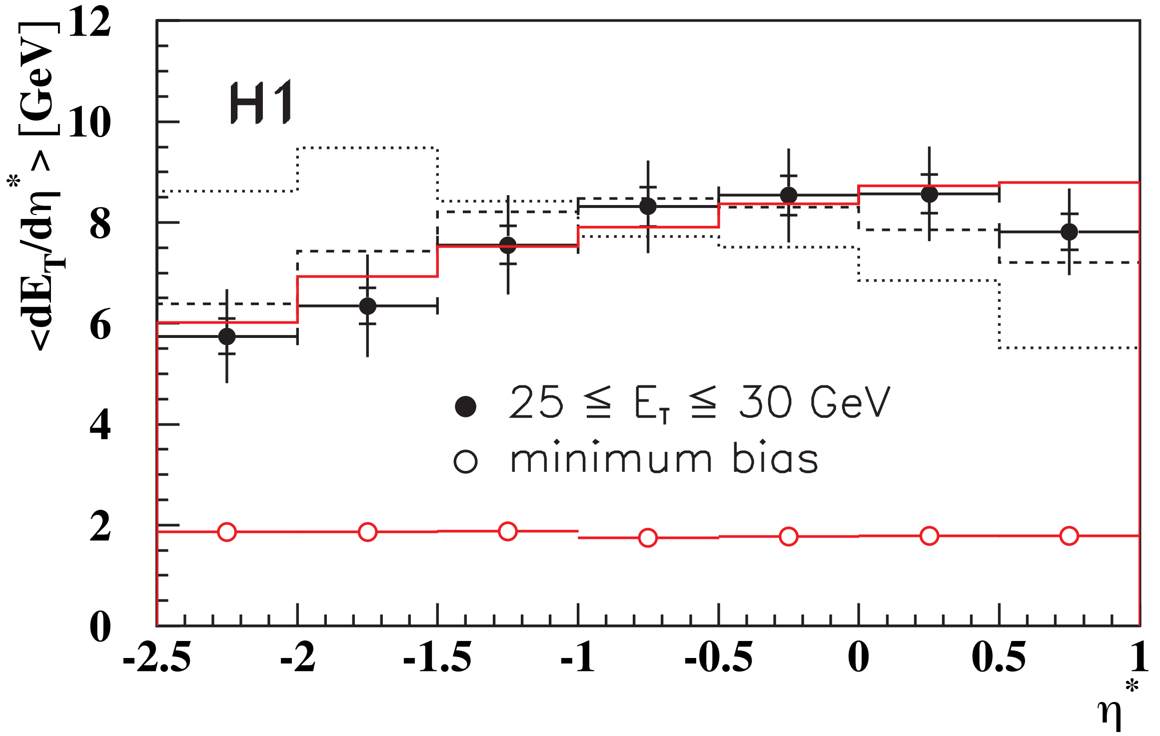

Energy density outside of jet cone, averaged over $-1 \leq \eta^{*} \leq 1$

(H1 Collab., ZPC 70, 1995)

Direct photon interactions: no shadowing

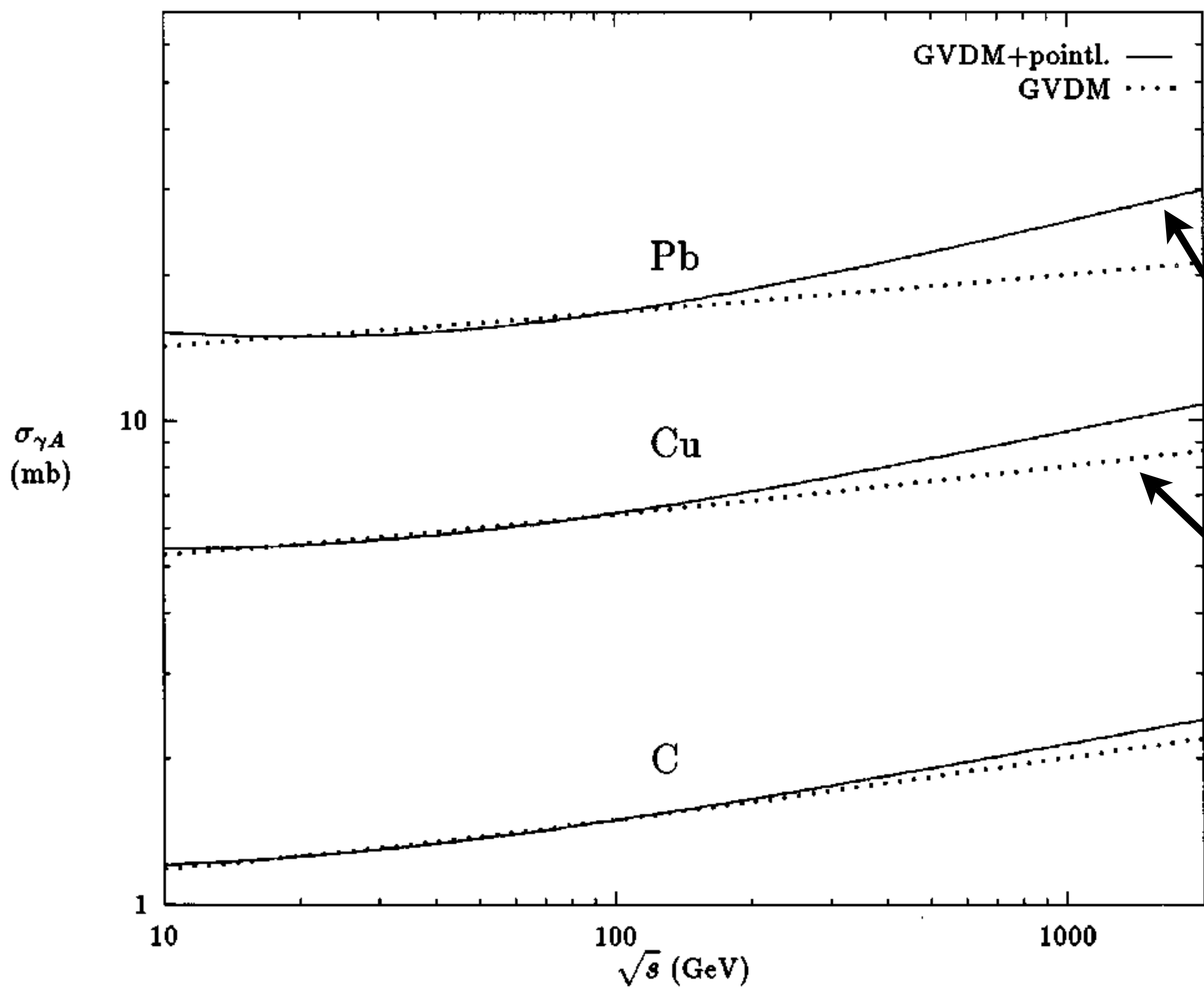

DPMJET III:

no shadowing for point-like photons, valid only for limited energy range

GVDM prediction

Treatment within dipole model:
Rogers, Strikman JPG 32 2006

Reconstruction of $W_{\gamma\gamma}$ at LEP

(Block & Kang, Int.J.Mod.Phys.A20, 2005)

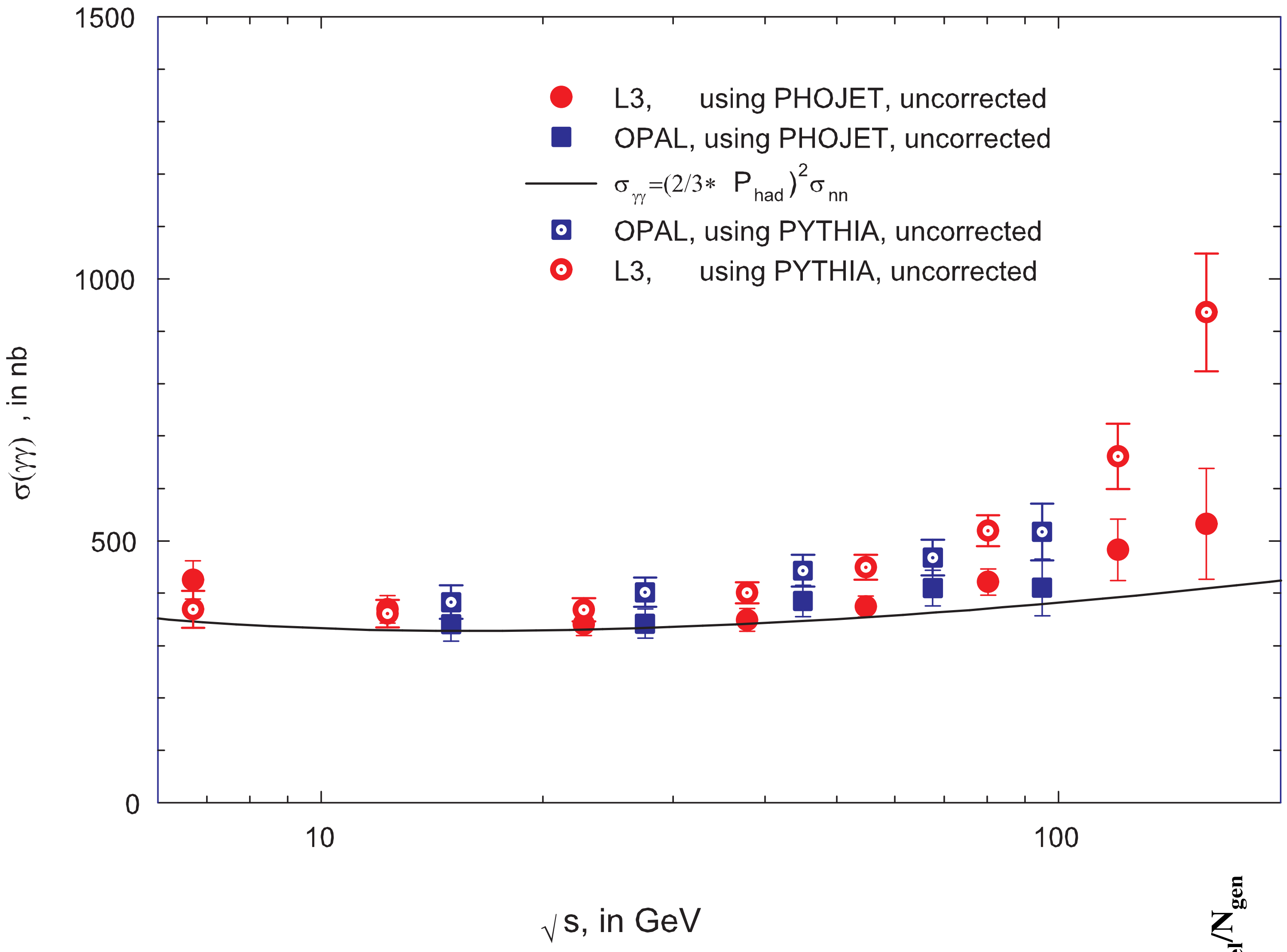

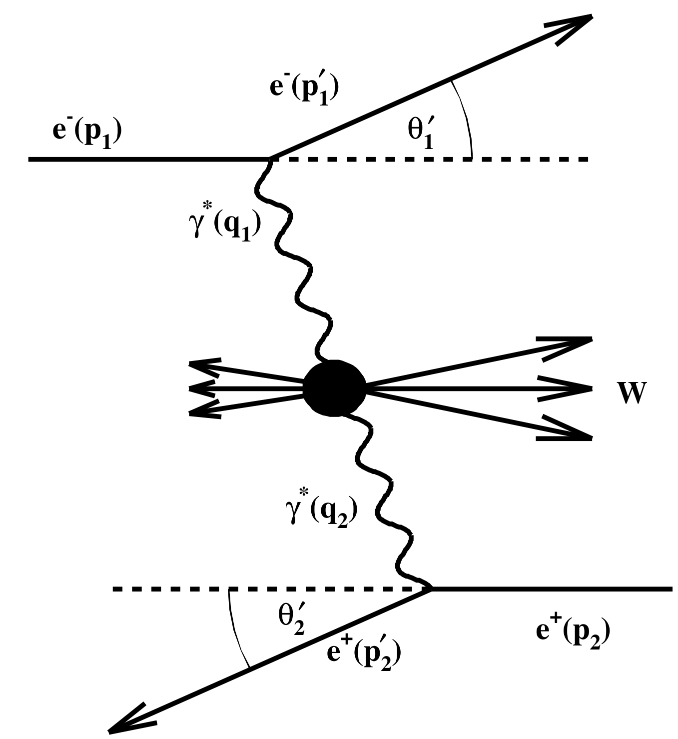

Always very strong model dependence of W reconstruction in untagged events

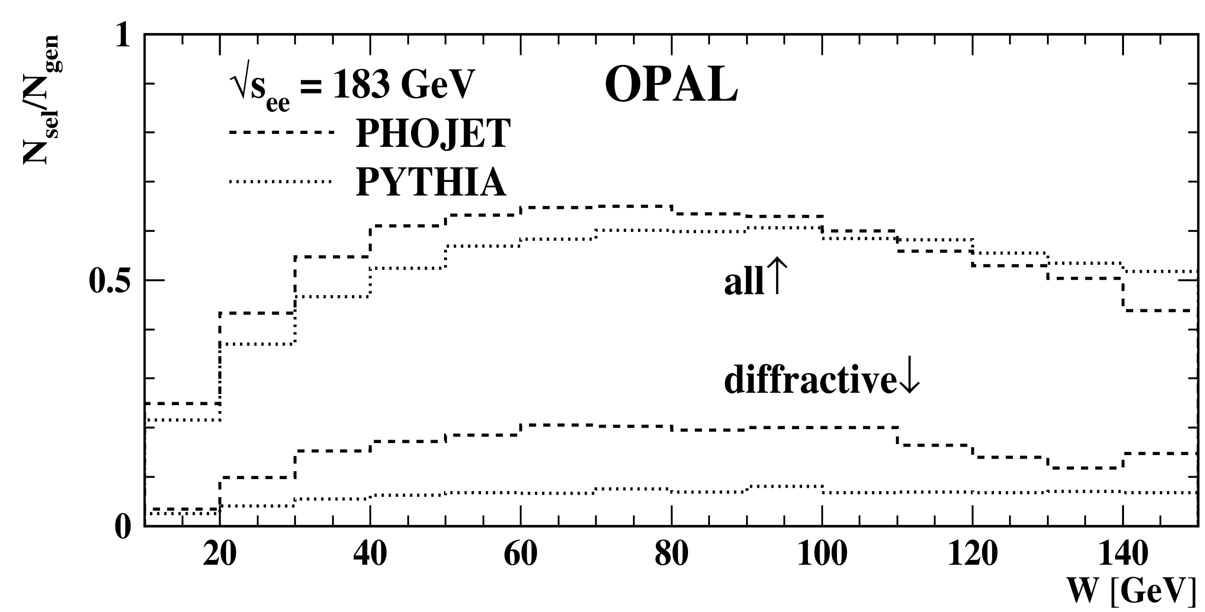

RHIC: nucleus-nucleus data

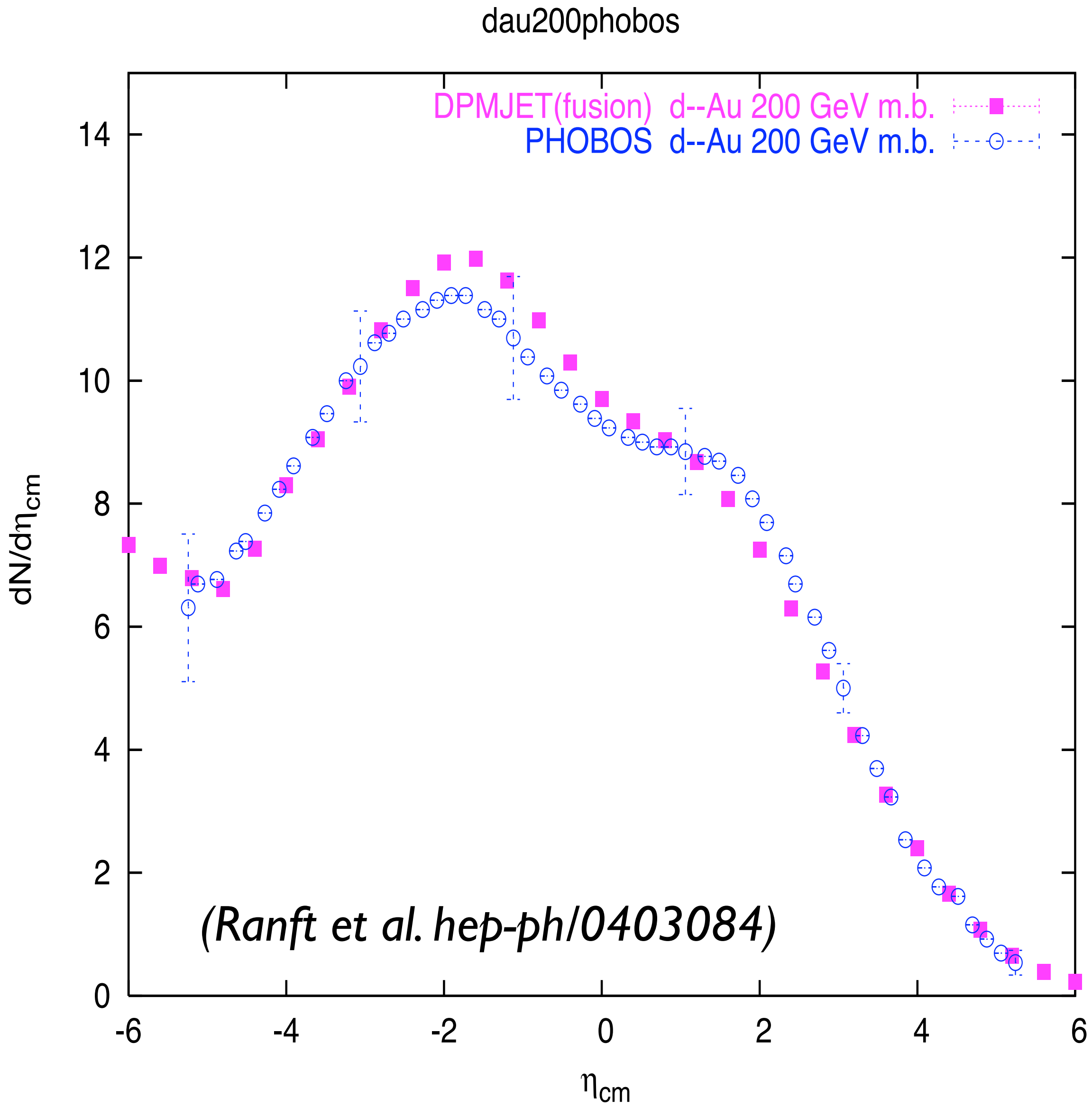

PHOBOS data:
d-Au @ 200 GeV cms

DPMJET III with string fusion

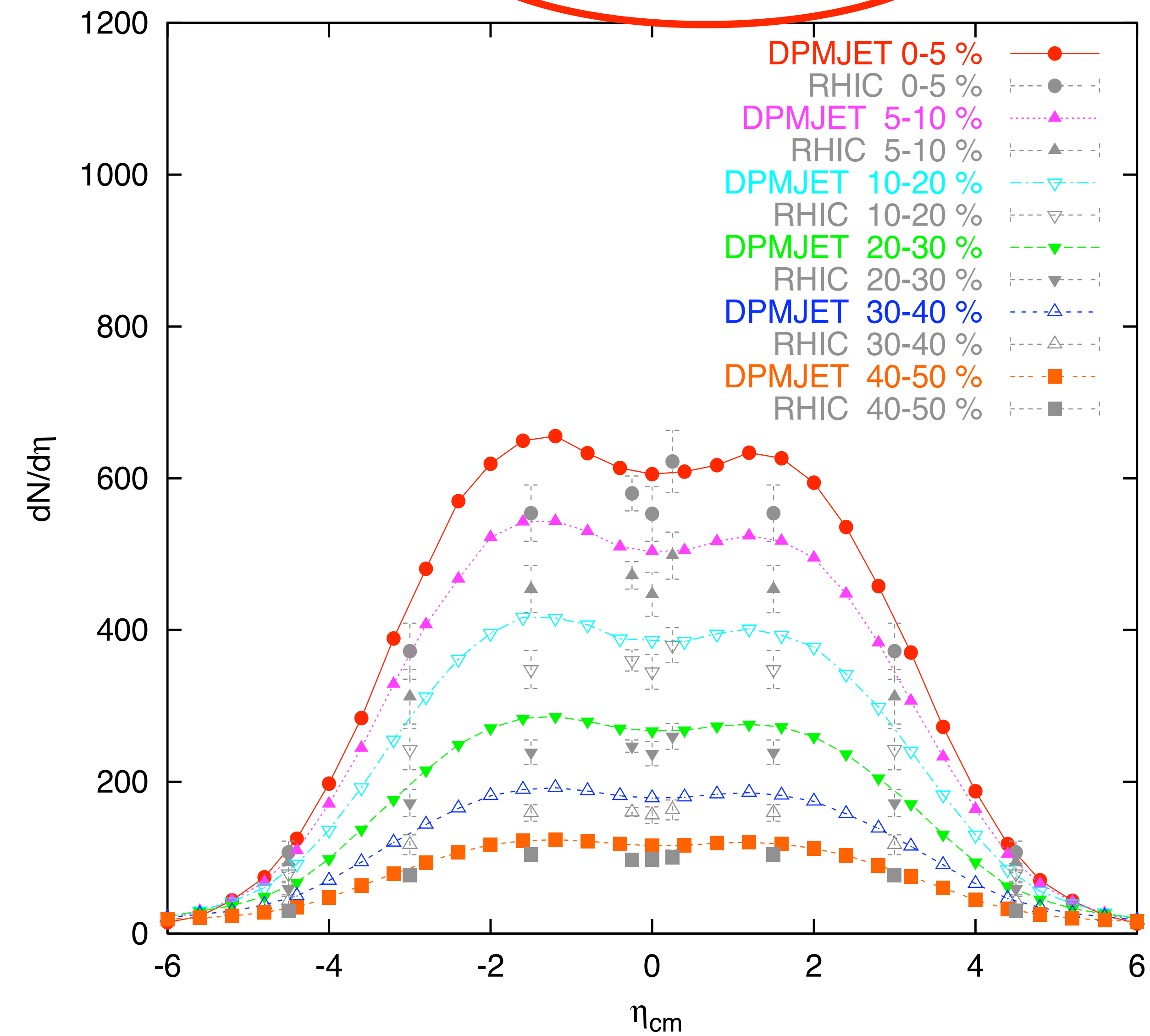

Au-Au, data compilation
(BRAHMS, PHENIX, PHOBOS)

Summary

Available (real/quasi-real photons):

- Low-energy region several well-tested MC models (SOPHIA, PEANUT, RELDIS, FLUKA)
- Intermediate energy region: DPMJET III (minimum bias studies)
- High-energy region: DPMJET III (with many caveats)
- Various photon flux MCs

Missing so far:

- Heavy quark production (diffractive and non-diffractive)
- MC based on dipole model and $k_\perp$ factorization
- Color transparency (cross section fluctuations + forward dijets)
- Rapidity gap (pomeron/diffraction) MC generator for nuclei

History of DPMJET

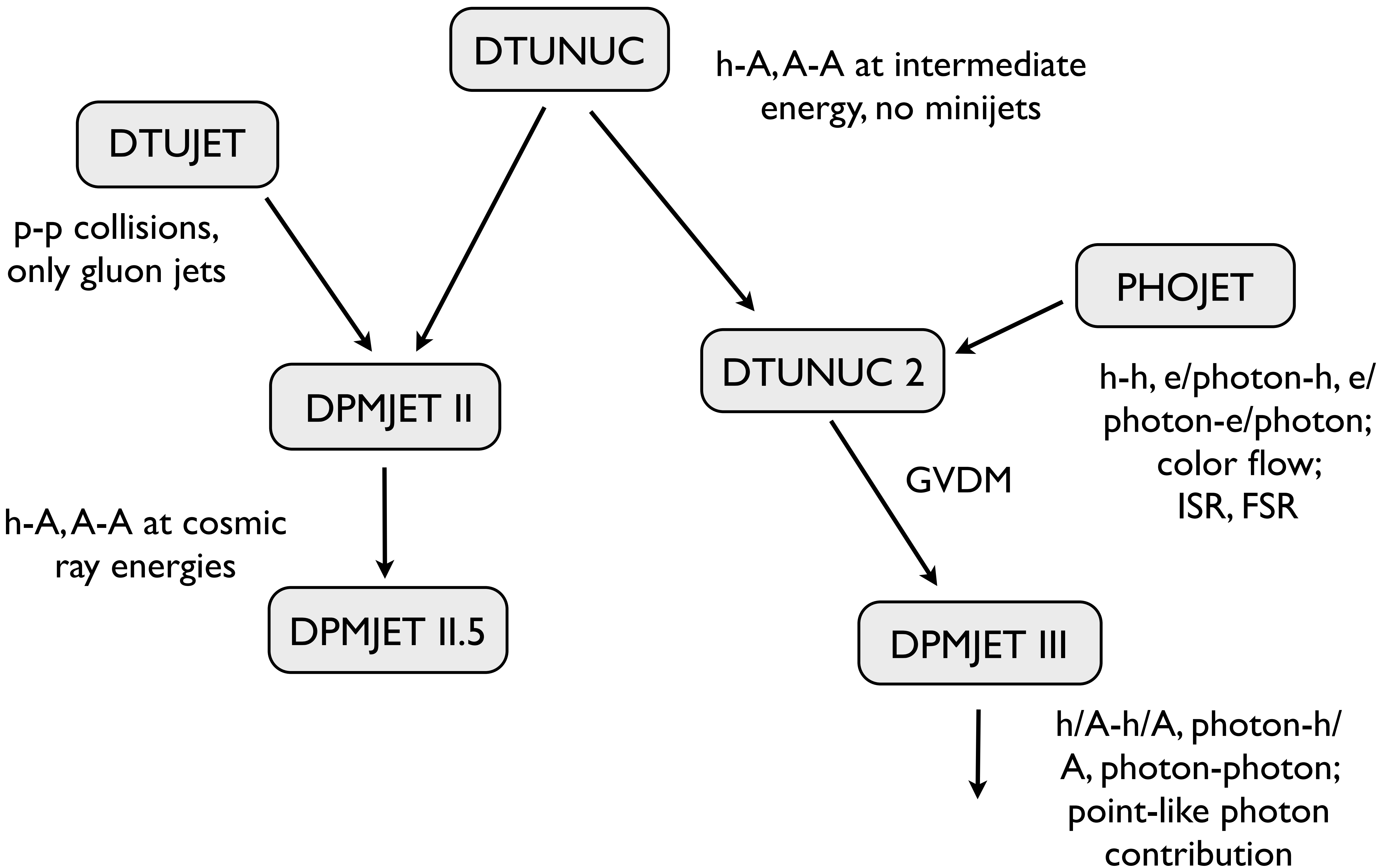

History of DPMJET